Prepared in Cooperation with the Minnesota Department of Natural Resources

Assessing the Water Quality and Habitat Dynamics of Deepwater Lakes with Coldwater Fish Populations

By Erik A. Smith and Richard L. Kiesling

U.S. Department of the Interior
U.S. Geological Survey

Contents

Introduction 1

Purpose and Scope 3

Relevance and Benefits 4

Acknowledgments 4

Methods 5

Model Implementation 5

Lake Carlos 6

Elk Lake 7

Trout Lake 8

Bathymetric Data and Computational Grid 8

Boundary and Initial Conditions 11

Hydraulic and Thermal Boundary Conditions 11

Lake Carlos 11

Elk Lake 13

Trout Lake 14

Chemical Boundary Conditions 15

Lake Profile Data 16

Initial Conditions 17

Model Parameters 18

Quality Assurance 19

Model Development 19

Model Calibration 19

Water Balance 20
Lake Carlos 21
Elk Lake 21
Trout Lake 22
Temperature 22
Lake Carlos 23
Elk Lake 24
Trout Lake 26
Dissolved Oxygen 27
Lake Carlos 28
Elk Lake 30
Trout Lake 31
Algae..32
Lake Carlos 33
Elk Lake 35
Trout Lake 36
Nutrients..38
Lake Carlos 39
Elk Lake 41
Trout Lake 44
Model validation 45
Lake Carlos 46
Elk Lake 48
Trout Lake 51

Model Limitations 53
Sensitivity Analysis 54
Historical Simulations 58
Summary 60
References Cited 61

Figures

Figure 1. Major Minnesota ecoregions and sentinel lakes. The super sentinel lakes are the focus of this study. ... 66
Figure 2. Location of the sampling locations in Lake Carlos, Minnesota. 67
Figure 3. Location of the sampling locations in Elk Lake, Minnesota. 68
Figure 4. Location of the sampling locations in Trout, Minnesota. 69
Figure 5. Volume-elevation and surface area-elevation curves for Lake Carlos between the measured bathymetry, provided by the Minnesota Department of Natural Resources (DNR), and as represented by the model grid. 70
Figure 6. Volume-elevation and surface area-elevation curves for Elk Lake between the measured bathymetry, provided by the Minnesota Department of Natural Resources (DNR), and as represented by the model grid. 71
Figure 7. Volume-elevation and surface area-elevation curves for Trout Lake between the measured bathymetry, provided by the Minnesota Department of Natural Resources (DNR), and as represented by the model grid. 72
Figure 8. Lake Carlos, as shown in (*A*) side view and (*B*) top view of the CE-QUAL-W2 computational grid. 73
Figure 9. Elk Lake, as shown in (*A*) side view and (*B*) top view of the CE-QUAL-W2 computational grid. 74
Figure 10. Trout Lake, as shown in (*A*) side view and (*B*) top view of the CE-QUAL-W2 computational grid. 75
Figure 11. Simulated and measured water surface elevation for Lake Carlos, April 22 to November 9, 2010. 76
Figure 12. Simulated and measured water surface elevation for Elk Lake, April 26 to November 8, 2011. 77
Figure 13. Simulated and measured water surface elevation for Trout Lake, April 28, 2010 to October 20, 2010. 78

Figure 14. Simulated and measured water temperature for the epilimnion (2-m) and hypolimnion (37-m) at Kecks Point (USGS station number 455843095212501) for Lake Carlos, April 22, 2010 to November 9, 2010. 79

Figure 15. Simulated and measured water temperature at Kecks Point (USGS station number 455843095212501) in Lake Carlos for 15 dates in 2010, with AME and RMSE quantities.. 80

Figure 16. Simulated and measured water temperature for the epilimnion (2-m and 7-m) and hypolimnion (20-m and 28-m) at south basin hole (USGS station number 471116095125301) in Elk Lake, April 26, 2011 to November 8, 2011. 81

Figure 17. Simulated and measured water temperature at south basin hole (USGS station number 471116095125301) in Elk Lake for 15 dates in 2011, with AME and RMSE quantities. 82

Figure 18. Simulated and measured water temperature for the epilimnion (0.5 meters) and hypolimnion (18.5 meters) at north basin hole (USGS station number 475214090100401) in Trout Lake, April 28, 2010 to October 20, 2010. 83

Figure 19. Simulated and measured water temperature at north basin hole (USGS station number 475214090100401) in Trout Lake for 14 dates in 2010, with AME and RMSE quantities.. 84

Figure 20. Simulated and measured dissolved oxygen concentrations at Kecks Point (USGS station number 455843095212501) in Lake Carlos for 11 dates in 2010, with AME and RMSE quantities.. 85

Figure 21. Simulated and measured dissolved oxygen concentrations at south basin hole (USGS station number 471116095125301) in Elk Lake for 15 dates in 2011, with AME and RMSE quantities. 86

Figure 22. Continuous simulated and measured dissolved oxygen concentrations at south basin hole (USGS station number 471116095125301) in Elk Lake for three different depths (2, 7 and 20 meters below the water surface), with AME and RMSE quantities, April 26, 2011 to November 8, 2011... 87

Figure 23. Simulated and measured dissolved oxygen concentrations at north basin (USGS station number 475214090100401) in Trout Lake for 15 dates in 2010, with AME and RMSE quantities.. 88

Figure 24. Simulated algal group distributions (diatoms, green, and blue-green algae) for three different segments in Lake Carlos, April 22, 2010 to November 9, 2010. 89

Figure 25. Simulated and measured chlorophyll *a* concentrations (in μg/L) for three different segments in Lake Carlos, April 22, 2010 to November 9, 2010. 90

Figure 26. Simulated algal group distributions (diatoms, green, and blue-green algae) for two different depths at south basin hole (USGS station number 471116095125301) in Elk Lake, April 26, 2011 to November 8, 2011. 91

Figure 27. Simulated and measured chlorophyll *a* concentrations (in μg/L) for two different depths at south basin hole (USGS station number 471116095125301) in Elk Lake, April 26, 2011 to November 8, 2011. 92

Figure 28. Simulated algal group distributions (diatoms, green, and blue-green algae) for two different depths at north basin hole (USGS station number 475214090100401) in Trout Lake, April 28, 2010 to October 20, 2010. 93

Figure 29. Simulated and measured chlorophyll *a* concentrations (in μg/L for two different depths at north basin hole (USGS station number 475214090100401) in Trout Lake, April 28, 2010 to October 20, 2010. 94

Figure 30. Simulated and measured ammonia (as N) concentrations (in mg/L) for three different segments in Lake Carlos, April 22, 2010 to November 9, 2010. 95

Figure 31. Simulated and measured nitrate-nitrite (as N) concentrations (in mg/L) for three different segments at Kecks Point (USGS station number 455843095212501) in Lake Carlos, April 22, 2010 to November 9, 2010. 96

Figure 32. Simulated and measured orthophosphorus (as P) concentrations (in mg/L) for three different segments at Kecks Point (USGS station number 455843095212501) in Lake Carlos, April 22, 2010 to November 9, 2010. 97

Figure 33. Simulated and measured total nitrogen concentrations (in mg/L) for three different segments at Kecks Point (USGS station number 455843095212501) in Lake Carlos, April 22, 2010 to November 9, 2010. 98

Figure 34. Simulated and measured total phosphorus concentrations (in μg/L) for three different segments at Kecks Point (USGS station number 455843095212501) in Lake Carlos, April 22, 2010 to November 9, 2010. 99

Figure 35. Simulated and measured ammonia (as N) concentrations (in mg/L) for two different depths at south basin hole (USGS station number 471116095125301) in Elk Lake, April 26, 2011 to November 8, 2011. 100

Figure 36. Simulated and measured nitrate-nitrite (as N) concentrations (in mg/L) for two different depths at south basin hole (USGS station number 471116095125301) in Elk Lake, April 26, 2011 to November 8, 2011. 101

Figure 37. Simulated and measured orthophosphorus (as P) concentrations (in mg/L) for two different depths at south basin hole (USGS station number 471116095125301) in Elk Lake, April 26, 2011 to November 8, 2011. 102

Figure 38. Simulated and measured total nitrogen concentrations (in mg/L) for two different depths at south basin hole (USGS station number 471116095125301) in Elk Lake, April 26, 2011 to November 8, 2011. 103

Figure 39. Simulated and measured total phosphorus concentrations (in μg/L) for two different depths at south basin hole (USGS station number 471116095125301) in Elk Lake, April 26, 2011 to November 8, 2011. 104

Figure 40. Simulated and measured ammonia (as N) concentrations (in mg/L) for two different depths at north basin hole (USGS station number 475214090100401) in Trout Lake, April 28, 2010 to October 20, 2010. 105

Figure 41. Simulated and measured nitrate-nitrite (as N) concentrations (in mg/L) for two different depths at north basin hole (USGS station number 475214090100401) in Trout Lake, April 28, 2010 to October 20, 2010. 106

Figure 42. Simulated and measured orthophosphorus (as P) concentrations (in mg/L) for two different depths at north basin hole (USGS station number 475214090100401) in Trout Lake, April 28, 2010 to October 20, 2010. 107

Figure 43. Simulated and measured total nitrogen concentrations (in mg/L) for two different depths at north basin hole (USGS station number 475214090100401) in Trout Lake, April 28, 2010 to October 20, 2010. 108

Figure 44. Simulated and measured total phosphorus concentrations (in μg/L) for two different depths at north basin hole (USGS station number 475214090100401) in Trout Lake, April 28, 2010 to October 20, 2010. 109

Figure 45. Simulated and measured water temperature for the epilimnion (2-m) and hypolimnion (37-m) at Kecks Point (USGS station number 455843095212501) in Lake Carlos, March 16, 2011 to September 28, 2011. 110

Figure 46. Simulated and measured water temperature at Kecks Point (USGS station number 455843095212501) in Lake Carlos for 11 dates in 2011, with AME and RMSE quantities. 111

Figure 47. Simulated and measured dissolved oxygen concentrations at Kecks Point (USGS station number 455843095212501) in Lake Carlos for 8 dates in 2011, with AME and RMSE quantities. 112

Figure 48. Simulated and measured chlorophyll *a* concentrations (in μg/L) for three different segments in Lake Carlos, March 16, 2011 to September 28, 2011. 113

Figure 49. Simulated and measured total nitrogen concentrations (in mg/L) for three different segments in Lake Carlos, March 16, 2011 to September 28, 2011. 114

Figure 50. Simulated and measured total phosphorus concentrations (in μg/L) for three different segments in Lake Carlos, March 16, 2011 to September 28, 2011. 115

Figure 51. Simulated and measured water temperature for the epilimnion (2-m and 8-m) and hypolimnion (19-m and 28-m) at south basin hole (USGS station number 471116095125301) in Elk Lake, July 13, 2010 to November 9, 2010. 116

Figure 52. Simulated and measured water temperature at south basin hole (USGS station number 471116095125301) in Elk Lake for 12 dates in 2010, with AME and RMSE quantities. 117

Figure 53. Simulated and measured dissolved oxygen concentrations at south basin hole (USGS station number 471116095125301) in Elk Lake for 10 dates in 2010, with AME and RMSE quantities. 118

Figure 54. Simulated and measured chlorophyll *a* concentrations (in μg/L) for two different depths at south basin hole (USGS station number 471116095125301) in Elk Lake, July 13, 2010 to November 9, 2010. 119

Figure 55. Simulated and measured total nitrogen concentrations (in mg/L) for two different depths at south basin hole (USGS station number 471116095125301) in Elk Lake, July 13, 2010 to November 9, 2010. 120

Figure 56. Simulated and measured total phosphorus concentrations (in μg/L) for two different depths at south basin hole (USGS station number 471116095125301) in Elk Lake, July 13, 2010 to November 9, 2010. 121

Figure 57. Simulated and measured water temperature at north basin hole (USGS station number 475214090100401) in Trout Lake for six dates in 2011, with AME and RMSE quantities. 122

Figure 58. Simulated and measured dissolved oxygen concentrations at north basin hole (USGS station number 475214090100401) in Trout Lake for nine dates in 2011, with AME and RMSE quantities. 123

Figure 59. Simulated and measured total nitrogen concentrations (in mg/L) for two different depths at north basin hole (USGS station number 475214090100401) in Trout Lake, May 19, 2011 to July 20, 2011 and September 8, 2011 to November 9, 2011. 124

Figure 60. Simulated and measured total phosphorus concentrations (in μg/L) for two different depths at north basin hole (USGS station number 475214090100401) in Trout Lake, May 19, 2011 to July 20, 2011 and September 8, 2011 to November 9, 2011. 125

Figure 61. Simulated and measured dissolved oxygen concentrations for Kecks Point (USGS station number 455843095212501) for 12 dates in 1979. 126

Figure 62. Simulated and measured dissolved oxygen concentrations for Kecks Point (USGS station number 455843095212501) for 14 dates in 2009. 127

Figure 63. Plots of the simulated dissolved oxygen output from Keck's point, Lake Carlos MN, for 2009 (1a) and 2010 (1b) compared to Jacobson et al. (2008) model of niche boundaries for lake cisco *Coregonus artedi*. 128

Tables

Table 1. Location of continuous pressure transducers, water-quality sondes, thermistors, and discrete water-quality measurements used for the development of either model input or calibration of water temperature, dissolved oxygen, and water-quality constituents in the three Sentinel Lakes studies. 129

Table 2. Initial constituent concentrations for all three sentinel lakes, both calibration and validation runs. 131

Table 3. Parameters used for the water-quality algorithms for Lake Carlos, Elk Lake and Trout Lake. 132

Table 4. Summary of AME and RMSE quantities for all three Sentinel lakes for the calibration runs. 137

Table 5. Summary of AME and RMSE quantities for all three Sentinel lakes for the validation runs. 140

Table 6. Summary of sensitivity analysis for all three Sentinel lakes, in percent change from calibration run. 143

Conversion Factors

Inch/Pound to SI

Multiply	By	To obtain
	Length	
inch (in.)	2.54	centimeter (cm)
inch (in.)	25.4	millimeter (mm)
foot (ft)	0.3048	meter (m)
mile (mi)	1.609	kilometer (km)
	Area	
acre	4,047	square meter (m^2)
square foot (ft^2)	0.09290	square meter (m^2)
square mile (mi^2)	2.590	square kilometer (km^2)
	Volume	
cubic foot (ft^3)	0.02832	cubic meter (m^3)
	Flow rate	
foot per second (ft/s)	0.3048	meter per second (m/s)
cubic foot per second (ft^3/s)	0.02832	cubic meter per second (m^3/s)
cubic foot per day (ft^3/d)	0.02832	cubic meter per day (m^3/d)
million gallons per day (Mgal/d)	0.04381	cubic meter per second (m^3/s)
	Mass	
ounce, avoirdupois (oz)	28.35	gram (g)
pound, avoirdupois (lb)	0.4536	kilogram (kg)

Temperature in degrees Celsius (°C) may be converted to degrees Fahrenheit (°F) as follows:

°F=(1.8×°C)+32

Vertical coordinate information is referenced to the insert datum name (and abbreviation) here for instance, “North American Vertical Datum of 1988 (NAVD 88).”

Horizontal coordinate information is referenced to the insert datum name (and abbreviation) here for instance, “North American Datum of 1983 (NAD 83).”

Altitude, as used in this report, refers to distance above the vertical datum.

Specific conductance is given in microsiemens per centimeter at 25 degrees Celsius (µS/cm at 25 °C).

Concentrations of chemical constituents in water are given either in milligrams per liter (mg/L) or micrograms per liter (µg/L).

Assessing the Water Quality and Habitat Dynamics of Deepwater Lakes with Coldwater Fish Populations

By Erik A. Smith and Richard L. Kiesling

Introduction

Water quality, habitat, and fish in Minnesota lakes are facing substantial risks from a number of physical, chemical, and biological stressors. In recent years, water resource scientists have been making the case for focused assessments and monitoring of "sentinel" systems (Jassby, 1998; Carpenter and others, 2007; Magner and Brooks, 2007, Williamson and others, 2008) to address how these stress agents change lakes over the long term. Lakes and their contributing watersheds are highly complex, and developing a mechanistic understanding of the linkage between watershed-based stressors and lake metabolism is best accomplished by taking a long-term, adaptive approach towards water resource management (Magnuson and others, 1990). Intensive, detailed study of representative systems is critical to understanding cause and effect mechanisms, but there is an equally important need to compare this detailed information to a broader set of similar systems. In the Minnesota Department of Natural Resources (DNR) Sustaining Lakes in a Changing Environment (SLICE) research program, these study design requirements are being met by coupling intensive, predictive modeling of three "super sentinel" lakes with a larger group of sentinel lakes distributed in a split-panel design of environmental monitoring (McDonald, 2003). The structure of the SLICE program also includes a long-term ecological monitoring component.

The ability to simulate the effects of large-scale agents of change (e.g., watershed land-use alterations or decade-level climate change) on lake ecosystems is a critical component of a proactive management plan for Minnesota lakes. A number of regional and state-wide lake modeling studies have illustrated the potential linkages between climate change, lake morphology, and fish habitat in the form of temperature and dissolved oxygen distributions for Minnesota and the north-central United States (e.g., see summaries in Stefan and Fang, 1994; Stefan and others, 1995, 1996; DeStasio and others, 1996; Fang and others, 1999, 2004a, 2004b). These models have documented the relative importance of lake-basin geometry, ice-free season, thermal stratification, dissolved oxygen stratification and wind-driven mixing to the development of sustainable fish habitat in deepwater lakes of the region. However, the potential trophic-dynamic response to simultaneous changes in climate and land-use is less well understood, as is the response of specific lakes to these historical and hypothetical changes. Questions also remain as to how the complex food webs that support fish guilds within these modeled systems will respond to the predicted physical changes in fish habitat (DeStasio and others, 1996).

The U.S. Geological Survey (USGS) entered into a cooperative agreement with the Minnesota Department of Natural Resources to develop predictive tools to evaluate the trophic response of three selected sentinel lakes (fig. 1, table 1), to current meteorological conditions. The three selected lakes contain deep, coldwater habitats that remain viable during the summer months for coldwater fish species.

Figure 1. Major Minnesota ecoregions and sentinel lakes. The super sentinel lakes are the focus of this study.

Table 1. Location of continuous pressure transducers, water-quality sondes, thermistors, and discrete water-quality measurements used for the development of either model input or calibration of water temperature, dissolved oxygen, and water-quality constituents in the three Sentinel Lakes studies.

Purpose and Scope

The purpose of this report is to outline the development, calibration, and validation of mechanistic, biophysical water quality models for three lakes in Minnesota that are classified as supporting deep, coldwater fisheries habitat: Lake Carlos in Douglas County (fig. 2), Elk Lake in Itasca State Park in Clearwater County (fig. 3), and Trout Lake in Cook County (fig. 4). The chosen modeling framework, CE-QUAL-W2, is a two-dimensional, laterally averaged, hydrodynamic and water-quality model originally developed by the U.S. Army Corps of Engineers (USACE) and currently supported at Portland State University. CE-QUAL-W2 addresses the interaction between nutrient cycling, primary production, and trophic dynamics to predict responses in the distribution of temperature and oxygen in lakes, a primary goal of this study. Through the calibration and validation phases of the CE-QUAL-W2 models, it is shown CE-QUAL-W2 adequately predicts temperature and oxygen profiles in the three selected sentinel lakes, based on measured inputs of water and nutrients.

Figure 2. Location of the sampling locations in Lake Carlos, Minnesota.

Figure 3. Location of the sampling locations in Elk Lake, Minnesota.

Figure 4. Location of the sampling locations in Trout, Minnesota.

The model calibration for each of the lakes looked at the degree of fit between the simulated water temperature and dissolved-oxygen concentrations to selected lake water temperature and dissolved-oxygen concentrations. Lake Carlos was calibrated using data collected from April 2010 through November 2010, Elk Lake was calibrated using data collected from May 2011 through November 2011, and Trout Lake was calibrated using data collected from April 2010 through October 2010. With the calibrated CE-QUAL-W2 models, the model validation for each of the lake models followed the same methodology of comparisons as the calibration phase, except for a different period of time. Lake Carlos was validated using data collected from March 2011 through September 2011, Elk Lake was validated using data collected from July 2010 through November 2010, and Trout Lake was validated using data collected from May 2011 through November 2011 when water-quality data was available.

Relevance and Benefits

The proposed work will develop predictive tools to evaluate the trophic response of sentinel lakes to current meteorological conditions. The calibrated and validated CE-QUAL-W2 models will be used in future work to simulate the consequences of land-use change and climate dynamics on lake ecosystems and provide decision makers with information on the potential trade-offs between proposed management actions and current practices. In addition, modeled responses of coldwater fisheries habitat to climate change scenarios will identify long-term management challenges associated with the negative impacts of climate change on high-value fish communities.

Acknowledgments

Funding for this study was provided by a grant from the Environmental and Natural Resource Trust Fund of Minnesota to the Minnesota Department of Natural Resources and from the U.S. Geological Survey Cooperative Water Program. We thank Dr. Scott Wells from Portland State University, Joel Galloway from the U. S Geological Survey, Brian Herwig and Tim Cross of the Minnesota DNR, Ray Valley formerly of the Minnesota DNR, and Steve Heiskary of the Minnesota Pollution Control Agency. Special thanks go to Emily Resseger, Sarah Elliott, and Jeff Ziegeweid of the Minnesota Water Science Center, USGS, and to staff of the Minnesota Pollution Control Agency for data collection to support model development.

Methods

Model Implementation

All three of the sentinel lakes (Carlos, Elk, Trout) were constructed using CE-QUAL-W2 version 3.60 (V3.6) (Cole and Wells, 2008) , a two-dimensional, laterally averaged, hydrodynamic and water-quality model originally developed by the U.S. Army Corps of Engineers (USACE) and currently supported at Portland State University. As the model is laterally averaged, it is best suited for water bodies with a fairly homogenous cross-section. CE-QUAL-W2 V3.6 calculates the hydrodynamic properties of water surface elevation, velocities, and temperature, and can simulate 28 water quality state variables in addition to temperature. An advantage of CE-QUAL-W2 over other hydrodynamic and water quality models is that the hydrodynamic and water quality modules are coupled together through an equation of state for density, which is dependent on temperature, suspended solids, and total dissolved solids. This enables the water quality model to feedback into the hydrodynamic portion of the model. Although the lateral averaging of CE-QUAL-W2 is better suited for long, narrow water bodies such as reservoirs, rivers, and estuaries, CE-QUAL-W2 has been successfully applied in lake settings (Sullivan and Rounds, 2004; Sullivan and others, 2007). Lake Carlos has a relatively long and narrow body well-suited for CE-QUAL-W2. Although Elk Lake and Trout Lake did not meet the same criterion of a long and narrow body, both of these lakes exhibited enough homogeneity in water-quality and water temperature data such that laterally averaging did not compromise the integrity of the model to meet study objectives. Vertical variations captured with CE-QUAL-W2 are important for distinguishing temporal variations in the lake epilimnion and hypolimnion. Initial calibration included a water balance based on water surface elevation and water temperature at varying stations for each lake. Further calibration targets included water temperature and dissolved oxygen depth profiles, in addition to discrete measurements of ammonia, nitrate-nitrite, total nitrogen, total phosphorus, orthophosphate, and chlorophyll *a*.

The individual lake models were developed in several phases. First, data was collected to provide the meteorological, hydrological, thermal, and water quality boundary conditions for the calibration year. A summary of the discrete and continuous constituents collected for all three sentinel lakes, further split by sampling locations, is shown in table 1. Calibration year selection for each lake was based on the most extensive data sets available, specifically for outflow discharge, water surface elevation, water temperature, and meteorological data, since these data sets were critical for driving the model hydrodynamics. All other data, including temperature and dissolved oxygen profiles, tributary inflow, and water quality data, were aggregated to best define either the initial boundary conditions and/or utilized later in the calibration and validation processes. Next, the model grid was constructed based on available lake bathymetry data. Data sets necessary to run CE-QUAL-W2 were formatted to fit the input data structure. Prior to initial water balance calibration, input parameters were selected, mainly based on default values either pre-populated within CE-QUAL-W2 (Cole and Wells, 2008) or previous USGS CE-QUAL-W2 modeling efforts (Galloway and Green, 2006; Galloway and others, 2008).

Lake Carlos

The water budget of Lake Carlos was initially calibrated for the period of April to November 2010 by comparing the measured and simulated water levels at the Long Prairie River (USGS station number 05244820), the main surface water outflow (fig. 2; table 1). Two gaged inflow tributaries, the outflow channels for Le Homme Dieu Lake (USGS station number 05244810) and Lake Darling (USGS station number 05244780) (fig. 2; table 1), were based on continuous discharge measurements for the entire calibration period. Adjustments were made to the gains and losses in the distributed tributary flow, which lumps all ungaged inflow and groundwater interactions, until a reasonable water balance was attained. After initial calibration, refined calibration focused on the vertical profiles of dissolved oxygen and temperature at Kecks Point (USGS station number 455843095212501). Additionally, the refined calibration step included the water quality parameters highlighted earlier (ammonia, nitrate-nitrite, total nitrogen, total phosphorus, orthophosphate, and chlorophyll *a*). Final refinement of model parameters, after several hundred iterations, was achieved with the realization of low absolute mean error (AME) and root mean square error (RMSE) values for most of the target constituents. AME and RMSE targets were operationally defined by other USGS reports utilizing CE-QUAL-W2, such as Pueblo Reservoir, southeastern Colorado (Galloway and others, 2008) and Table Rock Lake, Missouri (Green and others, 2003). Details of calculating the AME and RMSE values are included in the Model Development section. Most model runs included one adjustment with a subsequent model run to characterize the parameter sensitivity.

Elk Lake

The water budget of Elk Lake was initially calibrated for the period of April to November 2011 by comparing the measured and modeled water levels at the Elk Lake outlet (USGS station number 05199950), the main surface water outflow located at the north end of the lake. Four ungaged inflow tributaries (USGS station number 05199935; USGS station number 05199940; USGS station number 05199943; USGS station number 05199945), located around the margins of Elk Lake (fig. 3; table 1), were fixed as a ratio to the outflow discharge based on the contributing watershed area for the inflow compared to the overall basin watershed area. This analysis was automatically calculated using StreamStats (Lorenz and others, 2009). As in Lake Carlos, adjustments were made to the gains and losses in the distributed tributary flow until a reasonable water balance and low AME/RMSE values could be achieved for lake level elevation. After initial calibration, further calibration targets included vertical profiles of dissolved oxygen and temperature for specific dates throughout the year in addition to water-quality constituents for the Elk Lake outlet and the northern basin (fig. 2; table 1). Similar to Lake Carlos, final refinement of model parameters was achieved with the actualization of low AME and RMSE values for most of the target constituents.

Trout Lake

The water budget of Trout Lake was initially calibrated for the period of April to late October 2010 by comparing the measured and modeled water levels at the Trout Lake outlet (USGS station number 04011150), the main surface water outflow located at the south end of the lake (fig. 4). Two ungaged inflow tributaries (USGS station number 04011140; USGS station number 04011145), located along the western margin of Trout Lake, were fixed as a ratio to the outflow discharge based on the contributing watershed area for the inflow compared to the overall basin watershed area (fig. 4; table 1). Similar to Elk Lake, this analysis was automatically calculated using StreamStats (Lorenz and others, 2009). As in both Lake Carlos and Elk Lake, adjustments were made to the gains and losses in the distributed tributary flow until a reasonable water balance and low AME/RMSE values could be achieved for lake level elevation. After initial calibration, further calibration targets included vertical profiles of dissolved oxygen and temperature for specific dates throughout the year in addition to water-quality constituents collected at the Trout Lake outflow and the northern basin. Similar to both Lake Carlos and Trout Lake, final refinement of model parameters was achieved with the actualization of low AME and RMSE values for most of the target constituents.

Bathymetric Data and Computational Grid

Information from a digital elevation model and any available bathymetric data was used to generate bathymetric cross-sections for the CE-QUAL-W2 model. Accurate model reconstruction is important given that it is the finite difference representation of the lake itself, so the hydrodynamics will influenced by the lake's geometry. This can be verified by comparison of the actual and modeled relations between lake volume and lake surface area to water-surface elevation (fig. 5-7).

Figure 5. Volume-elevation and surface area-elevation curves for Lake Carlos between the measured bathymetry, provided by the Minnesota Department of Natural Resources (DNR), and as represented by the model grid.

Figure 6. Volume-elevation and surface area-elevation curves for Elk Lake between the measured bathymetry, provided by the Minnesota Department of Natural Resources (DNR), and as represented by the model grid.

Figure 7. Volume-elevation and surface area-elevation curves for Trout Lake between the measured bathymetry, provided by the Minnesota Department of Natural Resources (DNR), and as represented by the model grid.

A watershed geographic information system (GIS) layer was obtained for each lake from either the Minnesota Lake Watershed Delineation Project (*http://www.dnr.state.mn.us/watersheds/lakeshed_project.html*, accessed August 2013) or generated from the U.S. Geological Survey Minnesota StreamStats application (Ries and others, 2004; Lorenz and other, 2009). The lake watershed GIS layer was used to define the maximum outer boundary for each lakes bathometric model grid. The best available elevation data was used and ranged from 1-meter LiDAR based digital elevation models (DEMs) (*http://www.mngeo.state.mn.us/chouse/elevation/lidar.html*, accessed August 2013) to 30-meter DEMs from the U.S Geological Survey National Elevation Dataset (*http://ned.usgs.gov*, accessed October 2012). Bathymetric surveys of each of the three lakes was available from the Minnesota Department of Natural Resources (MN DNR) as GIS layers, either originally obtained from lake surveys or lake contour maps (*http://deli.dnr.state.mn.us/data_catalog.html*, accessed August 2013). The basic process was to combine the land elevation layer with the bathymetric data to produce a gridded, two-dimensional model of the surface area and depth of each lake. The next step was to identify the deepest elevation value of the lake, and then to divide the lake model into 1-meter slices starting at the bottom of the lake and ending approximately two meters above the static water level elevation. All model grid cells represented in each 1-meter slice was identified and converted to a GIS polygon dataset. All slice polygons were then compiled into a single polygon GIS dataset and the area of each polygon was calculated by the GIS. Each lake model also includes the area of land that would become inundated if the water level increased by two meters above the lake's base elevation (static water level elevation). The base lake elevation was obtained from 1:24,000 U.S. Geological Survey topographic maps or from lake level data from the Minnesota DNR Lake Finder website (*http://www.dnr.state.mn.us/lakefind/index.html*, accessed August 2013).

After completion of the GIS polygon dataset, each lake was segmented into lateral segments (fig. 8-10). Within each lateral segment, 1-meter layers were drawn from the bottom of the lake up to two meters above the static lake level elevation. Distance along the longitudinal axis for individual CE-QUAL-W2 lateral segments varied considerably. Considerations for the number of segments selected included a balance between full-scale representation of the real structure of the lake and segment structure that avoids numerical instability. Segments were grouped together into branches, with all of the branches grouped together representing the computational grid of the water body. Despite the ability to use different branches to represent separate bays or embayments, such as the north end of Lake Carlos (fig. 2), these embayments or arms were included into a single water branch for the sake of model simplicity for all three lakes. Figures 8-10 show each of the three lakes in side view as the CE-QUAL-W2 computational grids. In reality, layers get smaller deeper and would also vary from segment to segment. Lake Carlos includes 22 computational segments (fig. 2; fig. 8), Elk Lake includes five computational segments (fig. 3; fig. 9), and Trout Lake includes three computational segments (fig. 4; fig. 10).

Figure 8. Lake Carlos, as shown in (*A*) side view and (*B*) top view of the CE-QUAL-W2 computational grid.

Figure 9. Elk Lake, as shown in (*A*) side view and (*B*) top view of the CE-QUAL-W2 computational grid.

Figure 10. Trout Lake, as shown in (*A*) side view and (*B*) top view of the CE-QUAL-W2 computational grid.

Boundary and Initial Conditions

Paramount to the success of the model was a high data density of biological, chemical, and physical lake characteristics from which lake parameters could be calculated and the model calibrated and validated. Several continuous flow and water quality monitoring systems were installed to calculate the initial and boundary conditions for the models, and to provide a robust calibration and validation data set. Streamflow was measured monthly at the inflows and outflows of all three lakes. Streamflow measurements were made according to methods described in Buchanan and Somers (1969) and Mueller and Wagner (2008). Water temperature for all water inflows and outflows was also collected and required for the CE-QUAL-W2 model.

The following sections will detail the specific boundary and initial conditions for each of the three sentinel lakes (Carlos, Trout, and Elk).

Hydraulic and Thermal Boundary Conditions

Lake Carlos

Lake inflow and water temperature data used in the CE-QUAL-W2 model for Lake Carlos was obtained from two separate outlet channels into Lake Carlos. The Lake Darling outlet (USGS station number 05244780) was measured in the channel connecting Lake Darling to Lake Carlos, located at the southern end of Lake Carlos (table 1; fig. 2). Lake Le Homme Dieu outlet (USGS station number 05244810) was measured near the outlet channel connecting Lake Le Homme Dieu to Lake Carlos, located along the eastern margin of Lake Carlos in the southern basin (fig. 2; table 1). Submersible pressure transducers were installed at ice off and were removed just prior to ice on for both outlets, collecting continuous water temperature and level measurements every 15 minutes. Streamflow was measured monthly at the inflows. Based on a linear regression analysis that predicts discharge from stage, discharge estimates for every 15 minutes were made for both the Lake Darling and Lake Le Homme Dieu outlets. For the purposes of the model, the Lake Darling outlet is considered the main inflow to the CE-QUAL-W2, flowing into segment 2 (fig. 2; table 1), and Lake Le Homme Dieu is a tributary flowing into segment 5 (fig. 2; table 1). Additional water flow was also assumed from ungaged locations in the lake in addition to groundwater flow, known as distributed flow. This is input into the model in daily time steps, distributed evenly across all the model segments; more detail of the distributed flow will be given in the water balance section of the model calibration.

The main outflow from Lake Carlos occurs through the Long Prairie River, located along the eastern margin of the southern basin (table 1; fig. 2), with stage and temperature data collected upstream from the metal weir at the start of the Long Prairie River (USGS station number 05244820). Similar to the methods for both the inflows, high-resolution (15-minutes) discharge estimates were based on a rating curve constructed from comparisons between transducer water levels recorded every 15 minutes and monthly streamflow measurements (Rantz and others, 1982a; Rantz and others, 1982b). As this was not located in segment 23, the final segment of the main waterbody branch, the outflow was treated as a withdrawal from segment 22 where the Long Prairie Outlet was located. Additionally, temperature was also collected every 15 minutes. Water-surface elevation for Lake Carlos was based on the transducer record collected at the Long Prairie River outlet.

Meteorological data was required for CE-QUAL-W2 given the importance of surface boundary conditions to the overall behavior of the model, specifically surface heat exchange, solar radiation absorption, wind stress, and gas exchange. The model required meteorological data including air temperature, dew point temperature, wind speed, wind direction, and cloud cover. All unit conversions from the meteorological data to the units required for the model were straightforward with the exception of cloud cover. The qualitative sky cover parameter (i.e., clear, scattered, obscured, broken, and overcast) was converted to an integer value, ranging from 0 to 10: clear = 0, scattered (1/8 to 4/8 cloud coverage) = 3, obscured = 5, broken (5/8 to 7/8 cloud coverage) = 7, overcast = 10. All of the required data were generally available at hourly intervals from the Alexandria Municipal Airport (USAF station ID 726557), located less than 10 km south of Lake Carlos. Based on the latitude and longitude of the lake and the required meteorological inputs, evapotranspiration as an internal CE-QUAL-W2 calculation was included in the water budget.

Elk Lake

The main outflow from Elk Lake occurred through the Chamber Creek outlet to Lake Itasca (USGS station number 05199950), located at the northwest end of Elk Lake, which discharged water to Lake Itasca (fig. 3; table 1). Similar to the methods described for Lake Carlos, high-resolution (15-minutes) discharge estimates were based on linear regression equation constructed from comparisons between transducer water levels recorded every 15 minutes and monthly streamflow measurements. Slight differences in the stage transformation to discharge for Elk Lake included the linear regression analysis performed as a power trendline equation on a log/log scale between stage and discharge. Also, the stage data included an adjustment for the point of zero flow (PZF). Additionally, temperature was also collected every 15 minutes. Water-surface elevation for Elk Lake was based on the transducer record collected at the Elk Lake outlet.

Lake inflow data was not collected for Elk Lake. Instead, the inflows to Elk Lake were computed from the outflow record. Four distinct ungaged inflow sites were identified around Elk Lake: Unnamed tributary to Elk Lake (USGS station number 05199935), GA-GWA-Dosh Creek (USGS station number 05199940), Spring 4 to Elk Lake (USGS station number 05199943), and Siegfried Creek (USGS station number 05199945) (fig. 3; table 1). Utilizing Minnesota StreamStats (Lorenz and others, 2009), an online tool for calculating peak discharge and basin characteristics for ungaged sites, the contributing watershed size for each of the four ungaged inflow sites was determined. Dividing the ungaged inflow site's contributing watershed area by the overall Elk Lake contributing watershed, the amount of expected discharge from the ungaged inflow site was calculated. This assumed the entire watershed contributed equally at all the times and the instantaneous outflow was the same as the sum of all the instantaneous inflows minus evapotranspiration. Although these assumptions were not necessarily true, it was the best approximation available for inflows as well as apportioning the inflows into the different segments (fig. 3; fig. 9).

All of the required data meteorological were generally available at hourly intervals from the Park Rapids Municipal Airport (USAF station ID 727543), located approximately 33 km southeast of Elk Lake. A weather station was installed at Elk Lake in 2011, including wind speed and direction, which was used in lieu of the Park Rapids wind data when available. The same meteorological data were required for the Elk Lake CE-QUAL-W2 model as Lake Carlos; for full details on the meteorological data requirements, see the Lake Carlos section for further details.

Trout Lake

The main outflow from Trout Lake occurred through the Trout Lake outlet (USGS station number 05199950), located at the south end of Trout Lake (fig. 4). Similar to the methods described for both Elk Lake, high-resolution (15-minutes) discharge estimates were based on a linear regression analysis constructed from comparisons between transducer water levels recorded every 15 minutes and monthly streamflow measurements. Additionally, temperature and water-surface elevation was also collected every 15 minutes.

Lake inflow data was not collected for Trout Lake. Following the same approach as Elk Lake, the inflows to Trout Lake were computed from the outflow record; for further details on allocating the inflows from the outflow record, see the Elk Lake section. Two distinct ungaged inflow sites were identified around Trout Lake: Trout Lake Tributary, northwest side (USGS station number 04011140) and Marsh Lake Outlet (USGS station number 04011145) (fig. 4; table 1).

All of the required data meteorological were generally available at hourly intervals from the Grand Marais-Cook County Municipal Airport (USAF station ID 727454), located approximately 14 km southwest of Trout Lake. The same meteorological data requirements were required for the Trout Lake CE-QUAL-W2 model as Lake Carlos, so see the Lake Carlos section for further details.

Chemical Boundary Conditions

Limnological characteristics, including processes that could affect trophic state were examined at one site for each of the three sentinel lakes: Lake Carlos west of Kecks Point (USGS station number 455843095212501); Trout Lake, east side (USGS station number 475214090100401); Elk Lake, south end (USGS station number 471116095125301). The sites were sampled monthly from May through November of 2010 and March through October of 2011 by USGS , and by MPCA staff monthly with the same schedule but two weeks offset, so that biweekly sampling was accomplished for both the 2010 and 2011 field seasons. Samples were collected near the surface and at depth (20 m, 40.65 m in Lake Carlos; 20 m in Elk Lake; 18 m in Trout Lake) and were analyzed to determine concentrations of alkalinity, nutrients, major ions, and chlorophyll *a*. Vertical profiles (1-meter intervals) of temperature, dissolved oxygen concentration, pH, specific conductance, and chlorophyll *a* were measured at each lake site. Secchi-disk transparency was measured at each vertical profile to determine the extent of light limitation to algal growth. Whole surface water was collected at the surface in June and August of 2010 at all three lakes and bioassays were run to determine lake nutrient limitation.

Sampling was conducted at the inflows and outflow of Lake Carlos (Le Homme Dieu outlet, Lake Darling outlet, and Lake Carlos outlet at Long Prairie River respectively), Elk Lake (Ga Gwa Dash Creek, Seigfried Creek, an unnamed tributary, two groundwater fed springs, and lake outlet), and Trout Lake (an unnamed tributary, Marsh Lake outlet, and lake outlet).

In addition, Elk Lake, its inflows, and groundwater near the two spring sites at Elk Lake in August 2010 and June 2011 using mini-piezometers. Water samples were analyzed for major ions and total nutrients.

USGS samples were analyzed by the USGS National Water Quality Laboratory (NWQL) in Denver and MPCA samples were analyzed by the Minnesota Department of Health Environmental Laboratory in St. Paul. All of the samples analyzed by NWQL have been previously reviewed and published, available online at the National Water Information System (NWIS) water-quality site by searching for the site number in table 1(*http://waterdata.usgs.gov/mn/nwis/qw/*, accessed August 2013). All of the samples analyzed by the Minnesota Department of Health Environmental Laboratory have been previously reviewed and published, available online at the DNR Lake Finder by searching by lake number (Lake Carlos = 21005700; Elk Lake = 15001000; Trout Lake = 16004900) and the subcategory of lake water quality (*http://www.dnr.state.mn.us/lakefind/index.html*, accessed August 2013). Chlorophyll *a* was determined by spectrophotometry in the Mounds View lab (Arar, 1997).

Lake Profile Data

Buoys with thermistor chains attached were installed in each lake in the spring of 2010, and remained in the lake through 2012 ice off. The thermistor chains were made up of HOBO Water Temp

Pro v2 Loggers attached to braided nylon rope with clips. The buoys were designed to float on the water surface during the 2010 ice-free season, and were then submerged 1-2 meters below water surface through the 2010-2011 winter and remained submerged for the duration of deployment. Thermistors were spaced at equal intervals from 1.5 meters to 3 meters (depending on the lake) through the 2010 ice free season, and then adjusted to a tighter interval of 1 meter around the thermocline with broader thermistor spacing in the hypolimnion. The HOBO thermistors logged temperature continuously at 15-minute intervals. In Lake Carlos, the thermistor chain was located at Kecks Point (USGS station number 455843095212501); Elk Lake, the thermistor chain was located at the south end (USGS station number 471116095125301); Trout Lake, the thermistor chain was located in the northeast basin (USGS station number 475214090100401).

In addition to the thermistor chain data, all three lakes had multiparameter YSI sondes (YSI model 6920) measuring continuous (generally at 15-minute intervals) vertical profiles of temperature, dissolved oxygen concentration, pH, and specific conductance at the thermistor chain locations for 2011. The procedures of Wagner and others (2006) was followed for the long-term deployment of the multiparameter probes. However, since only Elk Lake was calibrated for 2011, Lake Carlos and Trout Lake lacked the continuous profiles as lake profile dissolved oxygen and water temperature calibration targets. Therefore, these two lakes relied on the periodic profile measurements for the calibration phase.

Initial Conditions

All three sentinel lakes had water-quality modeling coupled with a hydrodynamic model. Each modeled constituent (including temperature) must have either an initial, single concentration for the entire lake or a grid-wide initial vertical profile of concentrations at the start of each model run. Initial conditions for each of the three lakes are shown in table 2, broken up by the calibration and validation years. As Lake Carlos had a more robust water-quality data set, separate initial conditions for all of the parameters were provided for the calibration and validation years. Elk Lake and Trout Lake had the same initial conditions with the exception of the water-surface elevation, initial temperature, dissolved oxygen, and algal group concentrations. Constituent concentrations were considered uniform throughout the lake for every segment and layer.

Table 2. Initial constituent concentrations for all three sentinel lakes, both calibration and validation runs.

Model Parameters

A limited number of parameters control the hydrodynamics and heat exchange for a CE-QUAL-W2 model. For the most part, the default values provided within CE-QUAL-W2 v3.6 or the accompanying manual were followed. Numerous CE-QUAL-W2 models have shown that the default hydraulic parameters were robust across different hydrologic settings, relatively insensitive to variations (Cole and Wells, 2008). It is important to note that CE-QUAL-W2 is time and space invariant, so these parameters were also fixed for a given lake model. The density control for all inflows in the model, allowed for the water inflows to match up with the layers within the lake that corresponded to the inflow density.

For the water quality calibration, over 130 coefficients control the constituent kinetics (table 3). An advantage of CE-QUAL-W2 is the modular design that allows control of the water quality constituents by adding specific subroutines. A significant number of these parameters were optional depending on the inclusion of groups such as epiphyton, zooplankton, macrophytes, and algal groups. Only the parameters required for the sentinel lakes applications were included in table 3. As with the hydraulic and heat exchange parameters that control the hydrodynamics, all of the parameters (coefficients) were time and space invariant. The option exists to vary some parameters, such as the extinction coefficient of water; however, not enough data was collected to justify dynamic control of any parameters.

Table 3. Parameters used for the water-quality algorithms for Lake Carlos, Elk Lake and Trout Lake.

Many of the parameters were the default values, while some of the remaining parameters were adjusted within a reasonable range during the calibration process. Guidance for all of the parameters also came from other USGS CE-QUAL-W2 model applications (Green and others, 2003; Sullivan and Rounds, 2004; Galloway and Green, 2006; Galloway and others, 2008; Sullivan and others, 2011).

Quality Assurance

A primary data quality objective was to ensure that samples were representative of the water bodies under investigation. Quality assurance was assessed with specific procedures, such as instrument calibration, to ensure data reliability and assess the quality of the sample data. The quality-assurance plan for this project followed USGS guidelines (Brunett and others, 1997). Field instruments were be maintained according to manufacturer's guidelines, calibration standards were properly stored, calibration for portable field instruments was undertaken at the start of each day (Gibs and others, 2012), field measurements were recorded in the field, and all field sampling equipment was cleaned before use according to the National Field Manual guidelines (Wilde, ed., 2004). Further quality assurance specific to NWQL is available online (*http://bqs.usgs.gov/labEvaluation.php*, accessed August 2013). Further quality assurance specific to Minnesota Department of Health Environmental Laboratory is available online (*http://www.health.state.mn.us/divs/phl/environmental/index.html*, accessed August 2013).

Model Development

Model Calibration

The model calibration for each of the lakes looked at the degree of fit between the simulated results and measured lake values. The two quantities utilized to evaluate the degree of fit were the absolute mean error (AME) and the root mean square error (RMSE). AME, computed by equation 1, is a measure on the average difference between the predicted (simulated) value and the measured value:

$$\text{AME} = \frac{1}{n}\sum_{i=1}^{n}\left|simulated\ value - measured\ value\right| \tag{1}$$

For example, an AME of 1.0 mg/L for the dissolved oxygen means that simulated model value is on average within 1.0 mg/L of the measured dissolved oxygen value. RMSE is a slightly different metric, in that it indicates the amount of deviation, or spread, a simulated model value is from the measured value. RMSE, as computed by equation 2, gives the deviation of the simulated value from the measured value approximately 67 percent of the time:

$$\text{RMSE} = \sqrt{\frac{1}{n}\sum_{i=1}^{n}(simulated\ value - measured\ value)^2} \tag{2}$$

The initial model calibration for each of the lakes only looked at the degree of fit between the simulated and measured outlet water temperature and the water surface elevation. By calibrating to outlet water temperature and water surface elevation first, the subsequent water-quality calibration was easier given effects such as wind stress, inflow water temperature, meteorological influences, and the amount of flow in and out of the lake had already been taken into account. The water-quality calibration followed which calibrated the model for dissolved oxygen, nutrients, water temperature (hypolimnion, epilimnion), and algae, using the AME and RMSE metrics.

Water Balance

The first step in the calibration process for all three lake models was the water balance. Before the temperature and water quality calibration could proceed, the uncertainty of differences between the simulated and measured water surface elevations was rectified. A water balance was considered complete when both the AME and RMSE quantities were below 0.01 meter for the simulated water-surface elevation.

Lake Carlos

The initial attempt to achieve a water balance for Lake Carlos included the two gaged tributaries, Lake Darling and Lake Le Homme Dieu (table 1), as the sole inflows for the calibration period of April 22, 2010 to November 9, 2010. However, the simulated water-surface elevation was below the measured water-surface elevation which suggests other sources of water to the lake including ungaged tributaries and groundwater. To account for the unaccounted inflow, a distributed tributary flow was added to all segments equally. This distributed tributary can either be positive or negative; large positive values were found to correlate with large precipitation events, while negative values usually existed during the driest portions of the calibration. Several iterations were completed until the AME and RMSE targets were reached (fig. 11).

Figure 11. Simulated and measured water surface elevation for Lake Carlos, April 22 to November 9, 2010.

Elk Lake

The initial attempt to achieve a water balance for Elk Lake included the four ungaged tributaries as the inflows for the calibration period of April 26, 2011 to November 8, 2011. As mentioned earlier in the boundary conditions, each of the four ungaged tributaries were calculated as a percentage of the outflow record fixed by the ratio the contributing watershed (individual ungaged tributary) to the overall watershed (Elk Lake). However, similar to Lake Carlos, the simulated water-surface elevation was below the measured water-surface elevation. This revealed the existence of other ungaged inflows, groundwater flow either into or out of the lake, or that the calculated tributary record was off. To account for the unaccounted inflow, a distributed tributary flow was added to all segments equally. Several iterations were completed until the AME and RMSE targets were reached (fig. 12).

Figure 12. Simulated and measured water surface elevation for Elk Lake, April 26 to November 8, 2011.

Trout Lake

The initial attempt to achieve a water balance for Trout Lake included the two ungaged tributaries as the inflows for the calibration period of April 28, 2010 to October 20, 2010. Similar to Elk Lake, both of the ungaged tributaries were calculated as a percentage of the outflow record fixed by the ratio the contributing watershed (individual ungaged tributary) to the overall watershed (Trout Lake). However, similar to Lake Carlos and Elk Lake, the simulated water-surface elevation was below the measured water-surface elevation. Following the same approach as Lake Carlos and Elk Lake, a distributed tributary flow was added to all segments equally. Several iterations were completed until the AME and RMSE targets were reached (fig. 13).

Figure 13. Simulated and measured water surface elevation for Trout Lake, April 28, 2010 to October 20, 2010.

Temperature

A critical calibration step is water temperature because of its influence on water density. Boundary conditions that affect water temperature include sediment temperature, initial lake water temperature, and temperature of inflows. Meteorological influences include air temperature, wind velocity, wind direction, and solar radiation. Since solar radiation was not directly available for any of the lake models, an internal calculation within the model was made based on the amount of cloud cover and the lake’s location (latitude, longitude). Wind effects can be further controlled by the wind sheltering coefficient, which takes into account the influence of boundary factors such as topography and tree cover on wind mixing. Several hydraulic parameters also have an influence on the water temperature. For example, the amount of re-radiated heat back to the water column from solar radiation that penetrates the entire water column (Cole and Wells, 2008). For all the three lake models, the CE-QUAL-W2 default value of 100 percent was utilized. Another set of critical parameters include the extinction coefficients, which specifies the water absorption of light and other ancillary extinction coefficients for organic matter, suspended sediment, and algae (table 3).

Lake Carlos

The epilimnion (as measured at 1.65 meters below the water surface) and hypolimnion (as measured at 40.65 meters below the water surface) at Kecks Point (fig. 14; table 4) were the initial calibration targets. A challenge for the temperature calibration was the tradeoff between the degree of fit, based on AME and RMSE quantities, for the epilimnion and the hypolimnion at Kecks Point. Without adjusting the initial lake water temperature and sediment temperature to unrealistically low values, or adjusting the default model parameters for the hydrodynamics, settling at close to 1.0°C for both the AME and RMSE in the hypolimnion seemed reasonable. The AME and RMSE quantities of 0.48°C and 0.67°C, respectively, for the epilimnion were comparatively lower and followed the variations reasonably well throughout the year. The correlation did deviate with warmer simulated epilimnion temperatures throughout most of the summer months, from late June through August. The primary cause of the deviation was the increased wind speed coefficient during this period, increased to 80 percent from 65-70 percent during the rest of the year. The wind speed coefficient controls the amount of the wind energy transferred to the lake, with lower coefficients caused by shifts in primary wind directions during the year and differences in terrain between the meteorological station and the lake itself. Slightly better AME and RMSE quantities did occur with a lower wind speed coefficient during the summer months; however, this had a dramatic effect on the dissolved oxygen correlation.

Table 4. Summary of AME and RMSE quantities for all three Sentinel lakes for the calibration runs.

Figure 14. Simulated and measured water temperature for the epilimnion (2-m) and hypolimnion (37-m) at Kecks Point (USGS station number 455843095212501) for Lake Carlos, April 22, 2010 to November 9, 2010.

A secondary calibration target was the outlet water temperature as measured at the Long Prairie River. However, given its location approximately 100 meters downstream from the lake, this was given a lower priority and is only shown in table 4.

Simulated water temperature in Lake Carlos was also compared to lake profile data at Kecks Point, available from either continuous thermistor profiles or point measurements by either MPCA or USGS personnel. A total of 15 dates are shown in figure 15. Low AME and RMSE values (at or below 1.2°C) provided confidence in the model's ability to predict water temperature. The model also approximated the location of the thermocline. The thermocline is the portion of the temperature profile with the steepest change in temperature, dividing the epilimnion and hypolimnion by definition. Earlier in the year, up until the end of June, the slope of the thermocline was shallower in the simulated temperatures compared to the measured temperature. However, as the year progressed, the difference between the measured and simulated temperature profile was lower, and the thermocline slope was closely approximated. The model does predict by about 10 days too early the lake overturn, as shown in the fully mixed, simulated profile on the final simulated date (November 9, 2010).

Figure 15. Simulated and measured water temperature at Kecks Point (USGS station number 455843095212501) in Lake Carlos for 15 dates in 2010, with AME and RMSE quantities.

Elk Lake

In Elk Lake, the principal calibration targets were two locations in the epilimnion (as measured at 2 and 7 meters below the water surface, respectively) and two locations in the hypolimnion (as measured at 20 and 28 meters below the water surface, respectively) at the deepest hole in the south basin (fig. 16; table 4). Three of the four depths matched reasonably well. The shallowest location (at 2 meters below water surface) had AME and RMSE quantities of 0.65°C and 0.80°C, respectively. The two hypolimnion locations also had low AME and RMSE quantities. At 20 meters below the surface, the AME and RMSE quantities were 0.69°C and 0.69°C, respectively. At 28 meters below the surface, the AME and RMSE quantities were 0.54°C and 0.74°C, respectively. The other epilimnion location, at 7 meters below the water surface, the AME and RMSE quantities were 0.78°C and 1.08°C, respectively. The cause of the slightly higher AME and RMSE for this final location, or lower correlation, was likely due to the deepening of the thermocline through this location over the course of the year. Unlike Lake Carlos, there does not seem to any major offsets that occur during one period of the year over another. The same wind sheltering coefficient of 67% was applied during most of the year (after June 2nd). Before this date, the wind sheltering coefficient was set to 50%; this alteration was due to the usage of wind measurements at the lake after this date as opposed to the more distant Park Rapids meteorological station before this date.

Figure 16. Simulated and measured water temperature for the epilimnion (2-m and 7-m) and hypolimnion (20-m and 28-m) at south basin hole (USGS station number 471116095125301) in Elk Lake, April 26, 2011 to November 8, 2011.

A secondary calibration target was the outlet water temperature as measured at the Elk Lake outlet (USGS station number 05199950). However, for the same reasons as the outlet location for Lake Carlos, this was given a lower priority and is only shown in table 4.

Simulated water temperature in Elk Lake was also compared to lake profile data at the south basin hole (USGS station number 471116095125301), available from either continuous thermistor profiles or point measurements by either MPCA or USGS personnel. A total of 15 dates are shown in figure 17. As mentioned in the Lake Carlos section, a high correlation low AME and RMSE quantities give further confidence in the model's ability to predict water temperature. For Elk Lake, the model consistently attained AME and RMSE values at or below 1.0°C, often even below 0.5°C. The simulated thermocline also matched very well the location and slope, as compared to the measured thermocline. As in Lake Carlos, the model did seem to predict lake thermal overturn in Elk Lake early by about 7-10 days.

Figure 17. Simulated and measured water temperature at south basin hole (USGS station number 471116095125301) in Elk Lake for 15 dates in 2011, with AME and RMSE quantities.

Trout Lake

In Trout Lake, the principal calibration targets were the epilimnion (as measured at 0.5 meters below the water surface) and hypolimnion (as measured at 18.5 meters below the water surface) at the north basin hole (USGS station number 475214090100401) (fig. 18; table 4). The epilimnion had low AME and RMSE quantities of 0.54°C and 0.61°C, respectively. The hypolimnion location had even lower AME and RMSE quantities of 0.23°C and 0.23°C, respectively. The epilimnion result was somewhat surprising given the potential volatility of such a shallow measurement location in the epilimnion of 0.5 meters, such as fluctuations from air temperature shifts, wind effects, and solar radiation. Simulated temperatures were lower than the measured temperatures in the epilimnion after September 1st; however, the difference between the measured and simulated values did not go beyond 1.0°C. The only shift in the wind sheltering coefficient was from 100% to 60% after September 15th.

Figure 18. Simulated and measured water temperature for the epilimnion (0.5 meters) and hypolimnion (18.5 meters) at north basin hole (USGS station number 475214090100401) in Trout Lake, April 28, 2010 to October 20, 2010.

A secondary calibration target was the outlet water temperature as measured at the Trout Lake outlet (USGS station number 04011150). However, for the same reasons as the outlet location for Lake Carlos and Elk Lake, this was given a lower priority and is only shown in table 4.

Simulated water temperature in Trout Lake was also compared to lake profile data at the north basin hole (USGS station number 475214090100401), available from either continuous thermistor profiles or point measurements by either MPCA or USGS personnel. A total of 14 dates are shown in figure 19. For Trout Lake, the model consistently attained AME and RMSE values at or below 0.9°C, often even below 0.6°C. The simulated thermocline was generally a little deeper as compared to the measured thermocline, but did generally match the slope. The final measurement date of October 20th was a little too early for lake overturn, so it was difficult to evaluate whether or not the same issue of early modeled lake overturn existed for Trout Lake as the other two lakes.

Figure 19. Simulated and measured water temperature at north basin hole (USGS station number 475214090100401) in Trout Lake for 14 dates in 2010, with AME and RMSE quantities.

Dissolved Oxygen

Coldwater fish species and other aquatic organisms cannot survive without adequate dissolved oxygen. Accurate dissolved oxygen modeling is especially critical in determining the size of summer habitat refugia for coldwater fish species, because their thermal requirements confines them below the epilimnion where they are vulnerable to mass dieoffs due to a lack of dissolved oxygen (DO). For example, Jacobson and others (2008) evaluated the lethal oxythermal niche boundary for ciscos in several Minnesota lakes. They found that lethal temperatures were progressively less for lower lethal DO concentrations. Since these CE-QUAL-W2 models will be used to guide management decisions (e.g., climatic effects on dissolved oxygen profiles), dissolved oxygen calibrations were important.

Within CE-QUAL-W2, there are many sources and sinks for dissolved oxygen, which makes dissolved oxygen likely the most complicated constituent to model. For sources, these include inflows (all sources), atmospheric exchange across the lake surface, and algal photosynthesis (Cole and Wells, 2008). For sinks, these include the decay in both the water column and lake sediments of dissolved organic matter (labile and refractory), particulate organic matter (labile and refractory), and sediment decay itself. Other modeled sinks include algal respiration, ammonia and nitrite nitrification, and exchange back to the atmosphere and into sediments. The values used for these parameters are covered in table 4 (Cole and Wells, 2008). With such complex interactions, especially when simultaneously trying to dynamically model algal communities, several hundred iterations were required for each of the final lake CE-QUAL-W2 models.

Lake Carlos

For the dissolved oxygen calibration, the principal calibration targets were the lake profile data at Kecks Point, available from biweekly point measurements by either MPCA or USGS personnel. Generally, measurements were recorded for each meter below water surface, although some gaps up to five meters did exist specifically in the hypolimnion where changes were less drastic. A total of 11 dates are shown in figure 20. Overall, the simulated dissolved oxygen concentrations compared well to the measured concentrations for Kecks Point. Generally, where the greatest change in dissolved oxygen occurred, the simulated concentrations matched both the depth and slope of the measured concentrations. For example, the negative dissolved oxygen gradient between five to 10 meters on June 24, 2010, and July 20, 2010 both matched reasonably well, and likely had higher AME and RMSE values (>1.0 mg/L) due to the mismatch in the depleted DO concentrations in simulated shallow epilimnion and the enriched dissolved oxygen concentrations in the simulated hypolimnion. The model simulation overestimated the observed DO below 25 m of depth. DO depletion appeared to occur much faster than modeled. However, as the year progressed, the variation between the simulated and measured DO concentrations were less variable both in the epilimnion, hypolimnion, and the transition between the high and low DO zones. For example, the model predicted the negative hetrograde oxygen profile in August. AME quantities were consistently below 1.0 mg/L during this period, with slightly higher RMSE quantities. The only date that was considerably off was the final observation on November 9, 2010, where the dissolved oxygen was fully mixed. This is related to the earlier thermal mixing of the lake, and its effect on DO.

Figure 20. Simulated and measured dissolved oxygen concentrations at Kecks Point (USGS station number 455843095212501) in Lake Carlos for 11 dates in 2010, with AME and RMSE quantities.

A complex interaction between different processes has a strong effect on the dissolved oxygen concentrations in a lake. The decay rate of the different organic matter pools, as shown in table 4, were reasonably high compared to Trout Lake and on par with Elk Lake. Decay rates have the strongest impact on the DO concentrations in the hypolimnion. Sediment oxygen demand was also high for Lake Carlos, set at either 1 or 3 mg/L, which can greatly alter the DO profiles in the entire lake. The nitrate decay rate was set to 0.2 mg/L, which is on par with the other two lakes but generally higher than other CE-QUAL-W2 models (Green and others, 2003; Sullivan and Rounds, 2004; Galloway and Green, 2006; Galloway and others, 2008; Sullivan and others, 2011). Additional effects on dissolved oxygen had to do with the transitions between different algal communities, which will be covered in the Algae section. Briefly, simplification of the algal groups into three simple communities (diatoms, green, and blue-green algae) can diminish the ability to realistically capture real algal communities, but with a lack of data on these different communities or the real parameters required (table 4) this can hamper the DO modeling. For example, the underprediction of dissolved oxygen earlier in the year (May-June) could be due to not adequately capturing all of the algal growth during this period.

Elk Lake

For the dissolved oxygen calibration, the principal calibration targets were the lake profile data at the south basin hole, available from biweekly point measurements by either MPCA or USGS personnel. Similar to Lake Carlos, measurements were recorded for each meter below water surface, although some gaps up to five meters did exist specifically in the hypolimnion where changes were less drastic. A total of 15 dates are shown in figure 21. Overall, simulated dissolved oxygen concentrations compared very well to the measured concentrations for this location. Generally, where the greatest change in dissolved oxygen occurred, simulated concentrations matched both the depth and slope of the measured concentrations with the exception of the later season dates of October 19, 2011 and November 8, 2011. Otherwise, AME and RMSE quantities were consistently below 1.0 mg/L during the entire model simulation. The largest deviation between the simulated and measured DO concentrations occurred in the epilimnion during the peak of the summer algal blooms. This is likely due to inadequately capturing either the size of the algal communities or the correct composition of the algal communities, which would have an effect on the dissolved oxygen as a byproduct of photosynthesis. However, the model does very well in capturing the extremely low to zero dissolved oxygen concentrations in the hypolimnion.

Figure 21. Simulated and measured dissolved oxygen concentrations at south basin hole (USGS station number 471116095125301) in Elk Lake for 15 dates in 2011, with AME and RMSE quantities.

An additional calibration did exist for Elk Lake due to the 2011 sonde deployment, which included DO measurements. The sonde deployments were at the same location as the point measurements. Three of the four depths are shown in figure 22 and in table 4. Reinforcing the interpretations for the different DO profiles in figure 21, the underprediction of simulated epilimnion dissolved oxygen can easily be seen at two meters below the water surface. At the middle depth (seven meters below the water surface), the simulated DO was closer to the measured DO concentrations. However, this was not necessarily captured by the AME and RMSE quantities (0.89 and 1.33 mg/L, respectively) due to the mistiming of the higher DO concentrations after mid-September. Finally, the simulated hypolimnion DO concentrations (20 meters below the water surface) show consistently low or near zero concentrations as compared to the measured DO.

Figure 22. Continuous simulated and measured dissolved oxygen concentrations at south basin hole (USGS station number 471116095125301) in Elk Lake for three different depths (2, 7 and 20 meters below the water surface), with AME and RMSE quantities, April 26, 2011 to November 8, 2011.

As mentioned in the Lake Carlos section, different processes had a strong effect on the dissolved oxygen concentrations in a lake. As in Lake Carlos, the decay rate of the different organic matter pools were reasonably high (table 4). Sediment oxygen demand was also high for Elk Lake, set to 2 mg/L. The nitrate decay rate was set to 0.4 mg/L. The combination of these three effects likely had the biggest impact on the extremely low dissolved oxygen concentrations in the lake's hypolimnion.

Trout Lake

For the dissolved oxygen calibration, the principal calibration targets were the lake profile data at north basin hole, available from biweekly point measurements by either MPCA or USGS personnel. Similar to Lake Carlos and Elk Lake, measurements were recorded for each meter below water surface, although some gaps up to five meters did exist specifically in the hypolimnion where changes were less drastic. A total of 15 dates are shown in figure 23. Out of the three lakes, Trout Lake performed the poorest for dissolved oxygen but still preserved most of the overall DO trends. The model did very well in terms of simulating increased DO that generally occurs between five to 10 meters for this lake. However, where the simulated results deviate is in terms of the magnitude of this trend or the depth to the depletion of dissolved oxygen at depth later in the year (October 11, 2010; October 20, 2010). AME and RMSE quantities were still consistently low, below 1.0 mg/L during the most of the model simulation.

Figure 23. Simulated and measured dissolved oxygen concentrations at north basin (USGS station number 475214090100401) in Trout Lake for 15 dates in 2010, with AME and RMSE quantities.

As mentioned in both the Lake Carlos and Elk Lake sections, different processes had a strong effect on the dissolved oxygen concentrations in a lake. Unlike Lake Carlos and Elk Lake, the decay rate of the different organic matter pools were overall lower (table 4). This was supported by overall much deeper maximum secchi depths in Trout Lake. Sediment oxygen demand was also much lower for Trout Lake, set to 0.33 mg/L. The nitrate decay rate was set to 0.1 mg/L. The combination of these three effects likely had the biggest impact on the steady, decreasing trend in dissolved oxygen concentrations in the lake’s hypolimnion, which does not reach <1 mg/L until the lower five meters of the lake.

Algae

For all three sentinel lakes, the paradigm of three general groups was pursued rather than a more diverse species-specific modeling regime. This was partially due to a lack of data as well as the uncertainty in parameterization for the different groups. The three algal groups included were diatoms, green algae, and blue-green algae. Rather than including zooplankton as separate group(s), the dynamics of zooplankton grazing were captured within algal specific constants such as the algal growth rate and the algal mortality rate (table 4). Algal growth temperature coefficients were consistent across all three lakes, in addition to the algal growth rates and the light saturation intensity at the maximum photosynthetic rate. The main guidance for the algal groups was provided by other CE-QUAL-W2 efforts, specifically the Lake Waco model (Flowers and others, 2001).

Lake Carlos

The simulated distribution of three primary algal groups for Lake Carlos is shown in figure 24. Three different locations are shown in the figure, including the simulated results (1 meter below the water surface) for the segment adjacent to the Le Homme Dieu inlet, Kecks Point, and the segment adjacent to the Long Prairie River. Few differences existed between the different locations in the lake. However, the timing of the three algal groups did vary across all three locations. Diatoms were the first group to peak, starting out in early May, peaking in mid-May to around 0.8 mg/L, and then the diatoms approached 0 mg/L in the surface layer by early July. Towards the end of June, as diatoms exhibit senescence, green and blue-green algae replaced diatoms as the primary algal groups in the lake and remained fairly steady until early October. Green algae were more abundant throughout this entire period, peaking at around 0.9 mg/L by early October in the segment adjacent to the Le Homme Dieu outlet. The overall concentrations were only slightly buffered for both green and blue-green algae in the other two simulated sections shown. Starting in early October, the blue-green algae began to recede and continued this trend towards 0 mg/L through the end of the simulation in early November.

Figure 24. Simulated algal group distributions (diatoms, green, and blue-green algae) for three different segments in Lake Carlos, April 22, 2010 to November 9, 2010.

Although there was not direct supporting data for algal group composition, an ancillary data set that helped interpret at least if the overall magnitude was in the right range was the chlorophyll *a* concentration data. Shown for the same locations as figure 24, figure 25 details the simulated results of the chlorophyll *a* concentrations in micrograms per liter. Measured data was primarily collected in the surface layer at Kecks Point, which shows the grab samples measurements made by either MPCA or USGS personnel. There was also a single measurement made for the other two locations. Overall, the simulated results were a fairly good approximation of the measured results, with AME and RMSE quantities of 2.7 and 2.9 μg/L, respectively, in the Kecks Point segment (fig. 25; table 4).

Figure 25. Simulated and measured chlorophyll *a* concentrations (in μg/L) for three different segments in Lake Carlos, April 22, 2010 to November 9, 2010.

The simulated concentrations of both the algal groups and chlorophyll *a* were highly dependent on the parameterization of the algal groups. Given the high number of parameters related to the algal groups and their overall impact on the dissolved oxygen, these parameters can be extremely difficult to quantify. Many of the parameters were highly sensitive, such as the algal mortality, algal settling rate, temperature coefficients on maximum growth, and the algal half-saturation constants for nitrogen and phosphorus-limited growth; however, several of the parameters were fixed for each group across all three lakes. The maximum algal respiration rate, algal excretion rate, algal mortality, and the algal half-saturation for both nitrogen and phosphorus were varied to optimize the fit between the chlorophyll *a* data and the dissolved oxygen profiles. For Lake Carlos, the settling rate was highest between the three lakes which limited the algal growth. Another group of parameters which limited growth were the constants chosen for the nitrogen and phosphorus-limited growth (Cole and Wells, 2008), set slightly higher overall compared to the other two lakes. The algal growth was also strongly related to the availability of nutrients, which was dependent on the initial lake concentrations and the ongoing replenishment of nutrients from the various inflow sources. The chlorophyll *a* concentrations were influenced by the same factors as the algal group composition, but also the chosen ratio between algal biomass and chlorophyll *a*. This ratio was 0.18 for all three groups in Lake Carlos, in terms of milligrams of algae per micrograms of chlorophyll *a*.

Elk Lake

The simulated distribution of three primary algal groups for Elk Lake is shown in figure 26. The simulated results at two different depths for the same location, the south basin hole, are shown: 2 meters below water surface and 20 meters below water surface. Similar to the algal group dynamics for Lake Carlos, the timing of the three algal groups did vary considerably. Diatoms were the first group to peak, starting out in early May, peaking in mid-May to around 3 mg/L, and then the diatoms approached 0 mg/L in the surface layer by mid-June. The spike in diatoms was more distinct for Elk Lake compared to Lake Carlos. As diatoms receded in late May, the diatoms were replaced by green algae and to a minor degree blue-green algae. Green algae peaked in abundance to 2.5 mg/L by mid-June, with a smaller secondary peak in mid-October. In between these two peaks, the green algae abundance receded to a low of 0.6 mg/L in mid-September. Blue-green algae increased at a slower rate, compared to green algae, and peaked in abundance by late September, but did not exceed 1.5 mg/L. In addition to the surface layer at two meters, the simulated results for 20 meters was also shown to illustrate the model's prediction of fairly high algal concentrations at depth for both green and blue-green algae. While not necessarily realistic, it is important to note the potential drawback of the parameterization scheme of the CE-QUAL-W2 model that can lead to unrealistically high algal concentrations at depth.

Figure 26. Simulated algal group distributions (diatoms, green, and blue-green algae) for two different depths at south basin hole (USGS station number 471116095125301) in Elk Lake, April 26, 2011 to November 8, 2011.

Similar to Lake Carlos, algal group composition was lacking and instead the chlorophyll *a* concentration data was utilized to interpret overall magnitudes. Shown for the same depths as figure 26, figure 27 details the simulated results of the chlorophyll *a* concentrations in micrograms per liter. Measured data was collected only in the surface layer for the south basin hole (USGS station number 471116095125301). Overall, the simulated results were a fairly good approximation of the measured results, with AME and RMSE quantities of 2.7 and 3.4 μg/L, respectively, without any major discrepancies between the simulated and measured results (fig. 27; table 4).

Figure 27. Simulated and measured chlorophyll *a* concentrations (in μg/L) for two different depths at south basin hole (USGS station number 471116095125301) in Elk Lake, April 26, 2011 to November 8, 2011.

As mentioned in the Lake Carlos section, the simulated concentrations were highly sensitive to parameters such as the algal mortality, algal settling rate, temperature coefficients on maximum growth, and the algal half-saturation constants for nitrogen and phosphorus-limited growth. For Elk Lake, the settling rate was only slightly lower than Lake Carlos. Considerable optimization for Elk Lake was taken with the algal half-saturation constants for the nitrogen and phosphorus-limited growth. The highest limits were set for diatoms, with much lower constants set for green and blue-green algae to maximize the known algal blooms for these two groups. As in Lake Carlos, the algal growth was also strongly related to the availability of nutrients, particularly sensitive to the much higher ammonia concentration (table 3). The chlorophyll *a* concentrations were highly influenced by the much higher ratio of 0.28 for all three groups in Elk Lake, in terms of milligrams of algae per micrograms of chlorophyll *a*.

Trout Lake

The simulated distribution of three primary algal groups for Trout Lake is shown in figure 28. The simulated results at two different depths for the same location, the deepest hole in the north basin, are shown: 1 meter below water surface and 18 meters below water surface. Similar to the algal group dynamics for Lake Carlos and Elk Lake, the timing of the three algal groups did vary considerably. However, the algal bloom dynamics were more subtle in comparison to the other two lakes. Generally, diatoms were stable at around 1 mg/L until mid-July when green algae increased. The green algae also had a stable concentration at 1 mg/L. Blue-green algae had one spike in early June, close to 1 mg/L, but this blue-green algae bloom was short-lived. At depth, all three groups were quite low.

Figure 28. Simulated algal group distributions (diatoms, green, and blue-green algae) for two different depths at north basin hole (USGS station number 475214090100401) in Trout Lake, April 28, 2010 to October 20, 2010.

Similar to both Lake Carlos and Elk Lake, there was not supporting data for algal group composition and instead the chlorophyll *a* concentration data was utilized to interpret overall magnitudes. Shown for the same depths as figure 28, figure 29 details the simulated results of the chlorophyll *a* concentrations in micrograms per liter. Measured data was collected for both the surface layer (1 meter below water surface) and at depth (18 meters below water surface) for the south basin hole (USGS station number 471116095125301). Overall, simulated results were better at 18 meters than at 1 meter when compared to the measured results, with AME and RMSE quantities of 5.0 and 5.3 μg/L, respectively, at 1 meter below water surface and 2.1 and 2.8 μg/L, respectively, at 18 meters below water surface (fig. 29; table 4).

Figure 29. Simulated and measured chlorophyll *a* concentrations (in μg/L for two different depths at north basin hole (USGS station number 475214090100401) in Trout Lake, April 28, 2010 to October 20, 2010.

For Trout Lake, the settling rate was the lowest for all three algal groups in comparison to the other two lakes. Considerable optimization was also taken for Trout Lake with the algal half-saturation constants for the nitrogen and phosphorus-limited growth given the low concentrations of both nitrogen and phosphorus in Trout Lake. Contrary to the other two lakes, the algal half-saturation constant for nitrogen was set to zero for the blue-green algae, which simulates nitrogen fixation in the CE-QUAL-W2 model. With overall much lower nutrient loads, as shown in the initial nutrient concentrations (table 3) but a sustained algal community, this assumption seemed reasonable for Trout Lake. The chlorophyll *a* concentrations were also highly influenced by the lower ratio of 0.12 for all three groups in Trout Lake, in terms of milligrams of algae per micrograms of chlorophyll *a*.

Nutrients

Nutrients for all three sentinel lakes are controlled by many processes. One of the most important controls is the amount of nutrients (loads) contributed by the different inflows, which will be different for each of the three lakes. These loads would be expected to vary across different ecozones, the soil fertility in the contributing watershed, and the variable nutrient inputs depending on land-use (i.e., row-crop agriculture versus deciduous forest). After the water is in the lake, inlake processing of the nutrients is the major driver of nutrient concentrations. The focus for evaluating the model will be given to three different constituents of nitrogen and two constituents of phosphorus: nitrate-nitrite, ammonia, total nitrogen, orthophosphorus, and total phosphorus.

Sources and sinks will largely be the same for all three lakes, although distinctions can be made in terms of the major inflows. Lake Carlos was largely controlled by the inflows from Lake Darling and Le Homme Dieu Lake, whereas Trout Lake and Elk Lake seem to have considerably more groundwater and/or spring sources relative to surface inflows. For nitrate-nitrite, sources include all inflows and ammonia nitrification; sinks include denitrification (both in the water column and sediments), algal uptake, and lake outflow (Cole and Wells, 2008). For ammonia, which lumps both ammonia (NH_3) and ammonium (NH_4^+), sources include all inflows, decay of all the organic matter pools, sediment release under anaerobic conditions, and algal respiration; sinks would include nitrification, algal uptake, and lake outflow (Cole and Wells, 2008). For orthophosphorus, sources include all inflows, decay of all the organic matter pools, sediment release under anaerobic conditions, and algal respiration; sinks would include particles settling with adsorbed phosphorus, algal uptake, and lake outflow (Cole and Wells, 2008). Total nitrogen, for purposes of the simulated and measured results, was classified as the concentration of nitrogen present in ammonia, nitrate-nitrite, and organically-bound nitrogen (both in living algal biomass and all of the organic matter pools). Total phosphorus, for purposes of the simulated and measured results, was classified as the concentration of phosphorus present in orthophosphorus and bound up in organic matter (both in living algal biomass and all of the organic matter pools).

The primary tools for evaluating the degree of fit for the nutrients were the AME and RMSE (table 4). It is worth noting that these quantities could often be largely offset by only one or two measured samples because of the low number of total samples.

Lake Carlos

Ammonia and nitrate-nitrite distributions in Lake Carlos were largely affected by the inflows and the lake hydrodynamics. Three different locations are shown in figure 30 for ammonia (shown as ammonia as N in mg/L), including the simulated results and measured data (1 meter below the water surface) for the segment adjacent to the Le Homme Dieu inlet, Kecks Point, and the segment adjacent to the Long Prairie River. An additional Kecks Point simulated results and measured data segment is shown on the right side at 20 meters below water surface. Few differences existed for the epilimnion locations (left side) in the lake. For most of the year, ammonia concentrations, both in the simulation and measured data, were relatively stable in the epilimnion. Algal uptake was likely fairly rapid, with replenishment by organic matter decay and inflows. At depth in the hypolimnion, there was a momentary buildup which peaked in late June. Part of this can be explained by organic matter decay without algal uptake, but also by inflow placement earlier in the year because of thermal density gradients. Nitrate-nitrite (fig. 31) is shown for the same locations as ammonia. Even further depletion occurred for nitrate-nitrite across all three epilimnion locations, likely due to the same factors as rapid algal uptake. At depth in the hypolimnion, nitrate-nitrite buildup in the simulated results was delayed from the ammonia due to ammonia nitrification of the earlier influx in the late spring and early summer. Towards the end of the simulation, without a steady source of ammonia for nitrification, the nitrate-nitrite becomes increasingly depleted, likely due to nitrate decay. Ammonia AME and RMSE quantities, due to the low concentrations, were low overall and ranged from <0.01 to 0.02 mg/L (table 4). Nitrate-nitrite AME quantities ranged from <0.01 to 0.05 mg/L, the highest value in the hypolimnion; nitrate-nitrite RMSE quantities ranged from <0.01 to 0.06 mg/L (table 4).

Figure 30. Simulated and measured ammonia (as N) concentrations (in mg/L) for three different segments in Lake Carlos, April 22, 2010 to November 9, 2010.

Figure 31. Simulated and measured nitrate-nitrite (as N) concentrations (in mg/L) for three different segments at Kecks Point (USGS station number 455843095212501) in Lake Carlos, April 22, 2010 to November 9, 2010.

Orthophosphorus distributions in Lake Carlos were largely affected by the inflows and the lake hydrodynamics. For most of the year, orthophosphorus concentrations, both in the simulation results and measured data, were relatively stable in the epilimnion. Algal uptake is fairly rapid, with replenishment by organic matter decay and inflows. However, at the end of the model run, a steady increase occurred primarily due to increased loads from the Le Homme Dieu inlet. This trend was even more pronounced in the hypolimnion, which was partially the increased loads but also the lack of algal uptake in the hypolimnion. Orthophosphorus AME and RMSE quantities overall, due to the low concentrations, were low and all were <0.01 mg/L (table 4).

Figure 32. Simulated and measured orthophosphorus (as P) concentrations (in mg/L) for three different segments at Kecks Point (USGS station number 455843095212501) in Lake Carlos, April 22, 2010 to November 9, 2010.

Total nitrogen and total phosphorus simulated results are shown in figures 33 and 34, respectively. The epilimnion total nitrogen AME quantities were all 0.12 mg/L, with total nitrogen RMSE quantities varying from 0.12 to 0.14 mg/L (table 4). The hypolimnion AME and RMSE values were 0.04 and 0.05 mg/L, respectively (table 4). The measured data suggested a relatively stable amount of total nitrogen in the lake, while the simulated results show a slow and steady decrease over the course of the model run. This decrease was likely due to the overall decay of the simulated organic matter pools and the decrease in simulated total algal biomass. Total phosphorus was affected by the same trends, but was a much smaller pool (by three orders of magnitude), and was an overall smaller portion of algal biomass. Also, the hypolimnion total phosphorus was stable because of the offset between increasing orthophosphorus concentrations (fig. 32) and the decreasing amount of overall algal biomass (fig. 24). Total phosphorus AME quantities varied from 1 to 3 μg/L; total phosphorus RMSE quantities varied from 1 to 4 μg/L (table 4).

Figure 33. Simulated and measured total nitrogen concentrations (in mg/L) for three different segments at Kecks Point (USGS station number 455843095212501) in Lake Carlos, April 22, 2010 to November 9, 2010.

Figure 34. Simulated and measured total phosphorus concentrations (in μg/L) for three different segments at Kecks Point (USGS station number 455843095212501) in Lake Carlos, April 22, 2010 to November 9, 2010.

Elk Lake

Ammonia and nitrate-nitrite distributions in Elk Lake were also largely affected by the inflows and the lake hydrodynamics. The ammonia simulated results and measured data are shown for two different depths for the same location, south basin hole: 2 meters below water surface and 20 meters below water surface (fig. 35). For the epilimnion, the initially high lake ammonia concentration was quickly depleted by algal uptake, as noted by the large diatom bloom in May (fig. 26). After this initial bloom, incoming ammonia from inflows as well as ammonia from algal respiration was quickly recycled into more algal biomass. In the hypolimnion, a much slower depletion occurred due to ammonia nitrification into nitrate, but without algal uptake a fairly large ammonia pool remained. The simulated epilimnion nitrate-nitrite concentrations show a small peak in mid-May, likely due to either algal excretion and/or ammonia nitrification (fig. 36). In the hypolimnion, a substantial buildup of nitrate occurred, likely due to the combined effects of inflows and ammonia nitrification, while this was offset later in the model run by nitrate decay (denitrification). Ammonia AME quantities varied from 0.07 to 0.42 mg/L, the highest in the hypolimnion; ammonia RMSE quantities varied from 0.09 to 0.46 mg/L (fig. 35; table 4). Nitrate-nitrite AME quantities ranged from <0.01 to 0.10 mg/L, the highest value also in the hypolimnion; nitrate-nitrite RMSE quantities ranged from <0.01 to 0.18 mg/L (fig. 36; table 4).

Figure 35. Simulated and measured ammonia (as N) concentrations (in mg/L) for two different depths at south basin hole (USGS station number 471116095125301) in Elk Lake, April 26, 2011 to November 8, 2011.

Figure 36. Simulated and measured nitrate-nitrite (as N) concentrations (in mg/L) for two different depths at south basin hole (USGS station number 471116095125301) in Elk Lake, April 26, 2011 to November 8, 2011.

Orthophosphorus distributions in Elk Lake were largely affected by the inflows and the lake hydrodynamics. For most of the year, orthophosphorus concentrations, both in the simulation and measured data, were relatively stable in the epilimnion. As in Lake Carlos, algal uptake was likely fairly rapid, with replenishment by organic matter decay and inflows. Early in the model run, orthophosphorus depletion coincided with the diatom bloom. In the hypolimnion, orthophosphorus concentrations slowly increased without major algal uptake and the steady decay of the various organic matter pools. Epilimnion orthophosphorus AME and RMSE quantities overall, due to the low concentrations, were low and all were <0.01 mg/L; the hypolimnion AME and RMSE quantities were 0.10 mg/L, higher due to the mismatch between the slow buildup in the simulation results which was not reflected in the measured data (fig. 37; table 4).

Figure 37. Simulated and measured orthophosphorus (as P) concentrations (in mg/L) for two different depths at south basin hole (USGS station number 471116095125301) in Elk Lake, April 26, 2011 to November 8, 2011.

Total nitrogen and total phosphorus simulated results are shown in figures 38 and 39, respectively. The epilimnion total nitrogen AME quantities were 0.12 and 0.17 mg/L, with RMSE quantities of 0.17 and 0.18 mg/L (table 4). The hypolimnion AME and RMSE values were 0.45 and 0.48 mg/L, respectively (table 4). As in Lake Carlos, the measured data suggested a relatively stable amount of total nitrogen in the lake, while the simulated results show a slow and steady decrease over the course of the model run. As in Lake Carlos, this was likely due to the overall decay of the various organic matter pools and the decrease in total algal biomass. Total phosphorus was affected by the same trends as Lake Carlos, with a stable hypolimnion total phosphorus concentration because of the offset between increasing orthophosphorus concentrations (fig. 37) and the decreased amount of overall algal biomass (fig. 26). Total phosphorus AME quantities varied from 5 to 10 μg/L; total phosphorus RMSE quantities varied from 6 to 16 μg/L (fig. 39; table 4).

Figure 38. Simulated and measured total nitrogen concentrations (in mg/L) for two different depths at south basin hole (USGS station number 471116095125301) in Elk Lake, April 26, 2011 to November 8, 2011.

Figure 39. Simulated and measured total phosphorus concentrations (in μg/L) for two different depths at south basin hole (USGS station number 471116095125301) in Elk Lake, April 26, 2011 to November 8, 2011.

Trout Lake

As in Lake Carlos and Elk Lake, ammonia and nitrate-nitrite distributions in Trout Lake were largely affected by the inflows and the lake hydrodynamics. The ammonia simulated results and measured data are shown for two different depths for the same location, north basin hole: 1 meter below water surface and 18 meters below water surface (fig. 40). Of the three lakes, Trout Lake has the lowest overall amount of nutrients. For example, the epilimnion ammonia concentrations were only ~0.01 mg/L at maximum. Even in the hypolimnion, only a small peak up to 0.02 mg/L occurred for both the simulated results and measured data. For nitrate-nitrite, the values were close to zero, showing that nitrate was utilized almost as quickly as it was generated from ammonia nitrification or from inflows (fig. 41). Ammonia AME quantities were low and only varied from <0.01 to 0.02 mg/L; ammonia RMSE quantities varied from <0.01 to 0.03 mg/L (fig. 40; table 4). Nitrate-nitrite AME and RMSE quantities ranged from <0.01 to 0.04 mg/L (fig. 41; table 4).

Figure 40. Simulated and measured ammonia (as N) concentrations (in mg/L) for two different depths at north basin hole (USGS station number 475214090100401) in Trout Lake, April 28, 2010 to October 20, 2010.

Figure 41. Simulated and measured nitrate-nitrite (as N) concentrations (in mg/L) for two different depths at north basin hole (USGS station number 475214090100401) in Trout Lake, April 28, 2010 to October 20, 2010.

Orthophosphorus distributions in Trout Lake were largely affected by the inflows and the lake hydrodynamics. The same trends are seen in Trout Lake as Elk Lake, with fairly rapid algal uptake and replenishment by organic matter decay and/or inflows. Similar to Elk Lake, hypolimnion orthophosphorus concentrations increased in the simulated results but not so in the measured data. Orthophosphorus AME and RMSE quantities overall, due to the low concentrations, were low and all were <0.01 mg/L (fig. 42; table 4).

Figure 42. Simulated and measured orthophosphorus (as P) concentrations (in mg/L) for two different depths at north basin hole (USGS station number 475214090100401) in Trout Lake, April 28, 2010 to October 20, 2010.

Total nitrogen and total phosphorus simulated results are shown in figures 43 and 44, respectively. The epilimnion total nitrogen AME quantities were 0.05 and 0.09 mg/L, with RMSE quantities of 0.08 and 0.09 mg/L (fig. 43; table 4). The hypolimnion AME and RMSE values were 0.07 and 0.08 mg/L, respectively (fig. 43; table 4). Total phosphorus AME quantities varied from 3 to 5 μg/L; total phosphorus RMSE quantities varied from 4 to 6 μg/L (fig. 44; table 4).

Figure 43. Simulated and measured total nitrogen concentrations (in mg/L) for two different depths at north basin hole (USGS station number 475214090100401) in Trout Lake, April 28, 2010 to October 20, 2010.

Figure 44. Simulated and measured total phosphorus concentrations (in μg/L) for two different depths at north basin hole (USGS station number 475214090100401) in Trout Lake, April 28, 2010 to October 20, 2010.

Model validation

The model validation for each of the lakes looked at the degree of fit between the simulated results and measured lake values in the same method as the model calibration. AME and RMSE were utilized to evaluate the degree of fit between the simulated and measured results. Emphasis on the model validation was placed on the temperature and dissolved oxygen results, with lesser emphasis placed on the water quality results although some of the data is shown and discussed (table 5). For purposes of the model validation, only the initial conditions were altered (table 3). None of the approximately 130 parameters, as shown in table 4, were altered. One slight difference was made for the Elk Lake model, as the wind sheltering coefficient was kept at 50% for the entire year due to the usage of only Park Rapids meteorological data.

Table 5. Summary of AME and RMSE quantities for all three Sentinel lakes for the validation runs.

Lake Carlos

The validated model was run from March 16, 2011 to September 28, 2011. The ability for the simulated results to predict the measured data was robust. As in the model calibration, the principal validation targets for temperature were the epilimnion (as measured at 1.65 meters below the water surface) and hypolimnion (as measured at 40.65 meters below the water surface) at Kecks Point (fig. 45; table 5). The AME and RMSE quantities were similar for both the epilimnion and hypolimnion. As in the model calibration, the correlation does deviate more with warmer simulated epilimnion and hypolimnion temperatures, from late June through August. However, the overall trends in temperature were well represented by the simulated results.

Figure 45. Simulated and measured water temperature for the epilimnion (2-m) and hypolimnion (37-m) at Kecks Point (USGS station number 455843095212501) in Lake Carlos, March 16, 2011 to September 28, 2011.

Simulated water temperature was also compared to lake profile measurements at Kecks Point. Similar to the continuous results shown in figure 45, the model's ability to predict water temperature profiles was consistent. AME and RMSE values were generally at or below 1.2°Cand approximated the location and slope of the thermocline. On several dates, only four points were available from the continuous sonde data, which also biased the AME and RMSE quantities to higher values. In particular, August 18, 2011 had the highest AME and RMSE, despite the simulation results showing the overall trend of the temperature decrease in the measured data.

Figure 46. Simulated and measured water temperature at Kecks Point (USGS station number 455843095212501) in Lake Carlos for 11 dates in 2011, with AME and RMSE quantities.

Overall, the simulated dissolved oxygen concentrations compared better to the measured concentrations than the initial model calibration. All of the AME and RMSE quantities were less than 1 mg/L, with all of the major trends simulated including the small increase in dissolved oxygen at depth in the later summer months (July 21, 2011; August 4, 2011).

Figure 47. Simulated and measured dissolved oxygen concentrations at Kecks Point (USGS station number 455843095212501) in Lake Carlos for 8 dates in 2011, with AME and RMSE quantities.

For the chlorophyll *a* validation, three different locations are shown, including the simulated results (1 meter below the water surface) for the segment adjacent to the Le Homme Dieu inlet, Kecks Point, and the segment adjacent to the Long Prairie River (fig. 48). Similar to the model calibration year in 2010, measured data was primarily collected in the surface layer at Kecks Point with a few ancillary points in the other two locations. Overall, the simulated results were a fairly good approximation of the measured results, with AME and RMSE quantities of 4.1 and 4.8 μg/L, respectively, in the Kecks Point segment (table 5). For the model validation, the simulated results consistently overpredicted the amount of chlorophyll *a* which would in turn reflect on the algal composition of the lake.

Figure 48. Simulated and measured chlorophyll *a* concentrations (in μg/L) for three different segments in Lake Carlos, March 16, 2011 to September 28, 2011.

Finally, the total nitrogen and total phosphorus simulated results are shown in figures 49 and 50, respectively. The same monitoring locations are shown, with the additional Kecks Point simulated and measured results shown on the right side at 20 meters below water surface. For three of the four locations, the model validation results were actually better than the model calibration for the total nitrogen (fig. 49; table 5). The AME and RMSE quantities were as low as 0.05 and 0.07 mg/L, respectively, in the segment adjacent to the Le Homme Dieu inlet. The highest AME and Revalues of

0.10 and 0.12 mg/L, respectively, for total nitrogen were in the section adjacent to the Long Prairie River (fig. 49). Total phosphorus, on the other hand, was better in the initial model calibration over the model validation; however, the simulated results still compared well to the measured data (fig. 50; table 5). In general, the simulated results underpredicted the total phosphorus particularly in the segments adjacent to the Le Homme Dieu inlet and the Long Prairie River (fig. 50). The AME for total phosphorus across the four locations varied from 2 to 6 μg/L, and the RMSE for total phosphorus varied from 3 to 7 μg/L.

Figure 49. Simulated and measured total nitrogen concentrations (in mg/L) for three different segments in Lake Carlos, March 16, 2011 to September 28, 2011.

Figure 50. Simulated and measured total phosphorus concentrations (in μg/L) for three different segments in Lake Carlos, March 16, 2011 to September 28, 2011.

Elk Lake

The validated model was run from July 13, 2010 to November 9, 2010. Due to the timing of transducer installation, the abridged period was the longest period available for model validation outside of the model calibration year in 2011. However, this period still offered a time frame to evaluate the robustness of the model under different meteorological and hydrologic conditions.

As in the model calibration, the principal validation targets for temperature were two locations in the epilimnion (as measured at 2 and 8 meters below the water surface, respectively) and two locations in the hypolimnion (as measured at 19 and 28 meters below the water surface, respectively) at the south basin hole (fig. 51; table 5). All four depths matched reasonably well, with three of the four depths better than the model calibration in 2011. The shallowest location (at 2 meters below water surface) had AME and RMSE quantities of 0.65°C and 0.74°C, respectively, very similar to the model calibration.

The other epilimnion location, at 8 meters below the water surface, the AME and RMSE quantities were 0.60°C and 0.76°C, respectively, improved over the model calibration. At 20 meters below the surface, the AME and RMSE quantities of 0.98°C and 1.11°C, respectively, the highest of the four locations. At 28 meters below the surface, the AME and RMSE quantities were 0.32°C and 0.39°C, respectively. The slightly higher AME and RMSE quantities at 20 meters were caused by the offset in temperature which occurred at depth, due to the mistiming of lake mixing by the CE-QUAL-W2 model. However, this offset was not as dramatic as the 2011 model calibration.

Figure 51. Simulated and measured water temperature for the epilimnion (2-m and 8-m) and hypolimnion (19-m and 28-m) at south basin hole (USGS station number 471116095125301) in Elk Lake, July 13, 2010 to November 9, 2010.

Simulated water temperature in Elk Lake was also compared to lake profile data at the south basin hole (USGS station number 471116095125301). A total of 12 dates are shown in figure 52. The model consistently attained AME and RMSE values at or below 1.0°C. As in the model calibration, the simulated thermocline also matched very well the location and slope of the measured thermocline. The only miscue of the simulated results was the early stages of lake mixing being slightly mistimed (October 26, 2010).

Figure 52. Simulated and measured water temperature at south basin hole (USGS station number 471116095125301) in Elk Lake for 12 dates in 2010, with AME and RMSE quantities.

As in the model calibration, the principal calibration targets for dissolved oxygen were the lake profile data at the south basin hole. A total of 10 dates are shown in figure 53. Overall, the comparisons between simulated and measured dissolved oxygen concentrations were better for the model validation.

The AME for the 10 dates ranges from 0.19 to 0.87 mg/L, and the RMSE for total phosphorus varied from 0.50 to 1.62 mg/L.

Figure 53. Simulated and measured dissolved oxygen concentrations at south basin hole (USGS station number 471116095125301) in Elk Lake for 10 dates in 2010, with AME and RMSE quantities.

As in the model calibration, chlorophyll *a* concentration data was utilized to interpret overall magnitude or size of the algal communities. With data only available for the shallow layer at 2 meters below the water surface, the simulated chlorophyll *a* results consistently overpredicted the measured data (fig. 54; table 5). Finally, the total nitrogen and total phosphorus simulated results are shown in figures 55 and 56, respectively. The same monitoring locations are shown as chlorophyll *a*. For both total nitrogen and total phosphorus, the model performed better in the epilimnion than the hypolimnion. The epilimnion AME quantities for total nitrogen and total phosphorus were 0.13 mg/L and 6 μg/L, respectively, and the epilimnion RMSE quantities for total nitrogen and total phosphorus were 0.16 mg/L and 7 μg/L, respectively. In the deep location (20 meters below water surface), the model underpredicted the amount of both constituents. It stands to reason that the model needs further refinement for predicting total nitrogen and total phosphorus in the hypolimnion. One possible mechanism to explain the hypolimnion values could be the missing zooplankton dynamics. For example, a shift from daphnia to copepods could result in a larger export of nitrogen and phosphorus to the hypolimnion, as the fecal pellets expelled by the copepods would likely export more nitrogen and phosphorus to the hypolimnion. The hypolimnion AME quantities for total nitrogen and total phosphorus were 0.52 mg/L and 42 μg/L, respectively, and the hypolimnion RMSE quantities for total nitrogen and total phosphorus were 0.52 mg/L and 49 μg/L, respectively.

Figure 54. Simulated and measured chlorophyll *a* concentrations (in μg/L) for two different depths at south basin hole (USGS station number 471116095125301) in Elk Lake, July 13, 2010 to November 9, 2010.

Figure 55. Simulated and measured total nitrogen concentrations (in mg/L) for two different depths at south basin hole (USGS station number 471116095125301) in Elk Lake, July 13, 2010 to November 9, 2010.

Figure 56. Simulated and measured total phosphorus concentrations (in μg/L) for two different depths at south basin hole (USGS station number 471116095125301) in Elk Lake, July 13, 2010 to November 9, 2010.

Trout Lake

The validated model was run in two separate periods from May 19, 2011 to July 20, 2011 and September 8, 2011 to November 9, 2011. A loss of the outlet pressure transducer record during the gap limited the model validation to this shortened period. As in the abridged Elk Lake model validation, the period still offered a time frame to evaluate the robustness of the model under different meteorological and hydrologic conditions.

Simulated water temperature in Trout Lake was only available for the model validation as lake profile data at the north basin hole (USGS station number 475214090100401). A total of six dates are shown in figure 57. Unlike the Lake Carlos and Elk Lake model validations, the Trout Lake model validation did not perform as well when compared to the measured profile data. A fairly large discrepancy occurred for June 1, 2011, when the simulated results predicted a much shallower thermocline. This discrepancy seems remedied two weeks later, so it is likely the simulation is slightly out-of-sync with the observed values. Overall, the AME values ranged from 0.12°C to 2.30°C, and the RMSE values ranged from 0.15°C to 2.76°C.

Figure 57. Simulated and measured water temperature at north basin hole (USGS station number 475214090100401) in Trout Lake for six dates in 2011, with AME and RMSE quantities.

As in the model calibration, the principal calibration targets for dissolved oxygen were the lake profile data at the north basin hole. A total of 9 dates are shown in figure 58. Overall, the comparisons between simulated and measured dissolved oxygen concentrations were better for the model validation. The linear decreasing trend in hypolimnion dissolved oxygen concentrations was fairly well approximated by the model (September 8, 2011; October 12, 2011); however, the model did overpredict bottom hyoplimnetic DO concentrations on a few dates (June 30, 2011; July 13, 2011). The AME quantities for the 9 dates varied from 0.11 to 0.92 mg/L, and the RMSE quantities varied from 0.15 to 2.12 mg/L.

Figure 58. Simulated and measured dissolved oxygen concentrations at north basin hole (USGS station number 475214090100401) in Trout Lake for nine dates in 2011, with AME and RMSE quantities.

Chlorophyll *a* concentration data was not available for the model validation, so only the total nitrogen and total phosphorus comparisons are shown. The total nitrogen and total phosphorus simulated results are shown in figures 59 and 60, respectively. The same monitoring locations are shown as the Trout Lake model calibration (fig. 43; figure 44). For total nitrogen, the epilimnion simulated results compared favorably with the exception of one high measured data point; the AMSE and RMSE quantities for total nitrogen were 0.11 and 0.16 mg/L, respectively (fig. 59; table 5). Only one measured total nitrogen sample was available for the hypolimnion, which the simulated results overpredicted. For total phosphorus, the epilimnion simulated results consistently overpredicted (fig. 60; table 5) although this was not out of line when considering the model calibration had the same issue (fig. 44; table 4). The epilimnion AME and RMSE quantities for total phosphorus were both 5 μg/L.

The hypolimnion simulated results compared better than the epilimnion; the hypolimnion AME and RMSE quantities for total phosphorus were 6 and 7 μg/L, respectively.

Figure 59. Simulated and measured total nitrogen concentrations (in mg/L) for two different depths at north basin hole (USGS station number 475214090100401) in Trout Lake, May 19, 2011 to July 20, 2011 and September 8, 2011 to November 9, 2011.

Figure 60. Simulated and measured total phosphorus concentrations (in μg/L) for two different depths at north basin hole (USGS station number 475214090100401) in Trout Lake, May 19, 2011 to July 20, 2011 and September 8, 2011 to November 9, 2011.

Model Limitations

A full understanding of model limitations is necessary to better evaluate the effectiveness of any water-quality model. Given that the CE-QUAL-W2 model is laterally averaged, processes that could impose variations perpendicular to the primary flow axis of the lake will not be represented. Related to this issue is potentially imposing a false flow direction in lakes without a strong dominant current. CE-QUAL-W2 vertically averages within a layer, although the discretization of all three lake models into 1-meter segments is likely sufficient. Vertical momentum is currently not included, so in cases where significant vertical acceleration is a possibility the model could give inaccurate results (Cole and Wells, 2008). Water quality limitations include the simplification of a complex aquatic ecosystem into a series of kinetic reactions expressed in source and sink terms (Cole and Wells, 2008). Also, recognition must be made of the inherent shortcomings of a fixed number of water quality samples to represent a dynamic system. Specific water-quality modules with shortcomings for CE-QUAL-W2 include the sediment oxygen demand (SOD), which is user-defined and is decoupled from the water column. Instead, SOD variation only occurs with temperature. A complete sediment diagenesis model, with a fully integrated sediment kinetics and the sediment-water interface, does not currently exist within CE-QUAL-W2 v. 3.6.Other existing CE-QUAL-W2 water-quality modules not included as part of these particular lake models included the macrophyte and zooplankton reservoirs, known to be important but were not include because of sparse data. Instead, the effect of macrophytes and zooplankton were accounted for within the parameterization scheme of SOD and the algal dynamics as an attempt to address this deficiency.

Not only do data limitations exist, but structural selections such as segment geometry, the number of vertical layers, and the numerical transport scheme chosen will impose a potential bias to the model's outcome. Boundary conditions are not fixed in nature; however, boundary conditions are limited by the availability of data and it was required to extrapolate the data to fit the needs of the CE-QUAL-W2 model. For example, water-quality data was either linearly interpolated between sampling dates, or the sampling data was used as input into a load-estimation software to generate daily time steps for the model. Gaps within the continuous record also caused shorter calibration and/or validation periods than desired. As an example, Trout Lake outflow was limited for the 2011 validation due to the loss of transducer data during the summer months, thereby splitting the validation period into two sections rather than one continuous validation.

Sensitivity Analysis

A sensitivity analysis was undertaken to understand the effects on the model results of controlled departures in the calibrated model parameters and input loads. Due to the large number of calibrated parameters in each of the three lake models (table 3), only six different constituents were altered in the sensitivity analysis. For each of the following parameters or input loads, the calibrated lake model value was increased by 20 percent and decreased by 20 percent: wind sheltering coefficient, inflow phosphorus, inflow nitrogen, inflow organic matter, sediment oxygen demand, and the extinction coefficient. In the case of the extinction coefficient, all of the component extinction coefficients were adjusted including the light extinction coefficients for pure water, inorganic suspended solids, organic suspended solids, and the three different algal groups (diatoms, green, blue-green). During model development and calibration phase, a more robust but less controlled sensitivity analysis was undertaken in each of the three lake models in order to attain a final calibrated model, meaning that far more than the six different constituents underwent sensitivity analysis. However, the six constituents chosen for this analysis were found to be some of the most sensitive parameters or input loads, as well as previous CE-QUAL-W2 lake models (Galloway and others, 2008; Green and others, 2003; Sullivan and Rounds, 2005; Galloway and Green, 2006). Vertical profiles (at 1-meter intervals) of water temperature and concentrations of dissolved oxygen, ammonia, nitrate-nitrite, orthophosphate, and chlorophyll *a* were compared at Kecks Point for Lake Carlos, the south basin hole for Elk Lake, and the deepest hole in the north basin for Trout Lake. Results are presented in the percent change from the calibrated value (table 6).

Table 6. Summary of sensitivity analysis for all three Sentinel lakes, in percent change from calibration run.

Water temperature in both the Lake Carlos and Elk Lake model was most sensitive to alterations in the wind sheltering coefficient, and only a small amount in the Trout Lake model. As the wind sheltering coefficient adjusts the resultant wind speed, this will affect the amount of mixing that occurs in the vertical dimension and thereby the depth of the thermocline over time. Decreases in the wind sheltering coefficient will result in lower wind speeds, leading to a shallower thermocline and higher surface water temperatures. Increases in the wind sheltering coefficient will result in higher wind speeds, leading to a deeper thermocline and lower surface water temperatures. In comparing the three lakes for the effect of the wind sheltering coefficient on water temperature, the larger the lake, the more sensitive the water temperature is to alterations in the wind sheltering coefficient. However, care must be taken to generalize this effect, as this trend only includes the three selected lakes and this is more likely an illustration of the importance of collecting wind speed and direction close to the lake, especially for larger lakes. The only other parameter with a substantial effect on water temperature was the extinction coefficient, with the strongest departures in Trout Lake albeit only three percent when the extinction coefficient was decreased by 20 percent.

Dissolved oxygen in both the Lake Carlos and Elk Lake model was also most sensitive to alterations in the wind sheltering coefficient and the extinction coefficient. Dissolved oxygen changes are strongly tied to water temperature dynamics, hence the connection between water temperature and dissolved oxygen sensitivity. This also explains the smaller sensitivity in dissolved oxygen for Trout Lake, which had a minor departure for both water temperature and dissolved oxygen in response to the wind sheltering coefficient. For both the Lake Carlos and Elk Lake models, sediment oxygen demand is a major sink for dissolved oxygen so departures in this parameter also had a strong effect, shown as zero-order SOD in table 4. Sediment oxygen demand is smaller in Trout Lake, therefore the effect on dissolved oxygen is smaller.

Unlike water temperature and dissolved oxygen, nutrient concentrations were affected by several of the different parameters or input loads (table 6). Ammonia was most affected by the wind sheltering coefficient and the sediment-oxygen demand for Lake Carlos. Due to the size of Lake Carlos, changes in the input loads (inflow phosphorus, inflow nitrogen, inflow organic matter) only had a small effect. The likely connection with the wind sheltering coefficient relates back to the water temperature, which will affect the timing and magnitude of algal growth for the three different algal groups. As the algal dynamics affect the ammonia concentrations, both during photosynthesis (uptake) and respiration (release), the effect of wind on water temperature will thereby affect algal growth and production. This also explains the same patterns on ammonia concentrations for Elk Lake and Trout Lake. Small perturbations in the ammonia concentrations were seen for changes in the input loads, although these effects were minor due to the size of the lake volume relative to the incoming load. Sediment oxygen demand also affects the ammonia concentration by governing the rate at which bacteria and other organisms metabolize organic matter, which will eventually release ammonia back into the water column. Nitrate-nitrite and orthophosphorus concentrations were also affected for the same reasons as ammonia, with a strong tie back to any factors that will control algal dynamics. The percent differences vary between ammonia, nitrate-nitrite, and orthophosphorus; however, the trends are the same with the exception of the sediment oxygen demand (table 6). Another departure from the above pattern occurs for orthophosphate. Because orthophosphate has a relatively small reservoir pool, alterations in the inflow phosphorus also had a minor effect on the orthophosphorus concentrations, particularly in Lake Carlos and Elk Lake.

Chlorophyll *a* is used as a surrogate for algal concentrations, so those parameters with a strong effect on algal growth will affect chlorophyll *a*. Wind sheltering coefficient had an effect on chlorophyll *a* in all three lakes because of the tie to water temperature on algal growth dynamics. In both Lake Carlos and Elk Lake, increasing the wind sheltering coefficient caused the chlorophyll *a* concentration to increase because the temperature regime shifted towards enhanced production for the three algal groups, whereas decreasing the wind sheltering coefficient caused either a negative or smaller positive response in chlorophyll *a*. In Trout Lake, the linkage between the wind sheltering coefficient and a change in the chlorophyll *a* concentration was weak. The extinction coefficient is also important because the penetration of light into the water column will have a strong impact on photosynthetic rates for algal growth dynamics. Finally, because the incoming loads of phosphorus and nitrogen are relatively low for all three lakes, only the inflow organic matter had a strong effect on algal growth. Since there is a larger organic matter pool, the eventual breakdown of the organic matter will eventually lead to larger ammonia, nitrate-nitrite, and orthophosphorus pools, which will lead to increased algal growth. Alternatively, any decrease in the inflow organic matter will have the opposite effect.

Historical Simulations

An additional analysis was undertaken to understand the robust nature of the model calibration and validation. Meteorological data required for the Lake Carlos CE-QUAL-W2 model were obtained for calendar years 1979 and 2009 including air temperature, dew point temperature, wind speed, wind direction, and cloud cover. Unit conversions from the meteorological data to the units required for the model were the same as for the calibration and validation datasets. The calibrated Lake Carlos model was run using the 1979 or 2009 meteorological data as input. The water budget for Lake Carlos was recalculated for the period of April to November of each simulation year in order to account for the change in evaporative loses from the individual lakes. No attempt was made to adjust the gaged inflow from the tributaries. Adjustments to the water balance were made through changes to the gains and losses in the distributed tributary flow which lumps all ungaged inflow and groundwater interactions together in one value. Within CE-QUAL-W2, the distributed tributary flow can either be positive or negative, and several iterations were completed before the water balance of the model was re-established. No adjustment was made to constituent loading associated with tributary inflow and mass loadings were held constant between the calibrated model and the lake simulations for 1979 and 2009.

Model output for dissolved oxygen and temperature were compared to observed field data collected for Lake Carlos in 1979 and 2009. The results of the historical simulations were compared to observed profile data from the Keck’s Point sampling location from 2010 as well as with historical profile data collected from Lake Carlos by the MN DNR as part of their routine monitoring. Results from 1979 (fig. 61), with the entire spectrum of depths simulated, show a slower rate of spring stratification development when compared to 2010 but also show the eventual development of a metalimnetic dissolved oxygen minimum. Fall destratification of the water column occurs earlier in 1979 than in 2010, in part because cooler fall temperatures and strong winds drive deep mixing events that produce isothermal conditions.

Figure 61. Simulated and measured dissolved oxygen concentrations for Kecks Point (USGS station number 455843095212501) for 12 dates in 1979.

Figure 62. Simulated and measured dissolved oxygen concentrations for Kecks Point (USGS station number 455843095212501) for 14 dates in 2009.

In contrast to the historical simulation results from 1979, the model output from 2009 shows an early spring stratification pattern similar to what was observed in 2010. The mid-summer stratification pattern suggests that a deep mixed layer in 2009 reduced the potential impact of an anoxic metalimnion forming over an oxic hypolimnion. However, the dynamic model output suggests that lethal or near-lethal conditions in the metalimnion were more pronounced and lasted for a longer period of time in 2009 when compared to 2010. This result is more apparent when comparing the lake model output of dissolved oxygen profiles to the predicted oxy-thermal lethal niche boundary model of Jacobson and others (2008). When simulated profile data are compared to the predicted lethality boundary condition, results from 2009 show a more frequent occurrence of a metalimnetic oxygen minimum overlay on top of a hypolimnetic oxic condition (fig. 63). This habitat structure is a common precursor to poor oxy-thermal fish habitat that can lead to fish mortality.

Figure 63. Plots of the simulated dissolved oxygen output from Keck's point, Lake Carlos MN, for 2009 (1a) and 2010 (1b) compared to Jacobson et al. (2008) model of niche boundaries for lake cisco *Coregonus artedi*.

Summary

The CE-QUAL-W2 model was able to capture the nature of lake ecosystem responses to inflows and nutrient loads. Model output predicted seasonal dynamics in physical and chemical parameters, including temperature and dissolved oxygen profiles as well as nutrient concentrations in the epilimnion and the hypolimnion. Specific examples of the model capabilities include comparisons between observed and predicted vertical profile data for Lakes Carlos metalimnetic oxygen minima (fig. 20) and Elk Lake mid-water column oxygen maximum (fig.21). This high level of model performance is repeated throughout the three lake simulations.

The ability of the model to simulate the physical and chemical components of lake ecosystem response went beyond the accurate tracking of vertical profiles from a specific date. The model also captured the trajectories of oxygen and temperature concentrations at multiple depths over time. This suggests the model was accurately simulating the underlying metabolic processes in each lake. For Lake Carlos, the simulated dissolved oxygen concentration in the metalimnion tracked the concentration minimum by accurately modeling the oxygen demand associated with decomposition of algal carbon below the photic zone. In Elk Lake, the simulated metalimnetic chlorophyll maximum produced the observed metalimnetic oxygen maximum. In both cases, modeled in-lake processes of primary production, algal mortality, and carbon and nutrient recycling predicted the observed dissolved oxygen dynamics. Both cases illustrate that the internal trophic dynamics in these deep, cold lakes drives much of the observed biogeochemistry.

The robust nature of the predictive capabilities of the model has been further tested through the application of the validated model to historic datasets for Lake Carlos. When the calibrated model was run with 1979 meteorological inputs, the simulated dissolved oxygen profiles tracked the observed data as well as the seasonal trajectories. These results were achieved despite the need to approximate changes to the water balance, suggesting that the long water residence times in Lake Carlos buffer the effects of year to year inflow variablility.

References Cited

Arar, E.J., 1997, *In vitro* determination of chlorophylls a, b, c_1 + c_2 and pheopigments in marine and freshwater algae by visible spectrophotometry: U.S. Environmental Protection Agency Report EPA–446.0-1, 26 p.

Brunett, J.O., Barber, N.L., Burns, A.W., Fogelman, R.P., Gillies, D.C., Lidwin, R.A., and Mack, T.J., 1997, A quality-assurance plan for district ground-water activities of the U.S. Geological Survey: U.S. Geological Survey Open-File Report 97-11, 44 p.

Buchanan, T.J., and Somers, W.P., 1969, Discharge measurements at gaging stations: Techniques of Water-Resources Investigations of the United States Geological Survey, Chapter A8, 71 p.

Carpenter, S.R., Benson, Barbara J., Biggs, R., Chipman, J.W., Foley, J.A., Golding, S.A., Hammer, R.B., Hanson, P.C., Johnson, P.T.J., Kamarainen, A.M., Kratz, Timothy K., Lathrop, R.C., McMahon, K.D., Provencher, B., Rusak, J.A., and others, 2007, Understanding regional change: a comparison of two lake districts: BioScience, v. 57, no. 4, p. 323–335.

Cole, T.M., and Wells, S.A., 2008, CE-QUAL-W2 : A two-dimensional, laterally averaged, hydrodynamic and water quality model, version 3.6: U.S. Army Corps of Engineers Instruction Report EL-08-1, 715 p.

DeStasio, B.T., Hill, D.K., Klienhans, J.M., Nibbelink, N.P., and Magnuson, John J., 1996, Potential effects of global climate change on small north-temperate lakes: Physics, fish, and plankton: Limnology and Oceanography, v. 41, no. 5, p. 1136–1149.

Fang, Xing, and Stefan, H., 1999, Projections of climate change effects on water temperature characteristics of small lakes in the contiguous US: Climatic Change, v. 42, p. 377–412.

Fang, Xing, Stefan, H.G., Eaton, J.G., McCormick, J.H., and Alam, S.R., 2004a, Simulation of thermal/dissolved oxygen habitat for fishes in lakes under different climate scenarios Part 1. Cool-water fish in the contiguous US: Ecological Modelling, v. 172, no. 1, p. 13–37.

Fang, Xing, Stefan, H.G., Eaton, J.G., McCormick, J.H., and Alam, S.R., 2004b, Simulation of thermal/dissolved oxygen habitat for fishes in lakes under different climate scenarios Part 2. Cold-water fish in the contiguous US: Ecological Modelling, v. 172, no. 1, p. 39–54.

Flowers, J.D., Hauck, L.M., and Kiesling, R.L., 2001, USDA : Lake Waco-Bosque River initiative water quality modeling of Lake Waco using CE-QUAL-W2 for assessment of phosphorus control strategies: Texas Institute for Applied Environmental Research TR0114, 73 p.

Galloway, J.M., and Green, W.R., 2006, Application of a two-dimensional reservoir water-quality model of Beaver Lake, Arkansas, for the evaluation of simulated changes in input water quality , 2001–2003: U.S. Geological Survey Scientific Investigations Report 2006–5302, 39 p.

Galloway, J.M., Ortiz, R.F., Bales, J.D., and Mau, D.P., 2008, Simulation of hydrodynamics and water quality in Pueblo Reservoir, southeastern Colorado, for 1985 through 1987 and 1999 through 2002: U.S. Geological Survey Scientific Investigations Report 2008-5056, 67 p.

Gibs, J., Wilde, F.D., and Heckathorn, H.A., 2012, Alkalinity and acid neutralizing capacity (ver. 3.0): U.S. Geological Survey Techniques of Water-Resources Investigations, book 9, chap. A6., sec. 6.8, March 2012, accessed August 2013, from http://pubs.water.usgs.gov/twri9A6/.

Green, W.R., Galloway, J.M., Richards, J.M., and Wesolowski, E.A., 2003, Simulation of hydrodynamics, temperature , and dissolved oxygen in Table Rock Lake, Missouri, 1996–1997: U.S. Geological Survey Water-Resources Investigations Report 03-4237, 46 p.

Jacobson, P.C., Jones, T.S., Rivers, P., and Pereira, D.L., 2008, Field estimation of a lethal oxythermal niche boundary for adult ciscoes in Minnesota lakes: Transactions of the American Fisheries Society, v. 137, no. 5, p. 1464–1474.

Jassby, A., 1998, Interannual variability at three inland water sites: implications for sentinel ecosystems: Ecological Applications, v. 8, no. 2, p. 277–287.

Lorenz, D.L., Sanocki, C.A., and Kocian, M.J., 2009, Techniques for estimating the magnitude and frequency of peak flows on small streams in Minnesota based on data through water year 2005: U.S. Geological Survey Scientific Investigations Report 2009–5250, 62 p.

Magner, J.A., and Brooks, K.N., 2008, Integrating sentinel watershed-systems into the monitoring and assessment of Minnesota's (USA) waters quality: Environmental Monitoring and Assessment, v. 138, no. 1-3, p. 149–158.

Magnuson, J.J., Benson, B.J., and Kratz, T.K., 1990, Temporal coherence in the limnology of a suite of lakes: Freshwater Biology, v. 23, p. 145–159.

McDonald, T.L., 2003, Review of environmental monitoring methods: survey designs.: Environmental Monitoring and Assessment, v. 85, no. 3, p. 277–292.

Mueller, D.S., and Wagner, C.R., 2008, Measuring discharge with acoustic doppler current profilers from a moving boat: U.S. Geological Survey Techniques and Methods 3-A22, 86 p.

Rantz, S.E., and others, 1982a, Measurement and computation of streamflow: Volume 1. Measurement of stage and discharge: Geological Survey Water-Supply Paper 2175, v. 1, 313 p.

Rantz, S.E., and others, 1982b, Measurement and computation of streamflow: Volume 2. Computation of Discharge: Geological Survey Water-Supply Paper 2175, v. 2, 373 p.

Ries III, K.G., Steeves, P.A., Coles, J.D., Rea, A.H., and Stewart, D.W., 2005, StreamStats: A U.S. Geological Survey web application for stream information: U.S. Geological Survey Fact Sheet FS 2004-3115, 4 p.

Stefan, H., Hondzo, M, and Fang, X, 1996, Simulated long-term temperature and dissolved oxygen characteristics of lakes in the north-central United States and associated fish habitat limits: Limnology and Oceanography, v. 41, no. 5, p. 1124–1135.

Stefan, H.G., and Fang, Xing, 1994, Dissolved oxygen model for regional lake analysis: Ecological Modelling, v. 71, no. 1-3, p. 37–68.

Stefan, H.G., Hondzo, Midhat, Eaton, J.G., and McCormick, J.H., 1995, Predicted effects of global climate change on fishes in Minnesota lakes, *in* Beamish, R.J. ed., Climate change and northern fish populations, Can J. Fish. Aquatics, p. 57–72.

Sullivan, A.B., and Rounds, S.A., 2004, Modeling hydrodynamics, temperature, and water quality in Henry Hagg Lake, Oregon, 2000-03: U.S. Geological Survey Scientific Investigations Report 2004-5261, 48 p.

Sullivan, A.B., Rounds, S.A., Deas, M.L., Asbill, J.R., Wellman, R.E., Stewart, M.A., Johnston, M.W., and Sogutlugil, I.E., 2011, Modeling hydrodynamics , water temperature, and water quality in the Klamath River upstream of Keno Dam, Oregon, 2006-09: U.S. Geological Survey Scientific Investigations Report 2011-5105, 82 p.

Sullivan, A.B., Rounds, S.A., Sobieszczyk, S., and Bragg, H.M., 2007, Modeling hydrodynamics , water temperature , and suspended sediment in Detroit Lake, Oregon: U.S. Geological Survey Scientific Investigations Report 2007-5008, 52 p.

Wagner, R.J., Boulger, R.W., Jr., Oblinger, C.J., and Smith, B.A., 2006, Guidelines and standard procedures for continuous water-quality monitors; Station operation, record computation, and data reporting (ver. 1.0):\ U.S. Geological Survey Scientific Techniques and Methods 1-D3, 96 p.

Wilde, F.D., ed., 2004, Cleaning of Equipment for water sampling (ver. 2.0): U.S. Geological Survey Techniques of Water-Resources Investigations, book 9, chap. A3, April 2004, accessed [date viewed], at http://pubs.water.usgs.gov/twri9A3/.

Williamson, C.E., Dodds, W., Kratz, Timothy K, and Palmer, M.A., 2008, Lakes and streams as sentinels of environmental change in terrestrial and atmospheric processes: Frontiers in Ecology and the Environment, v. 6, no. 5, p. 247–254.

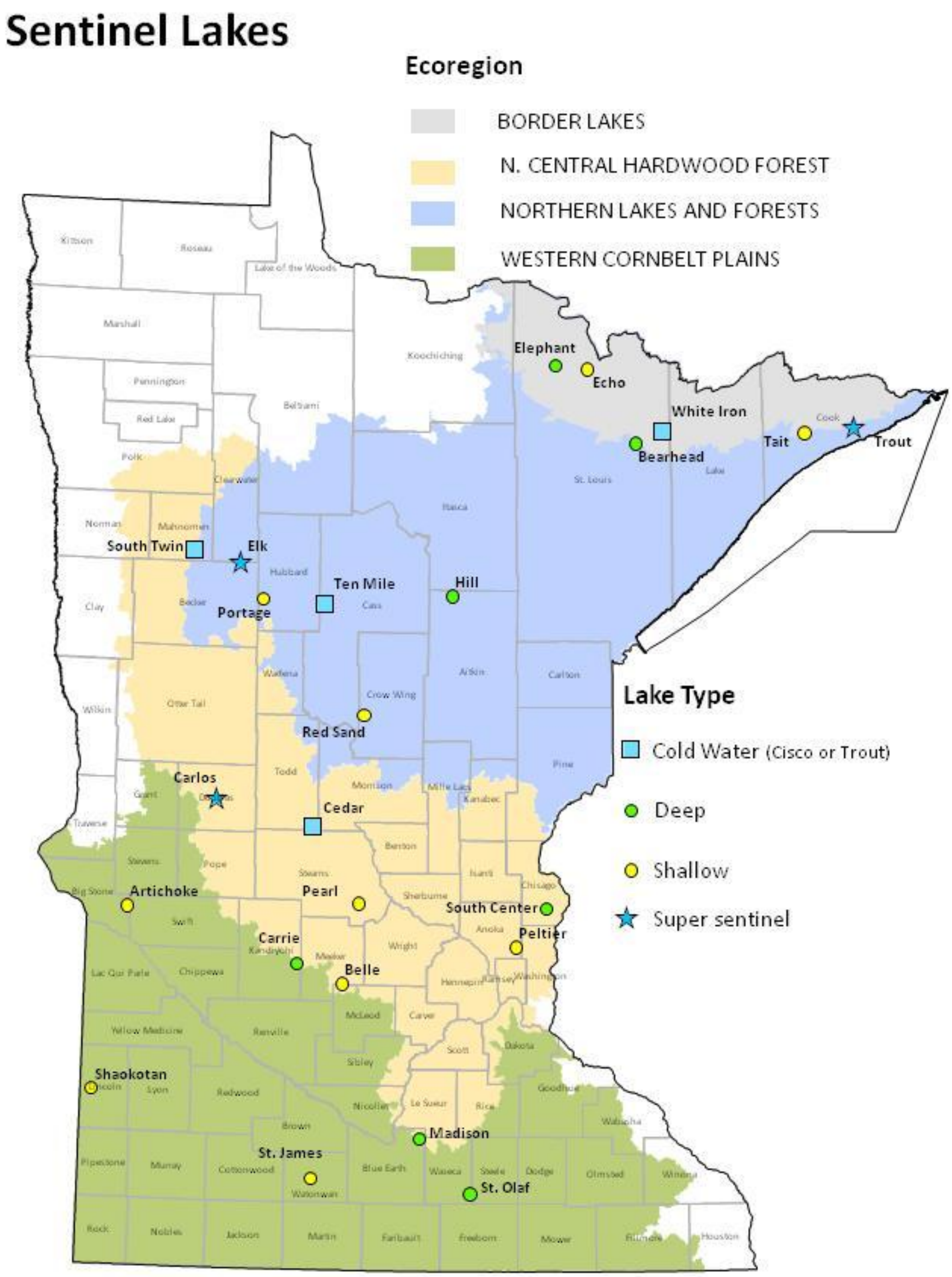

Figure 1. Major Minnesota ecoregions and sentinel lakes. The super sentinel lakes are the focus of this study.

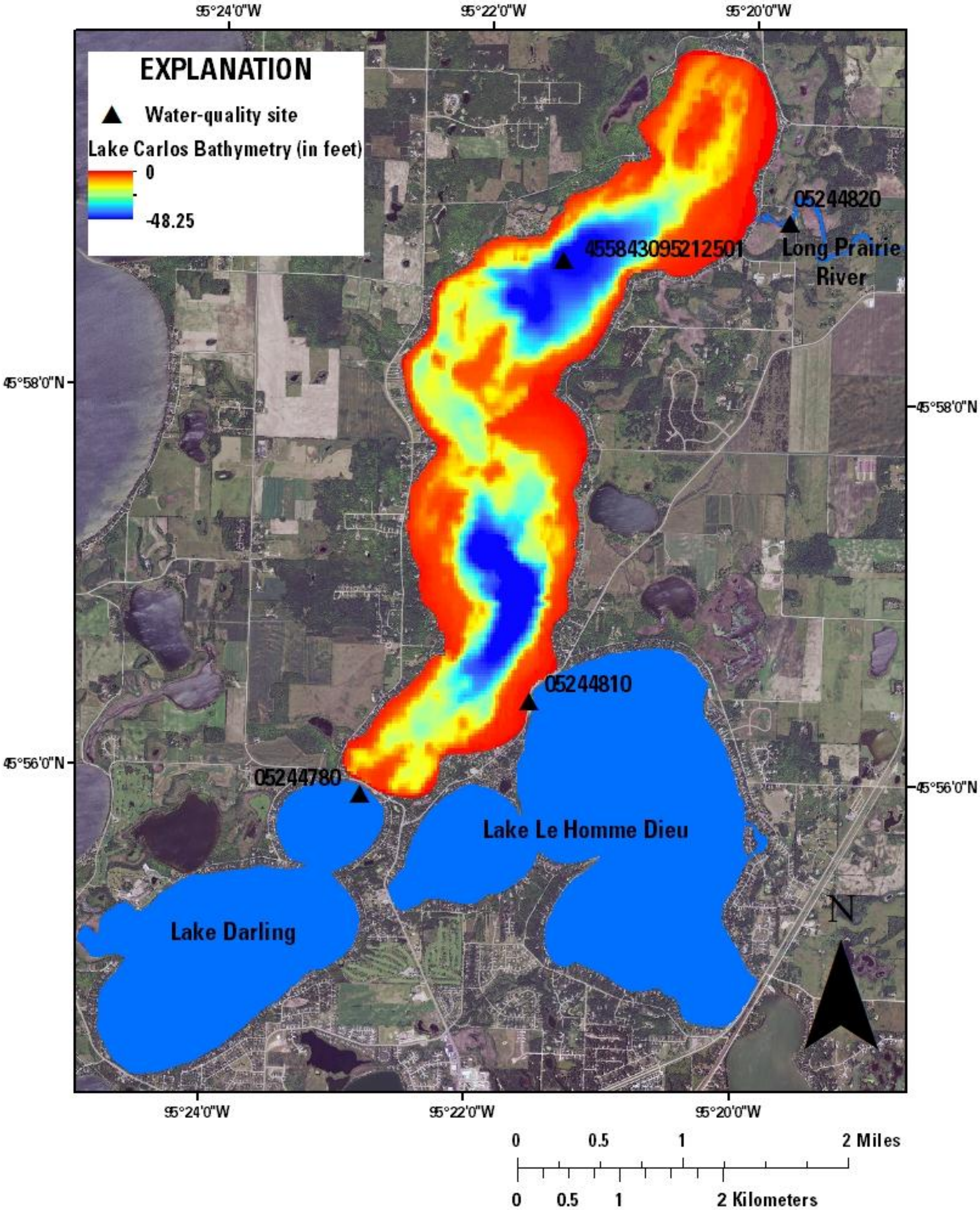

Figure 2. Location of the sampling locations in Lake Carlos, Minnesota.

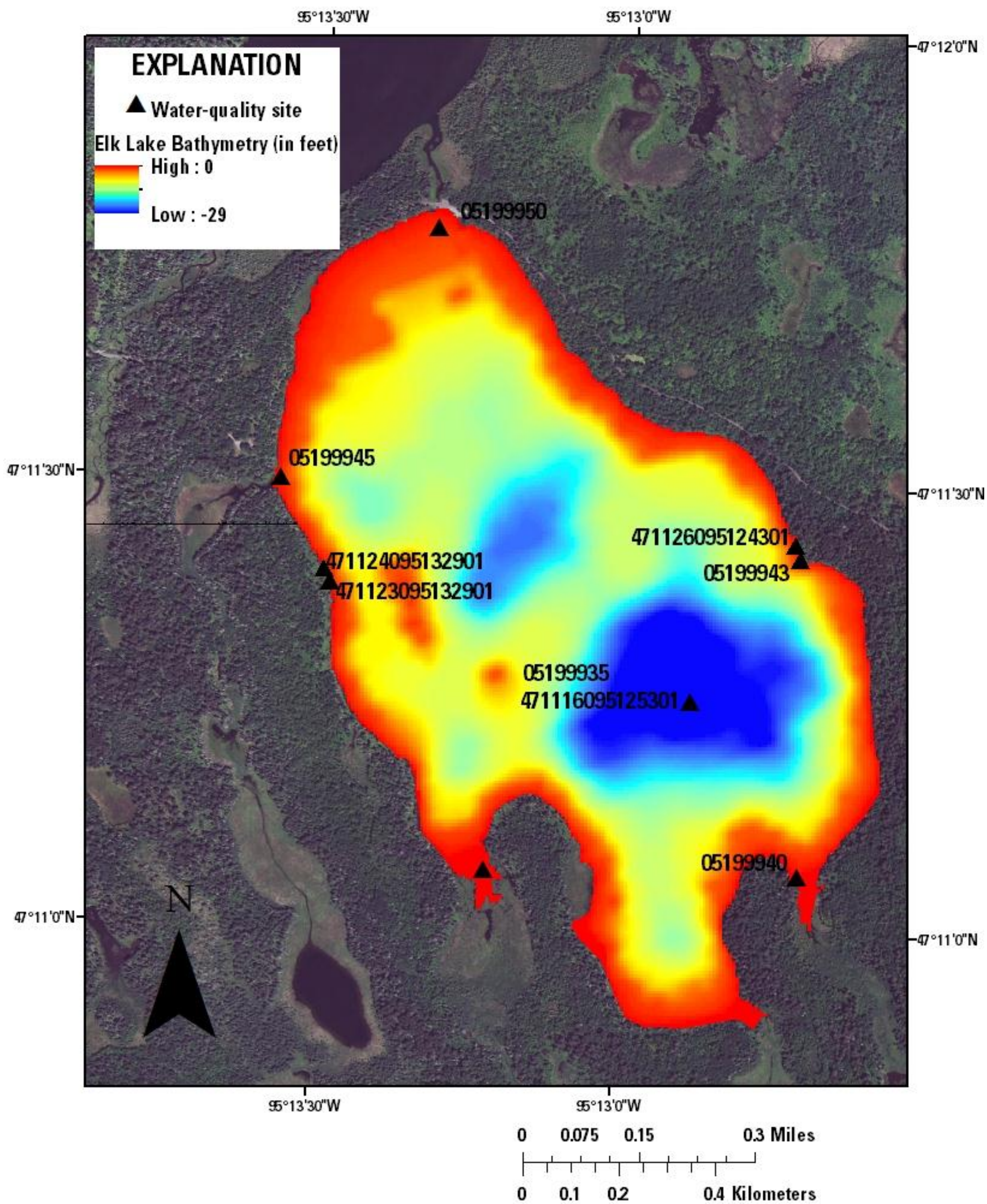

Figure 3. Location of the sampling locations in Elk Lake, Minnesota.

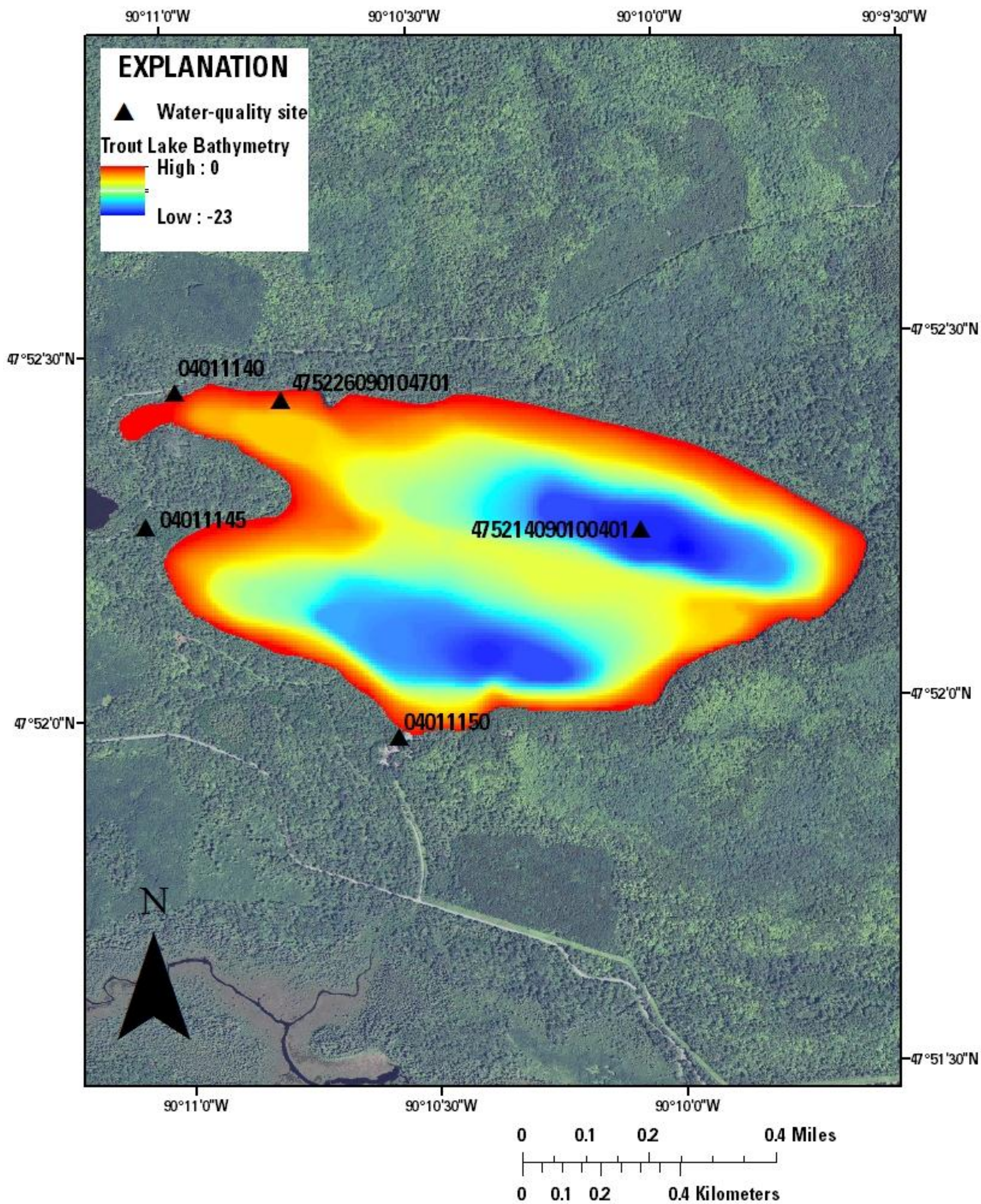

Figure 4. Location of the sampling locations in Trout Lake, Minnesota.

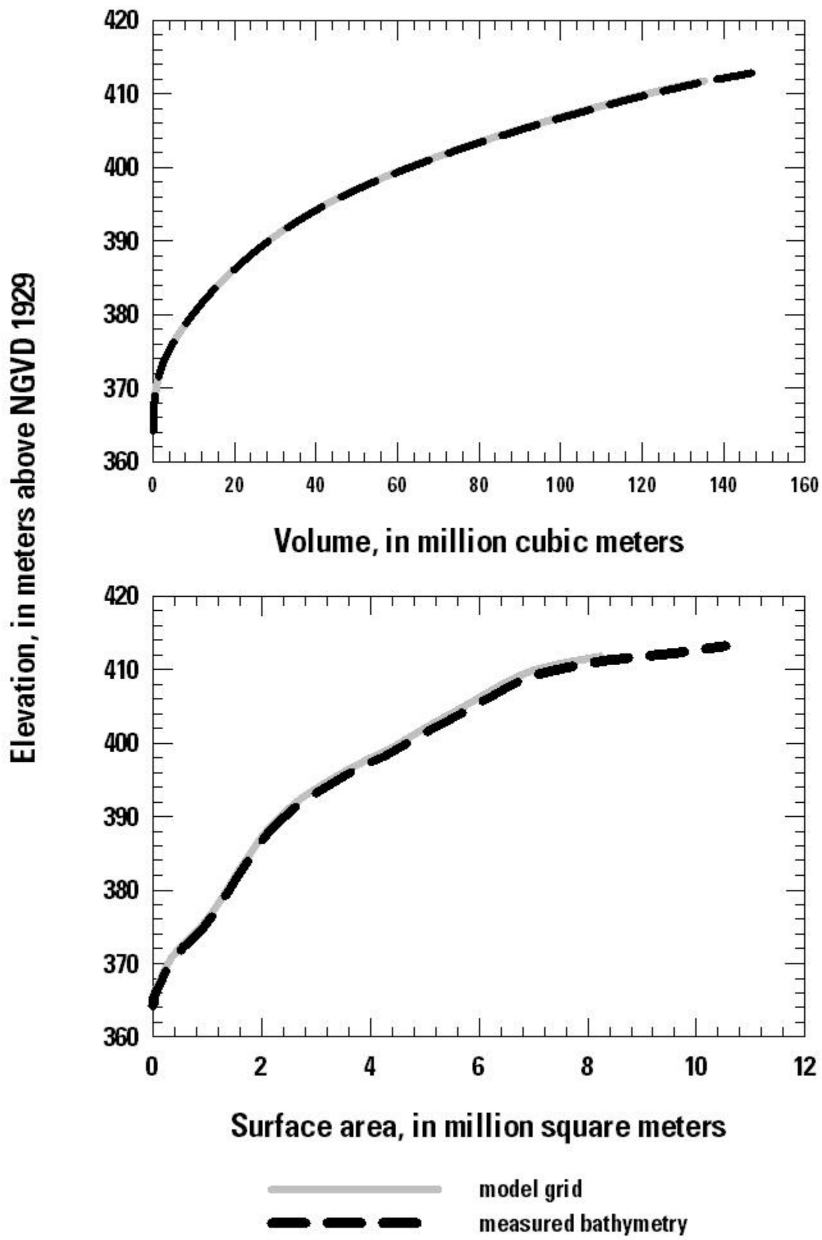

Figure 5. Volume-elevation and surface area-elevation curves for Lake Carlos between the measured bathymetry, provided by the Minnesota Department of Natural Resources (DNR), and as represented by the model grid.

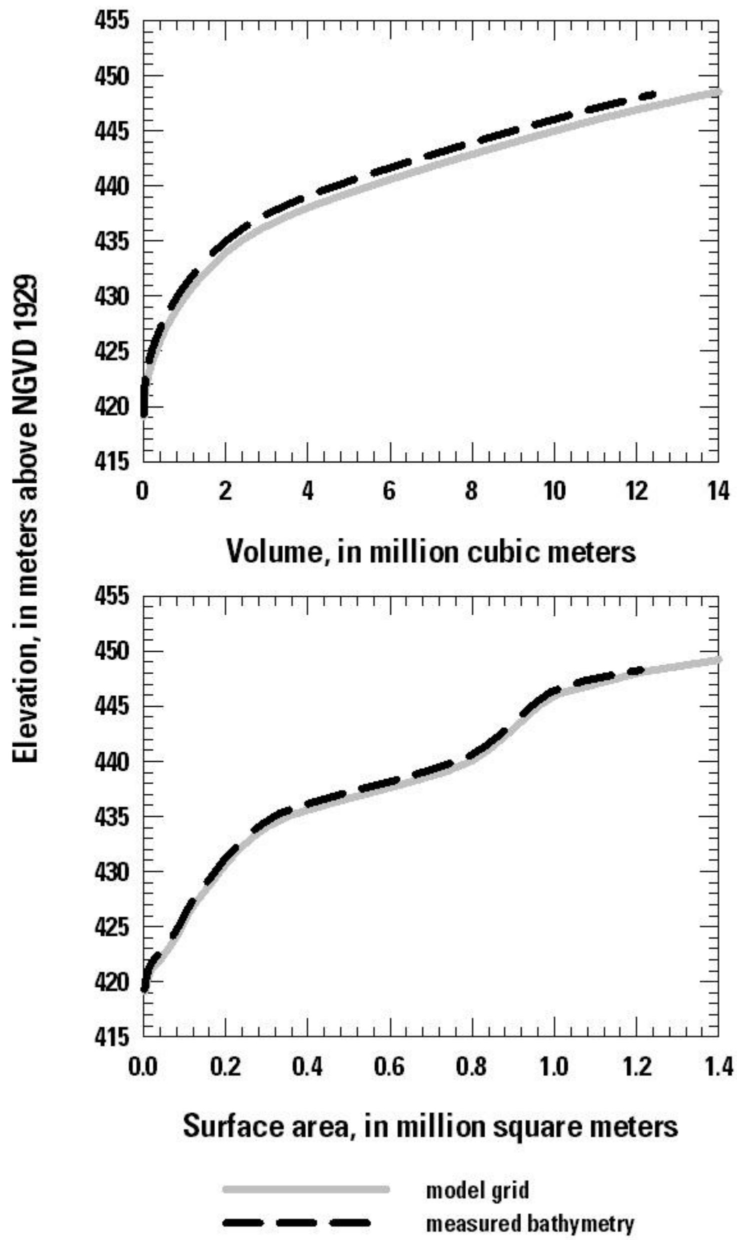

Figure 6. Volume-elevation and surface area-elevation curves for Elk Lake between the measured bathymetry, provided by the Minnesota Department of Natural Resources (DNR), and as represented by the model grid.

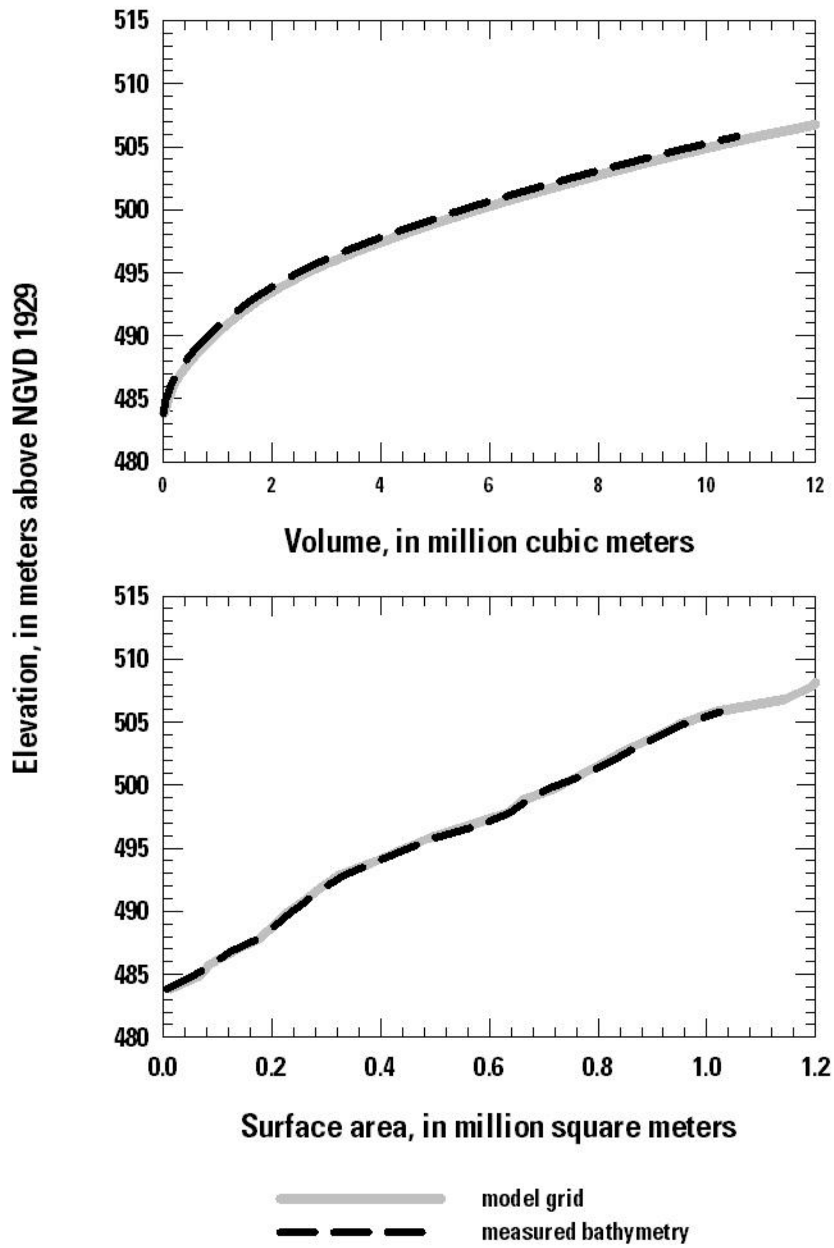

Figure 7. Volume-elevation and surface area-elevation curves for Trout Lake between the measured bathymetry, provided by the Minnesota Department of Natural Resources (DNR), and as represented by the model grid.

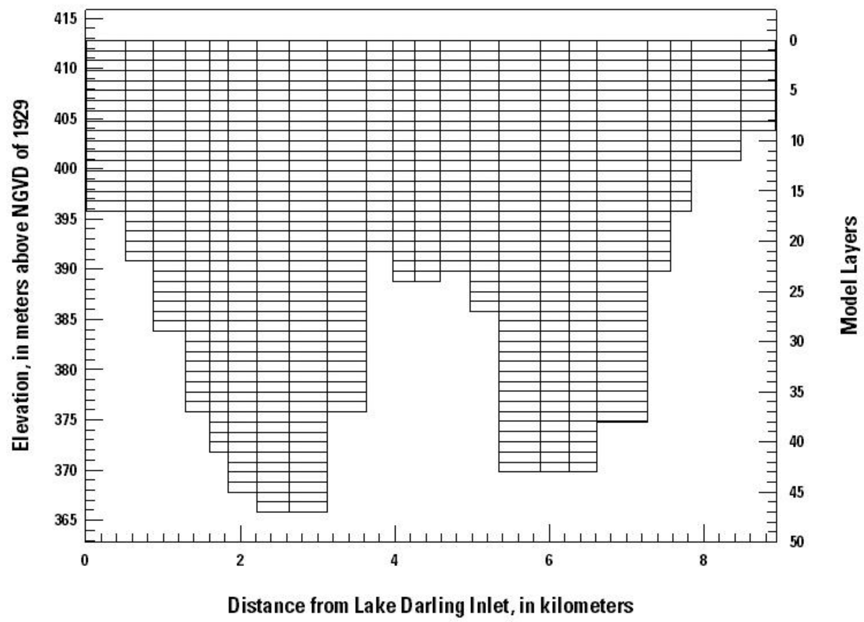

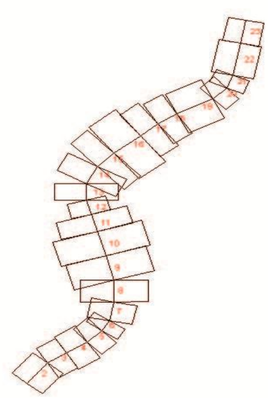

Figure 8. Lake Carlos, as shown in (A) side view and (B) top view of the CE-QUAL-W2 computational grid.

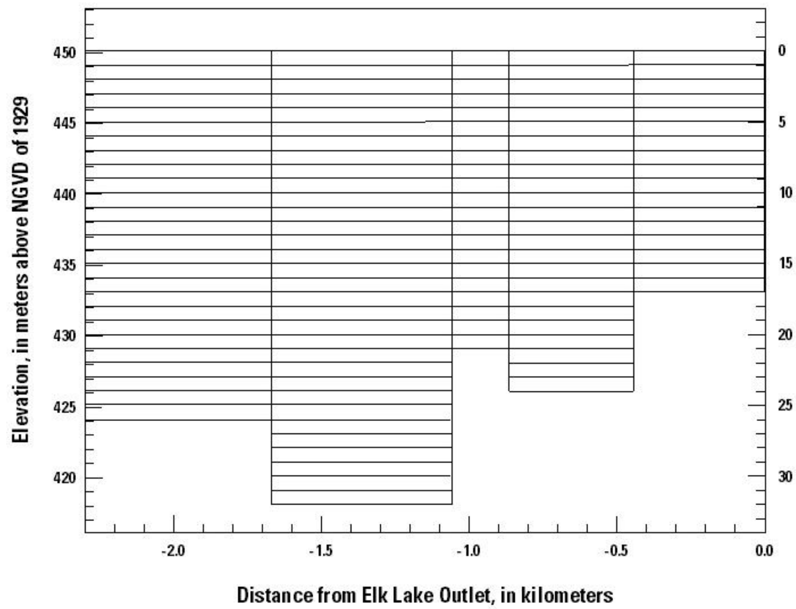

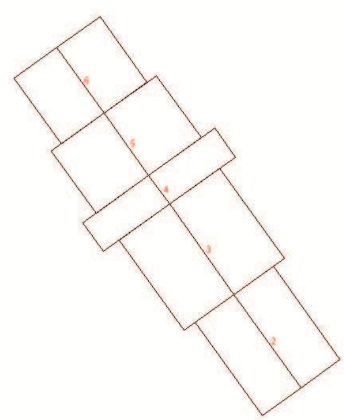

Figure 9. Elk Lake, as shown in (A) side view and (B) top view of the CE-QUAL-W2 computational grid.

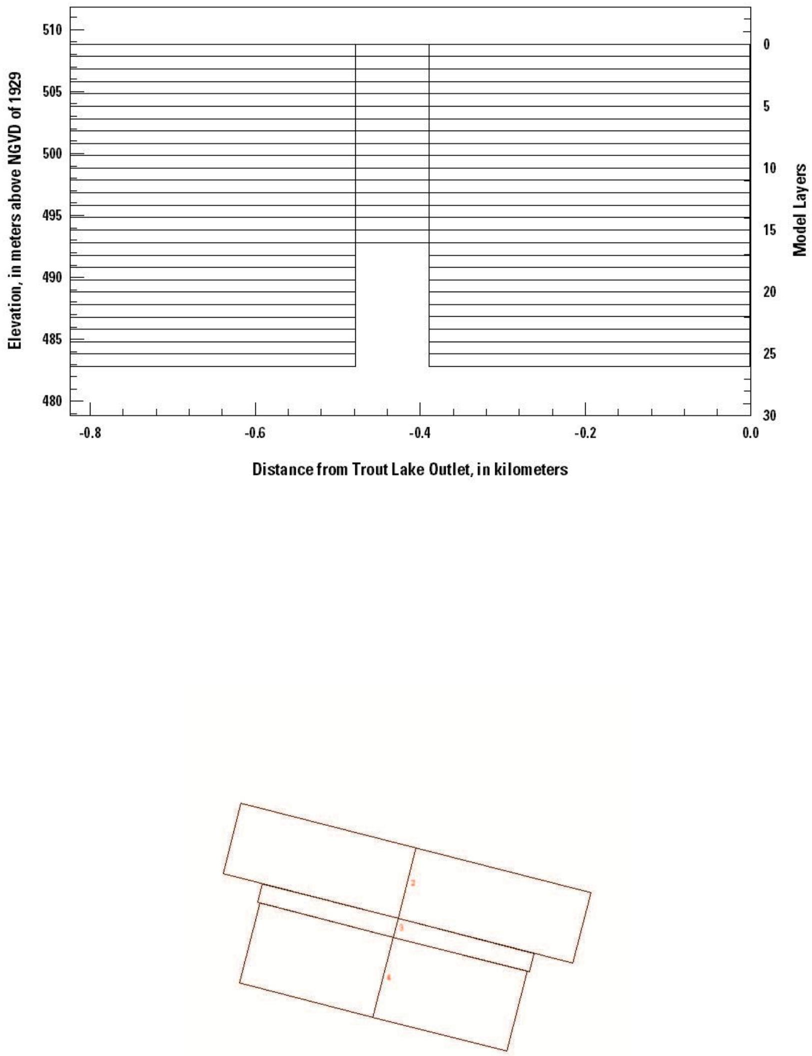

Figure 10. Trout Lake, as shown in (A) side view and (B) top view of the CE-QUAL-W2 computational grid.

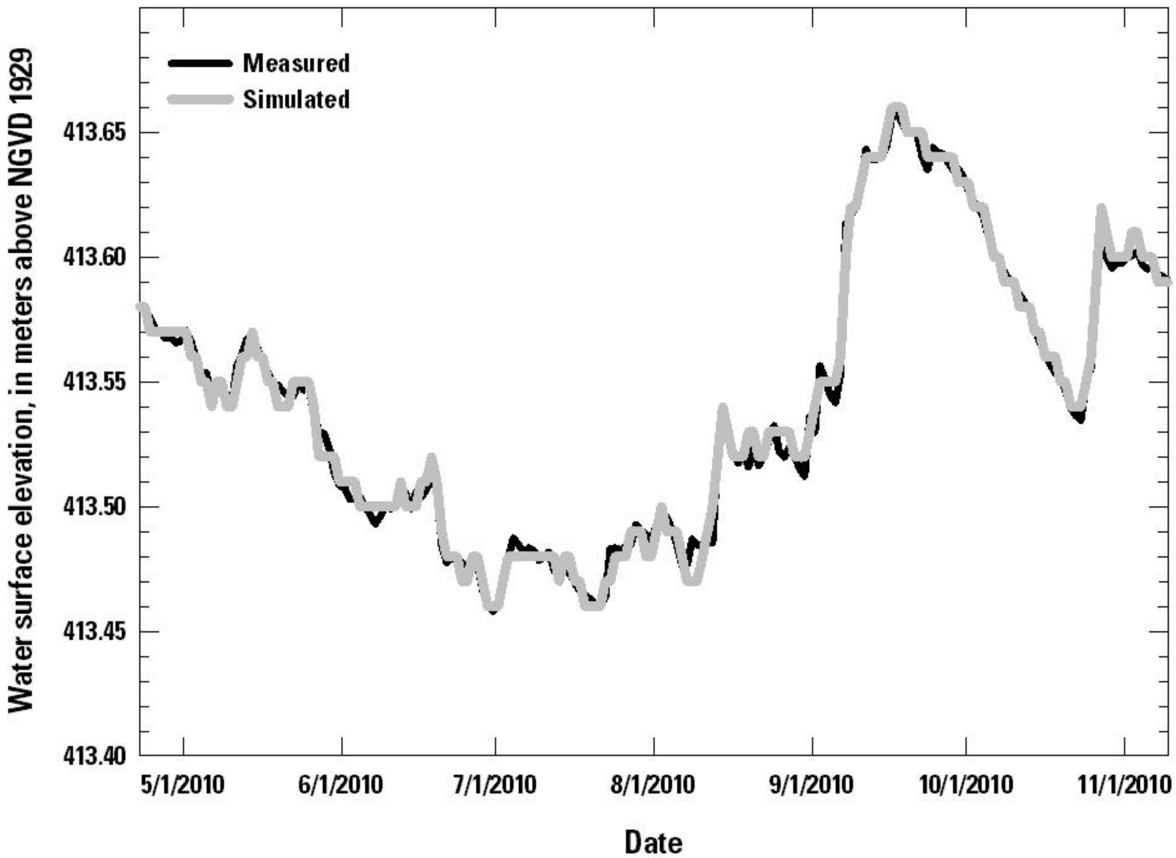

Figure 11. Simulated and measured water surface elevation for Lake Carlos, April 22 to November 9, 2010.

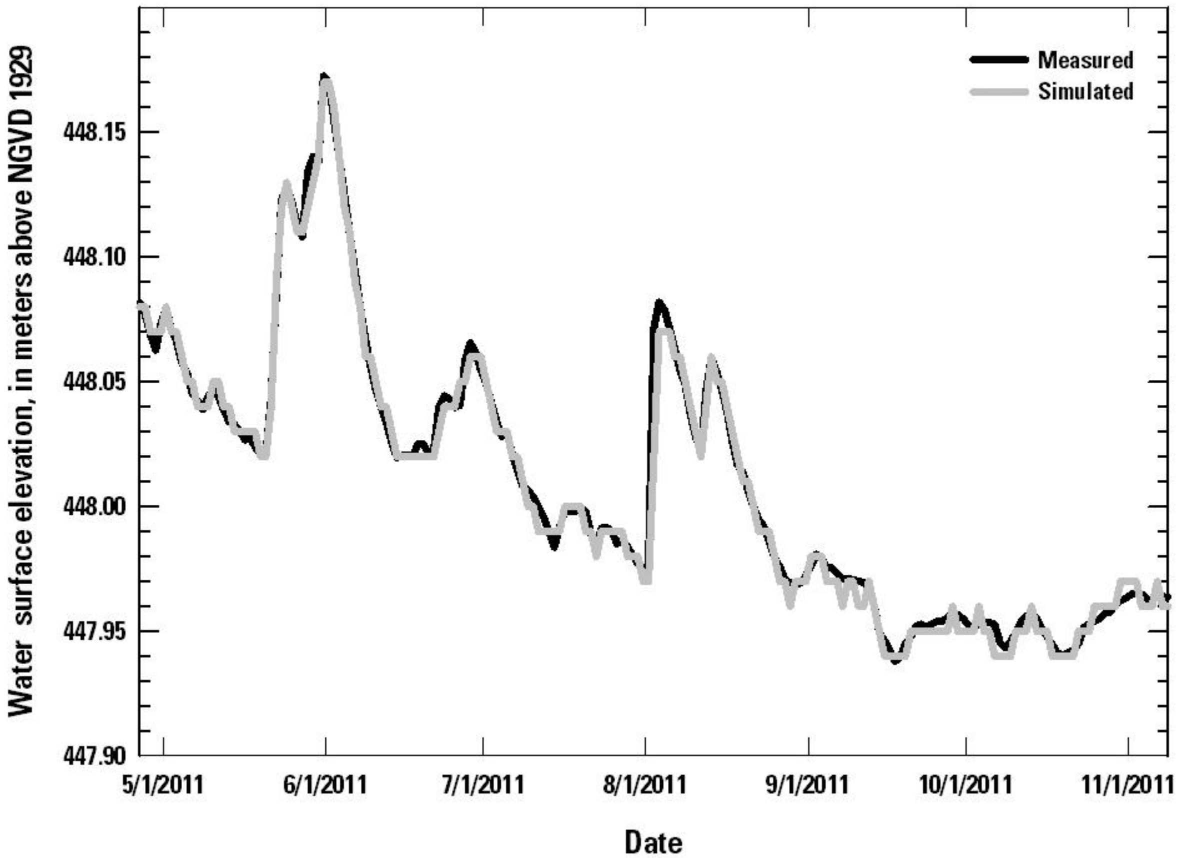

Figure 12. Simulated and measured water surface elevation for Elk Lake, April 26 to November 8, 2011.

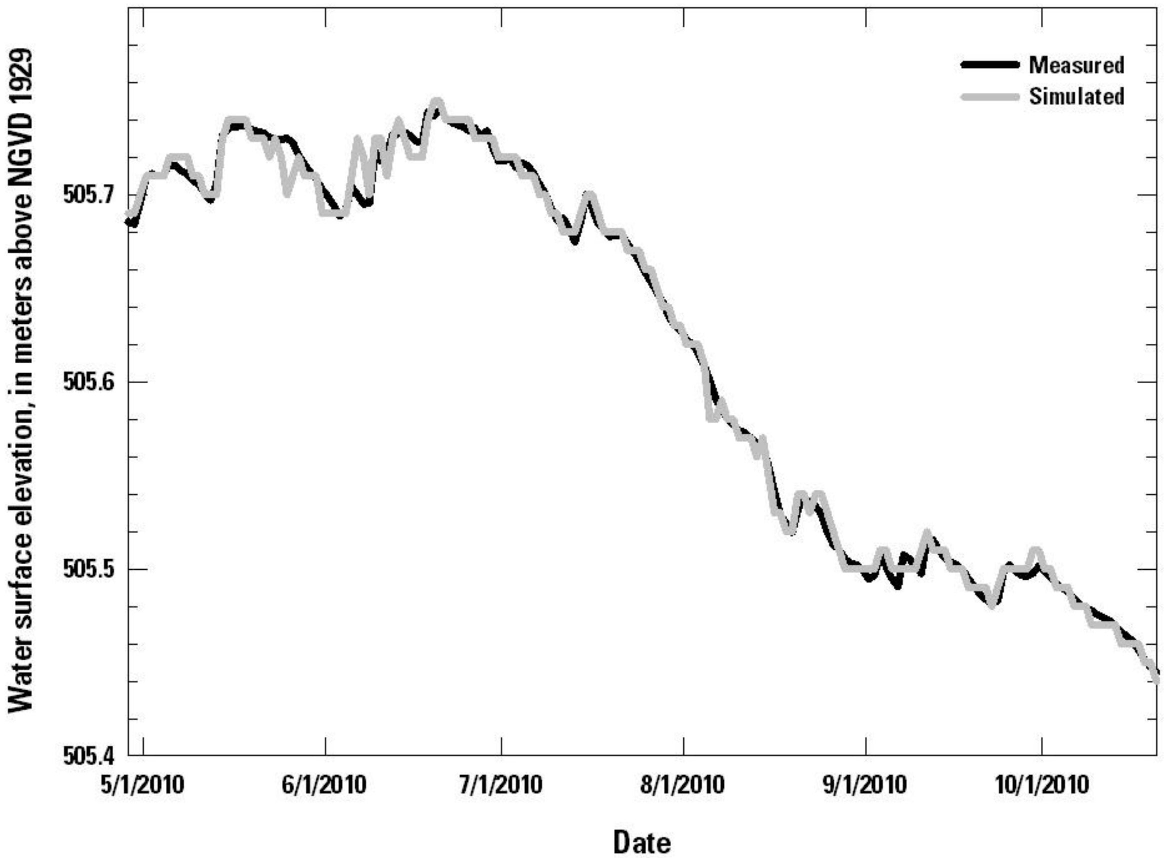

Figure 13. Simulated and measured water surface elevation for Trout Lake, April 28, 2010 to October 20, 2010.

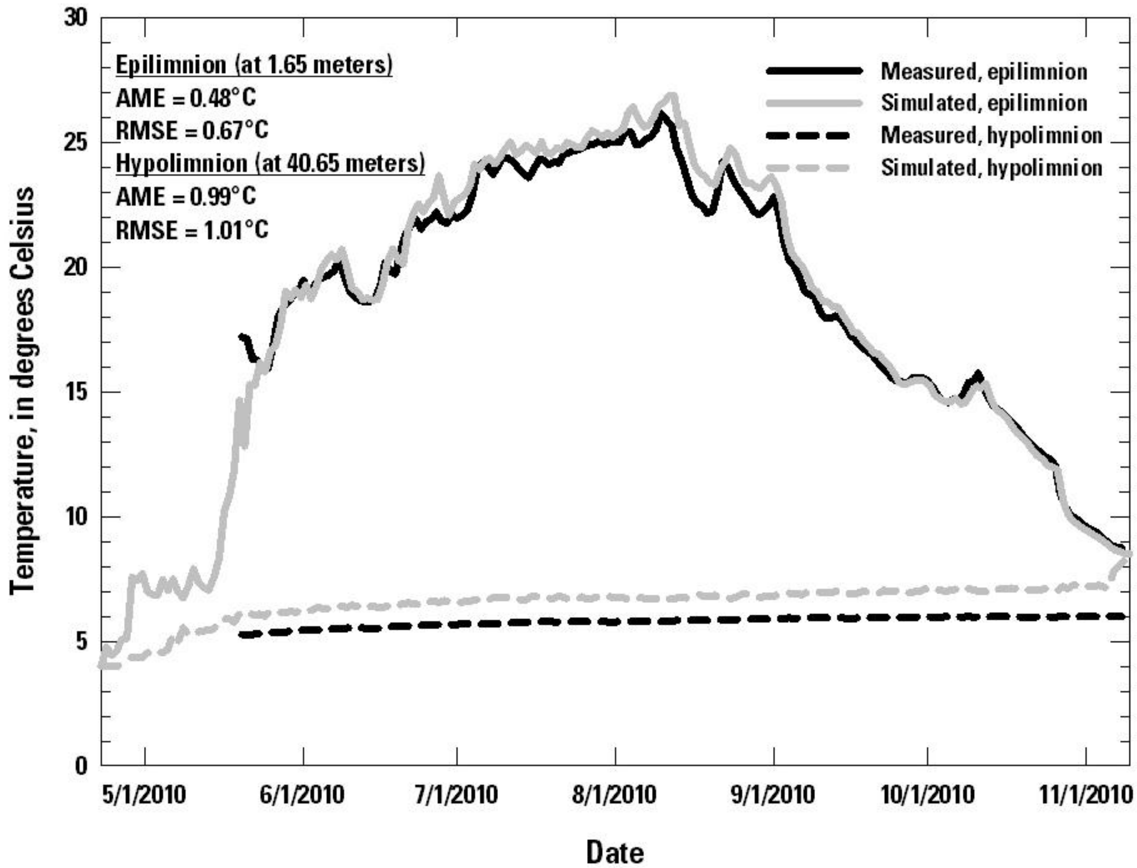

Figure 14. Simulated and measured water temperature for the epilimnion (2-m) and hypolimnion (37-m) at Kecks Point (USGS station number 455843095212501) for Lake Carlos, April 22, 2010 to November 9, 2010.

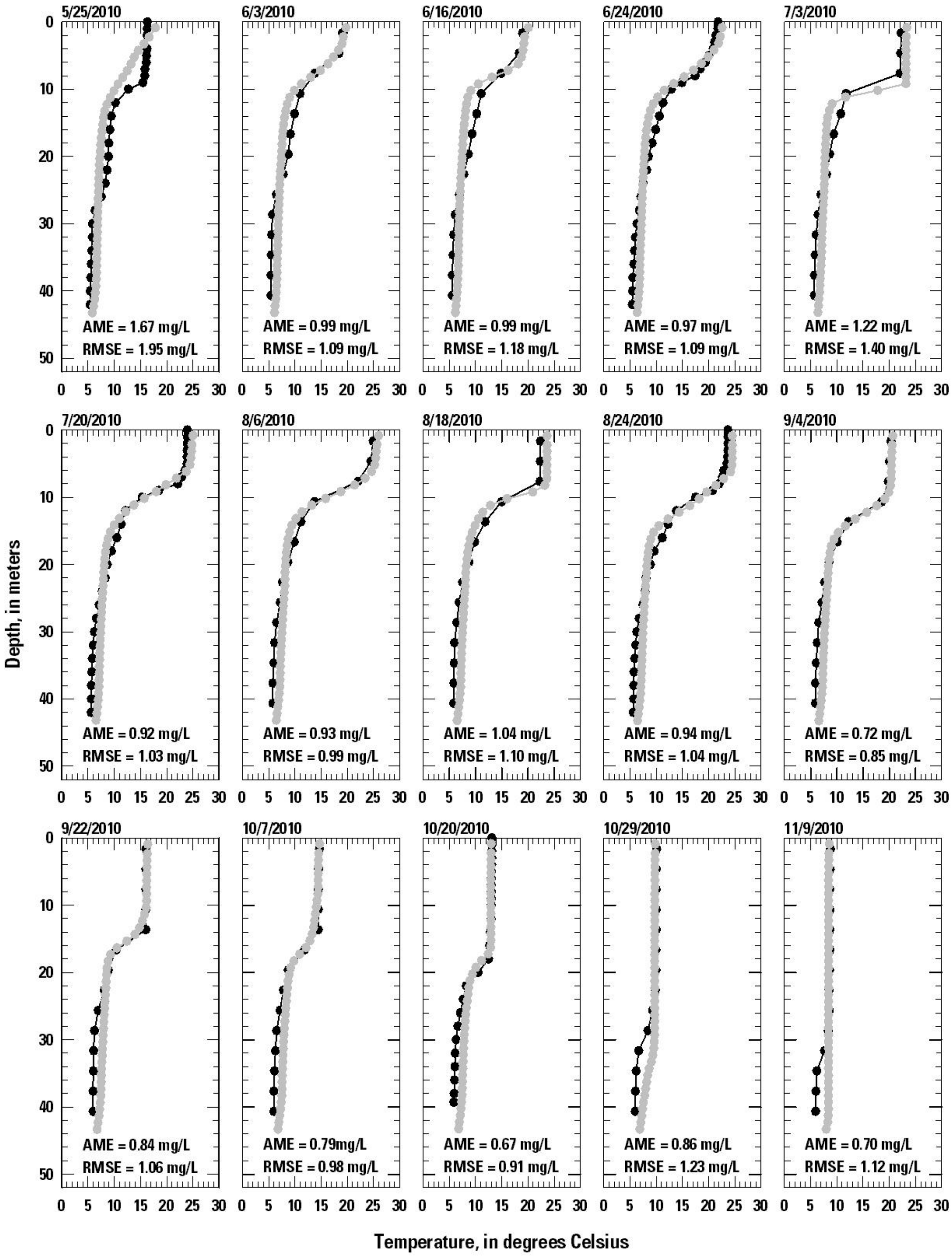

Figure 15. Simulated (gray) and measured (black) water temperature at Kecks Point (USGS station number 455843095212501) in Lake Carlos for 15 dates in 2010, with AME and RMSE quantities..

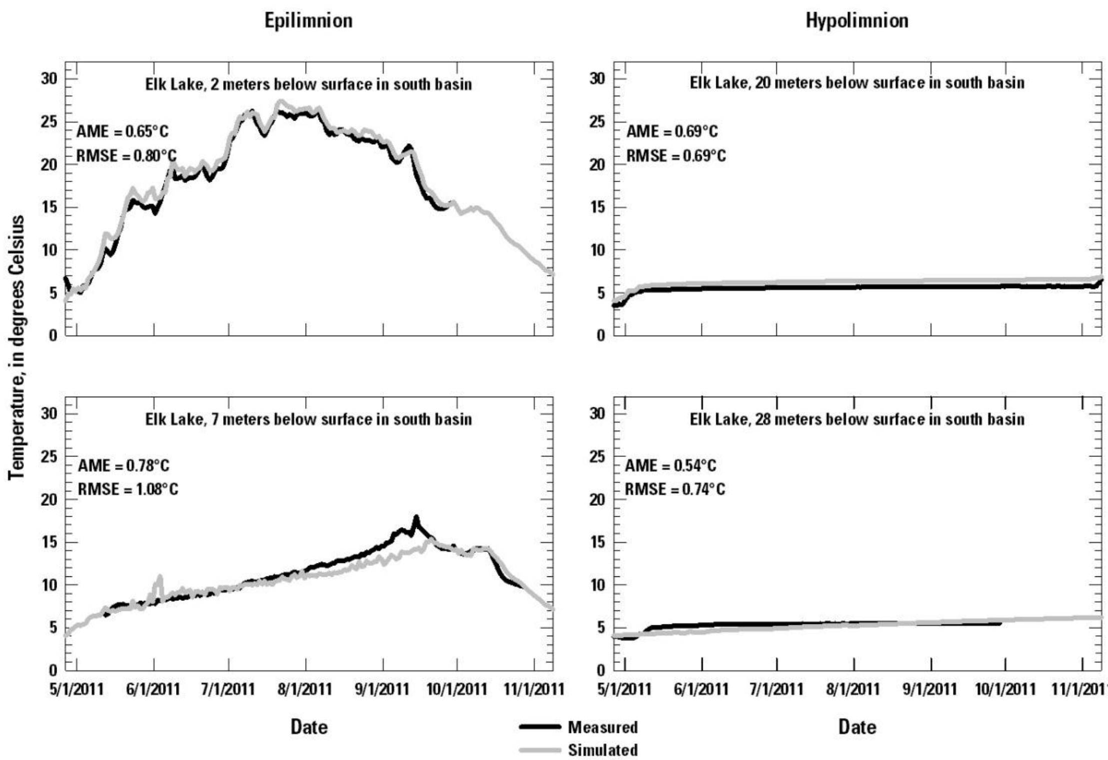

Figure 16. Simulated and measured water temperature for the epilimnion (2-m and 7-m) and hypolimnion (20-m and 28-m) at south basin hole (USGS station number 471116095125301) in Elk Lake, April 26, 2011 to November 8, 2011.

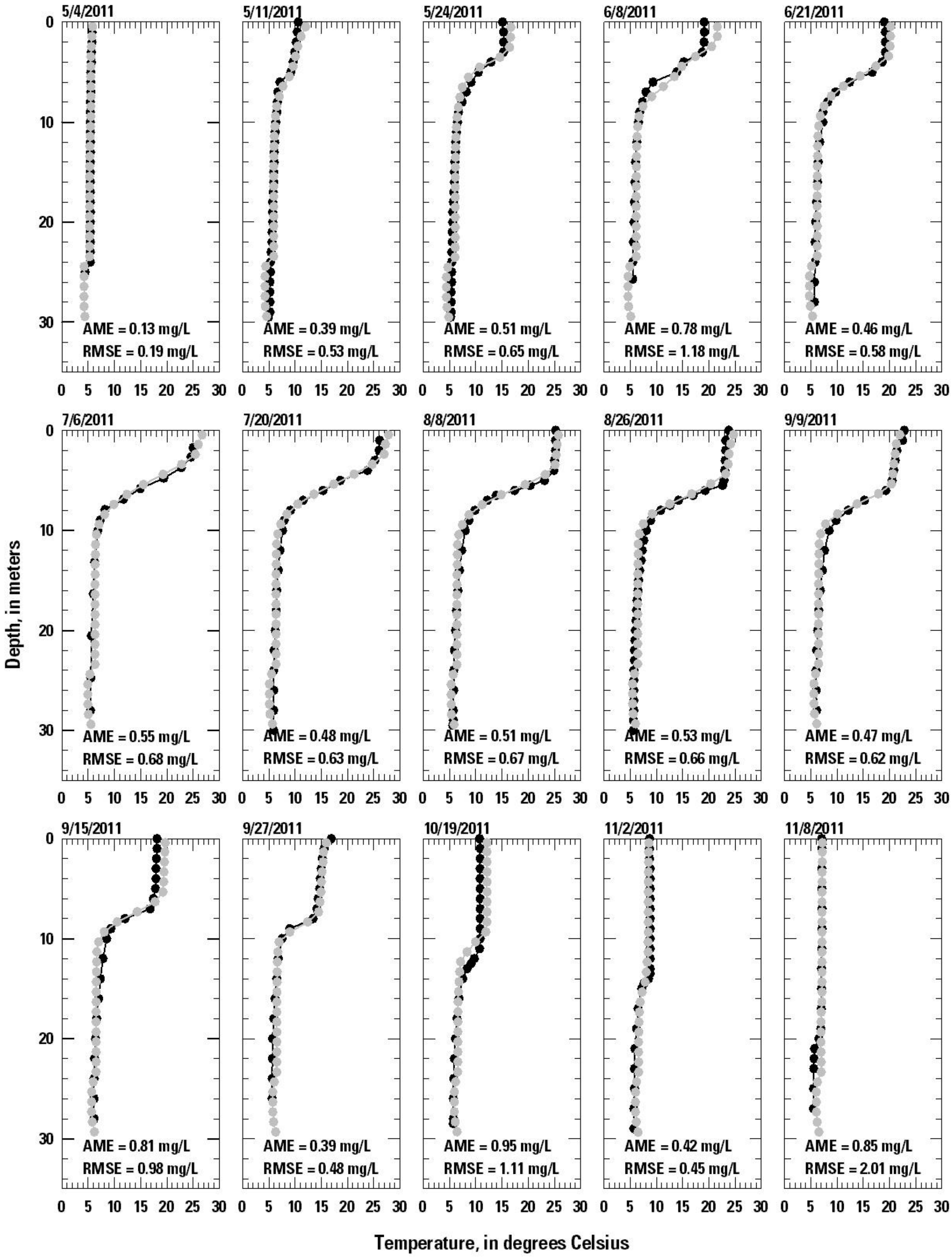

Figure 17. Simulated (gray) and measured (black) water temperature at south basin hole (USGS station number 471116095125301) in Elk Lake for 15 dates in 2011, with AME and RMSE quantities.

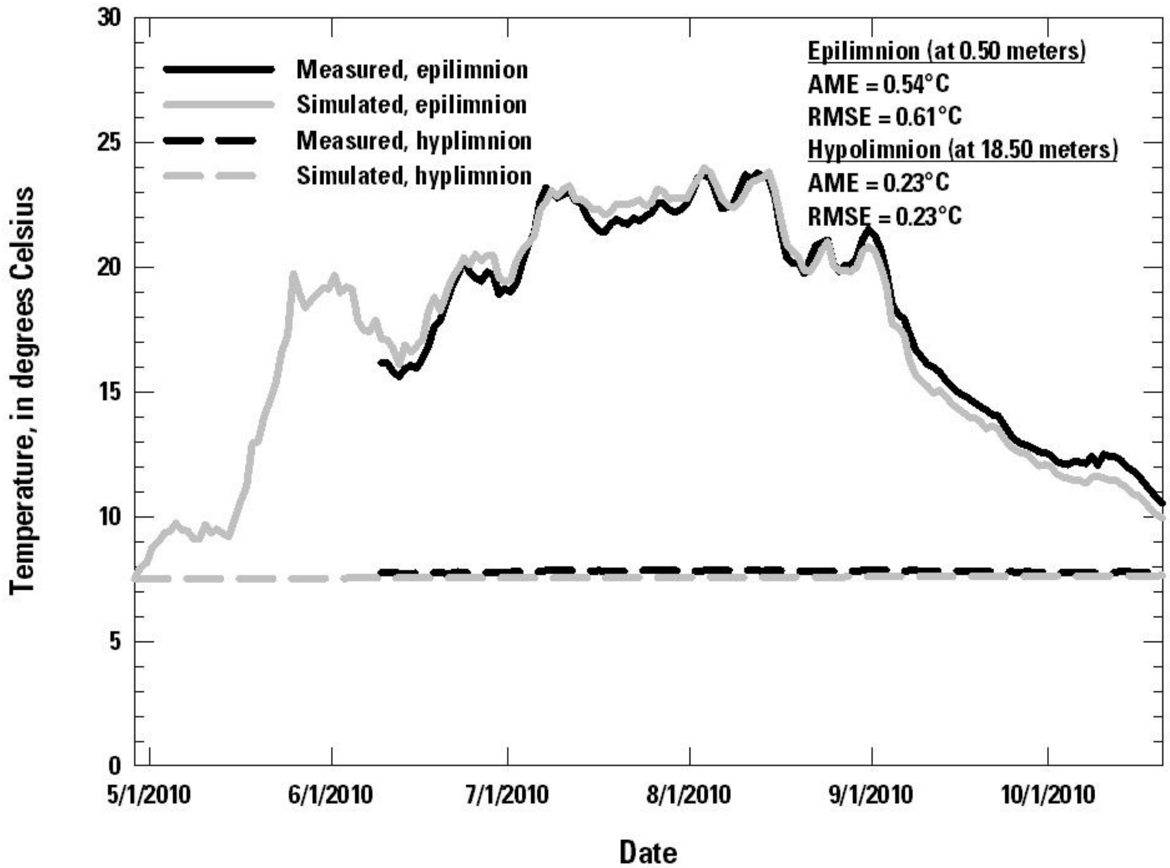

Figure 18. Simulated and measured water temperature for the epilimnion (0.5 meters) and hypolimnion (18.5 meters) at north basin hole (USGS station number 475214090100401) in Trout Lake, April 28, 2010 to October 20, 2010.

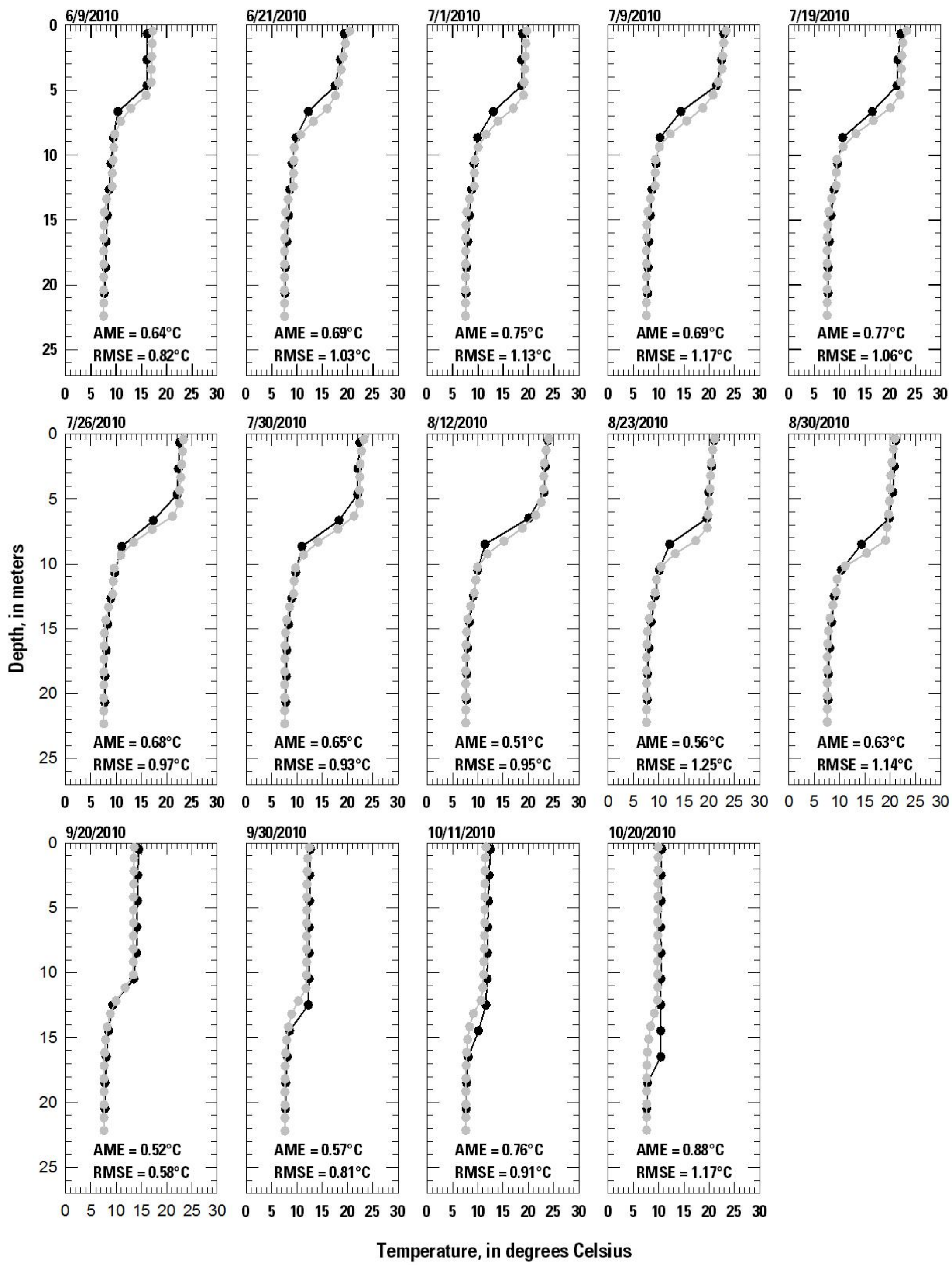

Figure 19. Simulated (gray) and measured (black) water temperature at north basin hole (USGS station number 475214090100401) in Trout Lake for 14 dates in 2010, with AME and RMSE quantities.

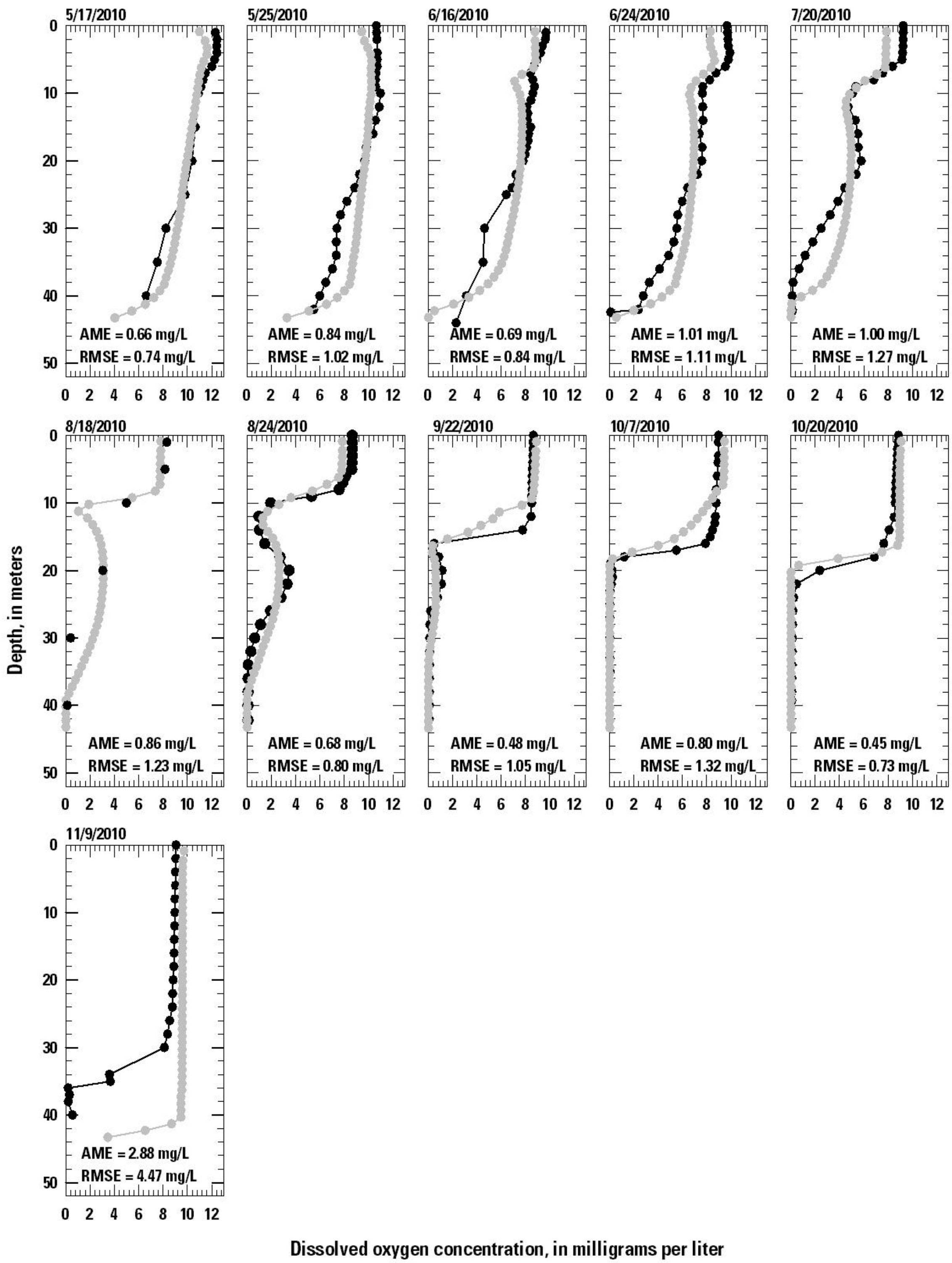

Figure 20. Simulated (gray) and measured (black) dissolved oxygen concentrations at Kecks Point (USGS station number 455843095212501) in Lake Carlos for 11 dates in 2010, with AME and RMSE quantities.

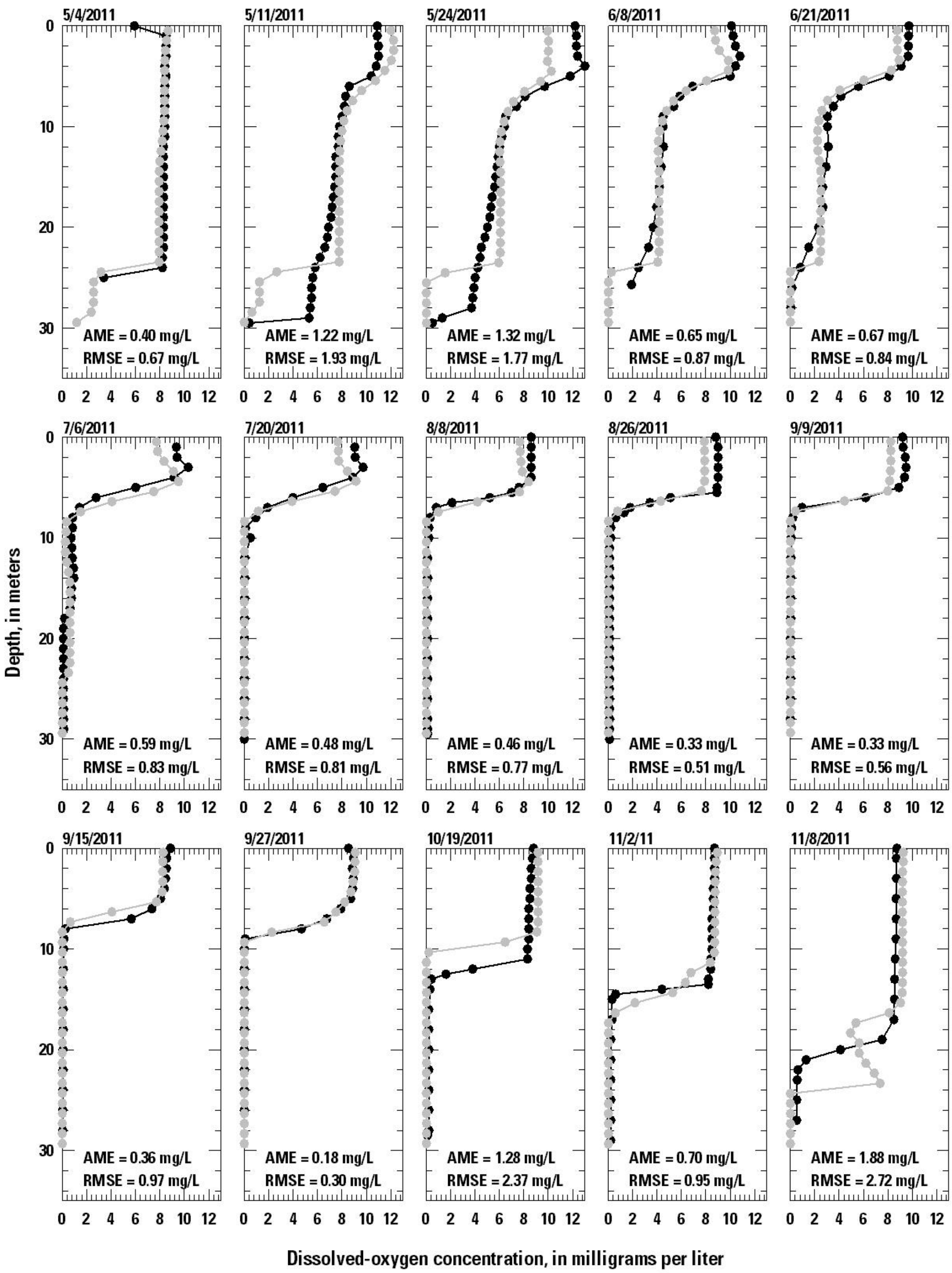

Figure 21. Simulated (gray) and measured (black) dissolved oxygen concentrations at south basin hole (USGS station number 471116095125301) in Elk Lake for 15 dates in 2011, with AME and RMSE quantities.

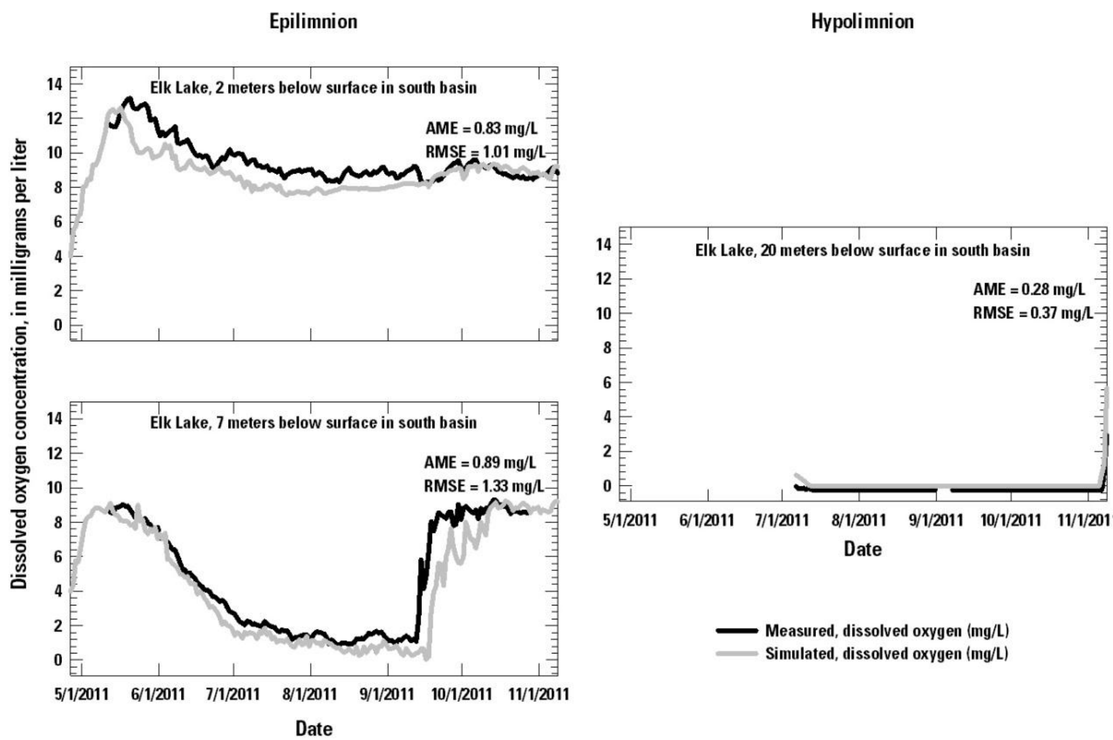

Figure 22. Continuous simulated and measured dissolved oxygen concentrations at south basin hole (USGS station number 471116095125301) in Elk Lake for three different depths (2, 7 and 20 meters below the water surface), with AME and RMSE quantities, April 26, 2011 to November 8, 2011.

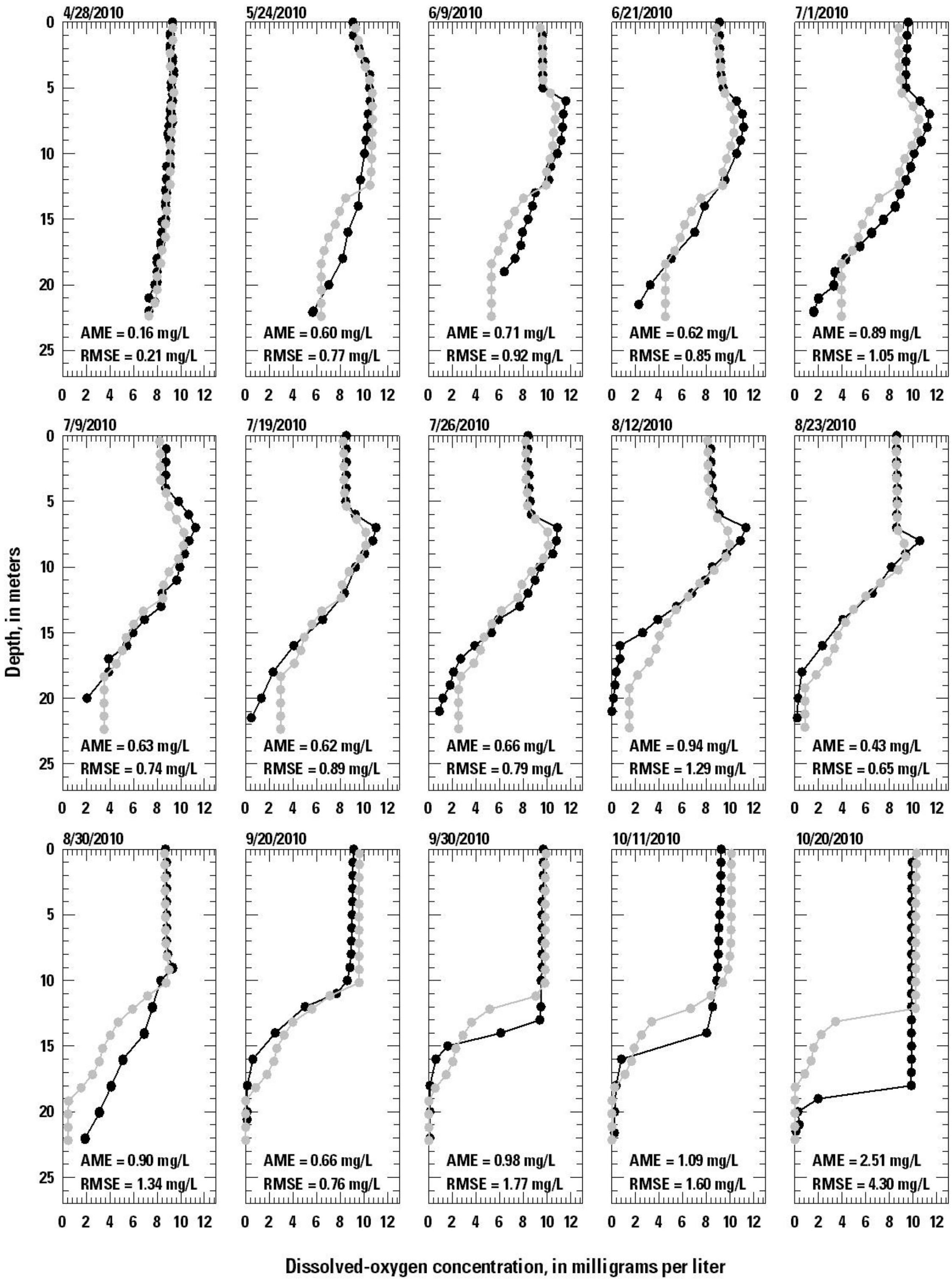

Figure 23. Simulated (gray) and measured (black) dissolved oxygen concentrations at north basin (USGS station number 475214090100401) in Trout Lake for 15 dates in 2010, with AME and RMSE quantities.

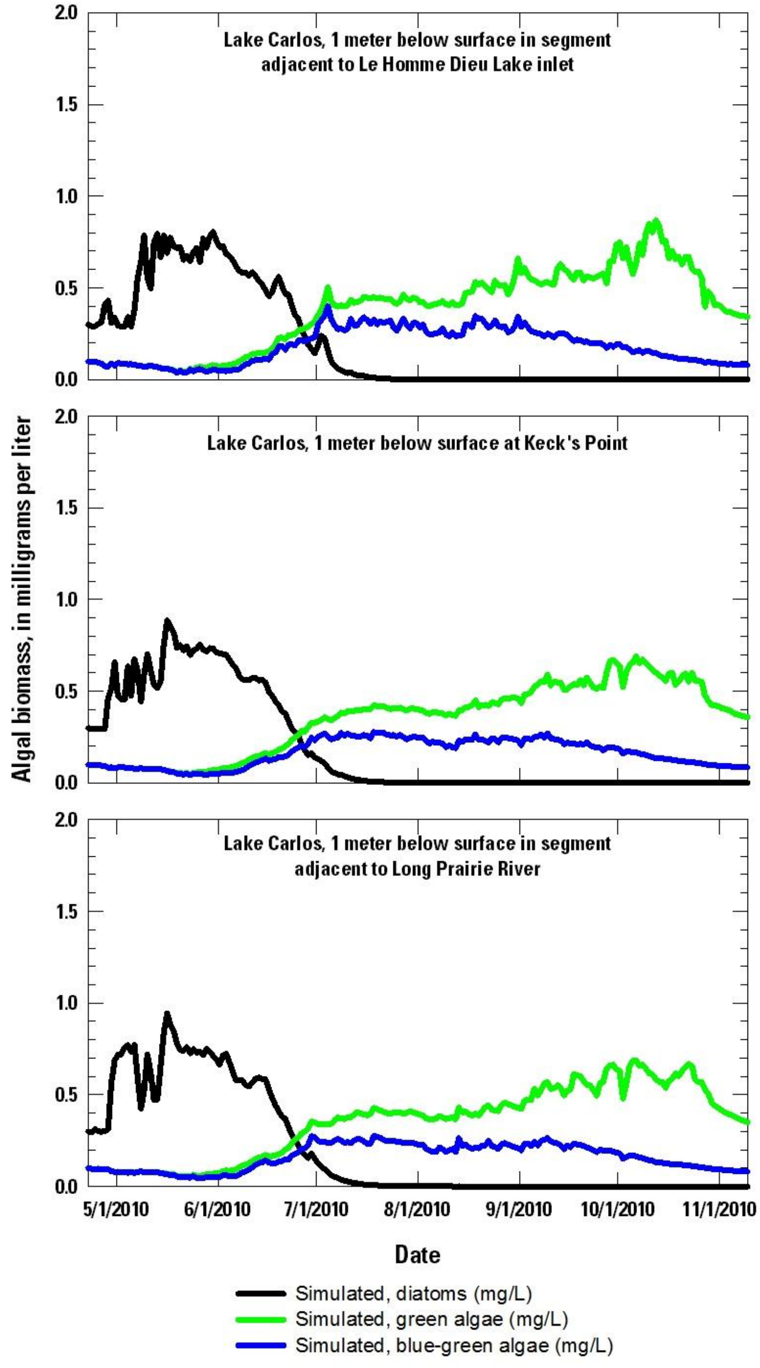

Figure 24. Simulated algal group distributions (diatoms, green, and blue-green algae) for three different segments in Lake Carlos, April 22, 2010 to November 9, 2010.

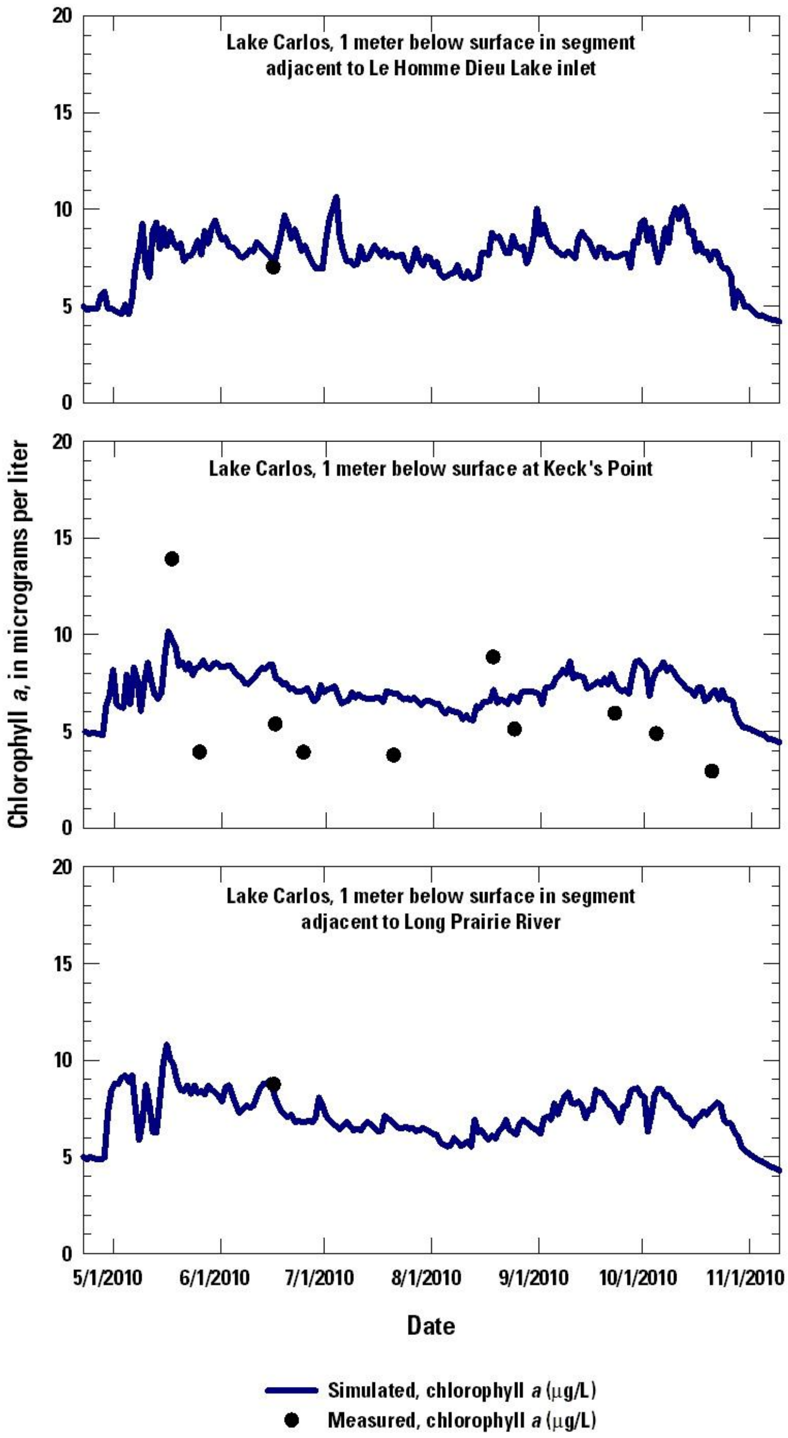

Figure 25. Simulated and measured chlorophyll *a* concentrations (in µg/L) for three different segments in Lake Carlos, April 22, 2010 to November 9, 2010.

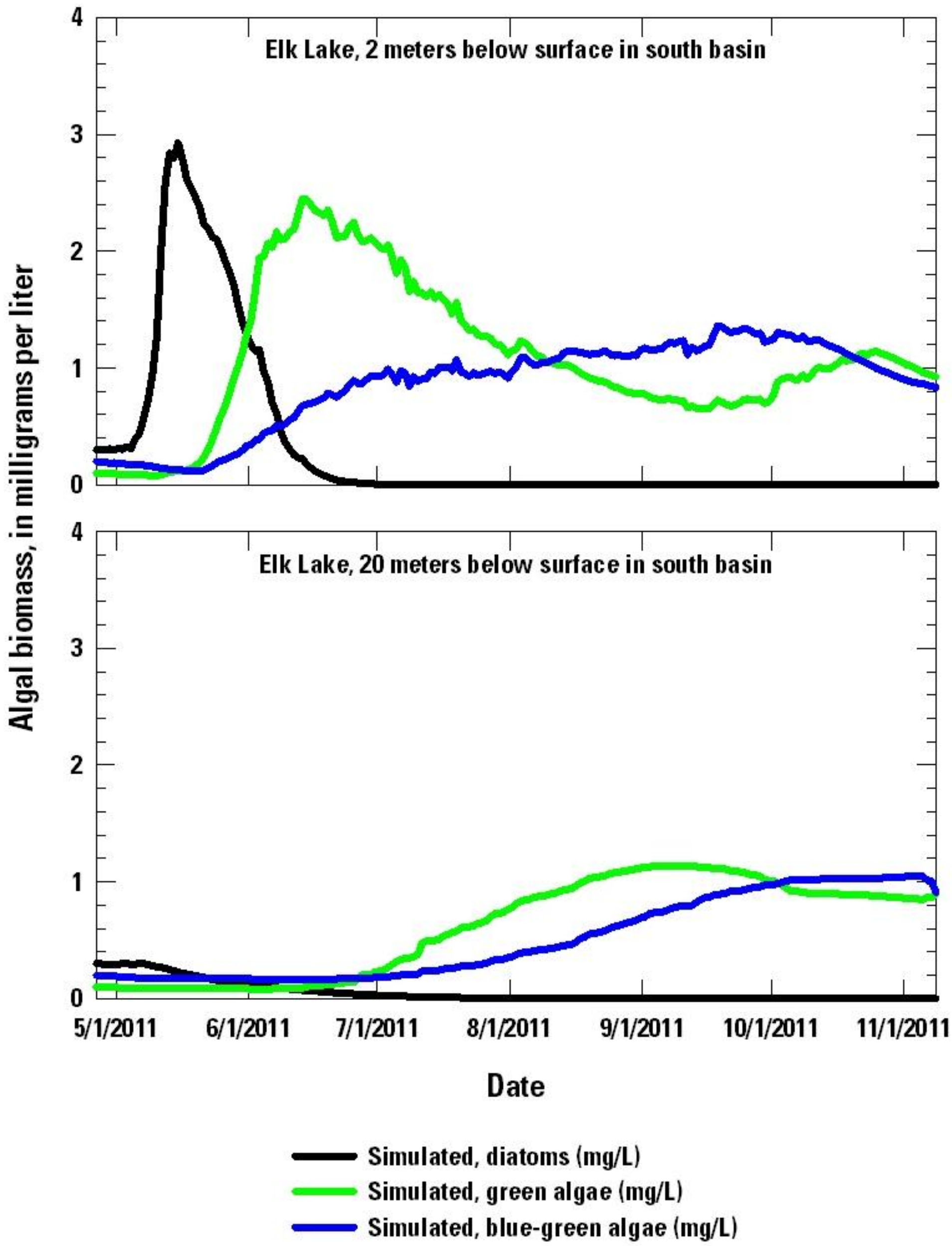

Figure 26. Simulated algal group distributions (diatoms, green, and blue-green algae) for two different depths at south basin hole (USGS station number 471116095125301) in Elk Lake, April 26, 2011 to November 8, 2011.

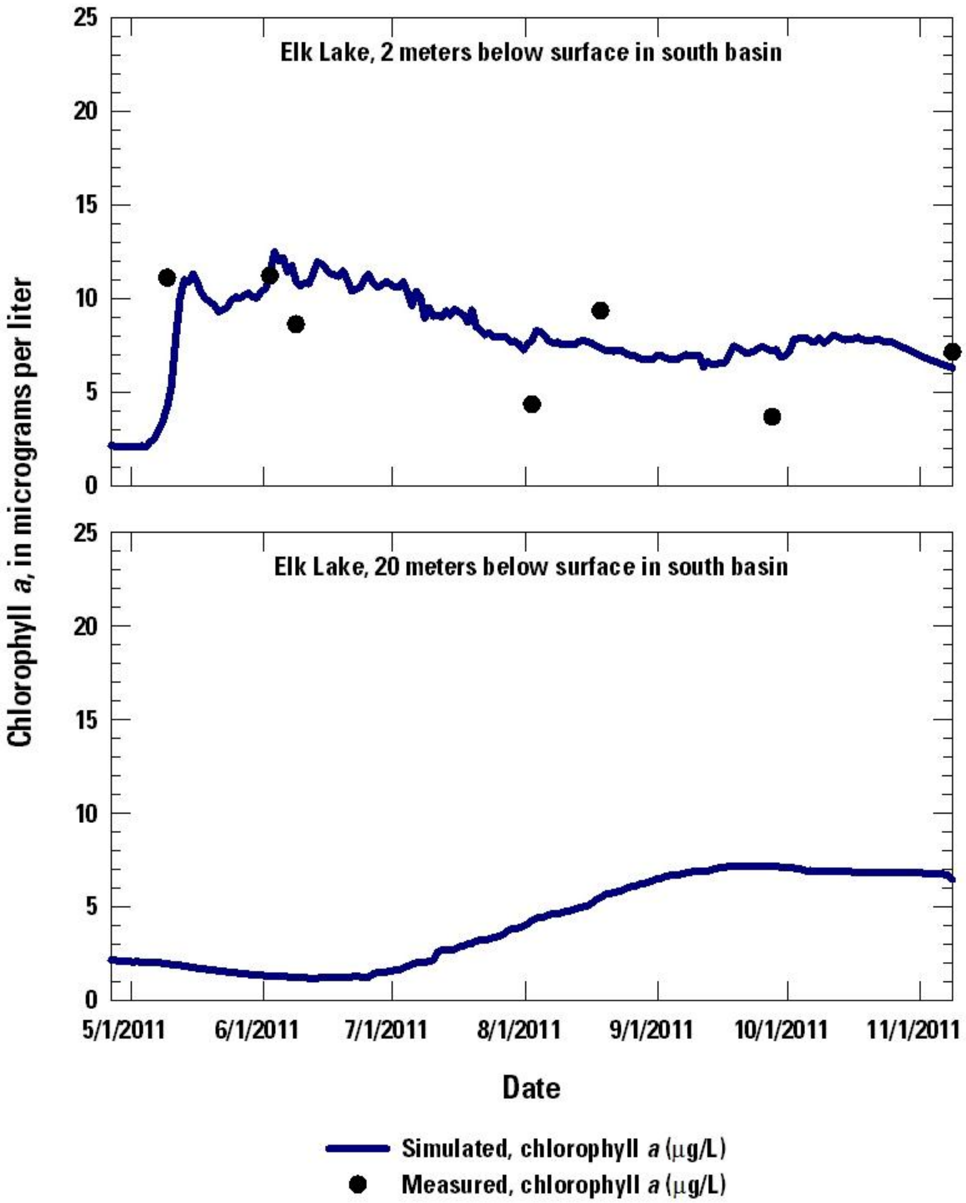

Figure 27. Simulated and measured chlorophyll *a* concentrations (in µg/L) for two different depths at south basin hole (USGS station number 471116095125301) in Elk Lake, April 26, 2011 to November 8, 2011.

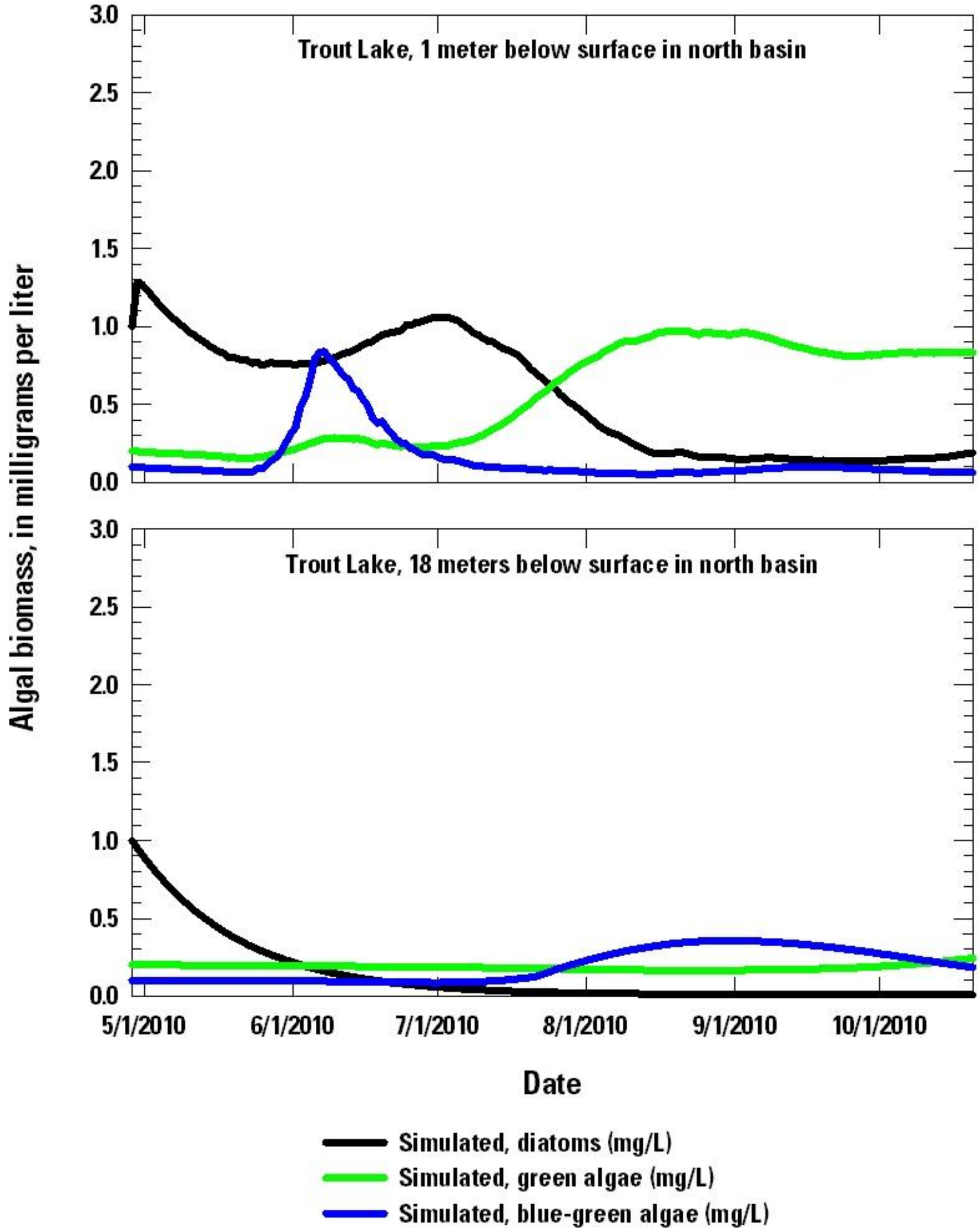

Figure 28. Simulated algal group distributions (diatoms, green, and blue-green algae) for two different depths at north basin hole (USGS station number 475214090100401) in Trout Lake, April 28, 2010 to October 20, 2010.

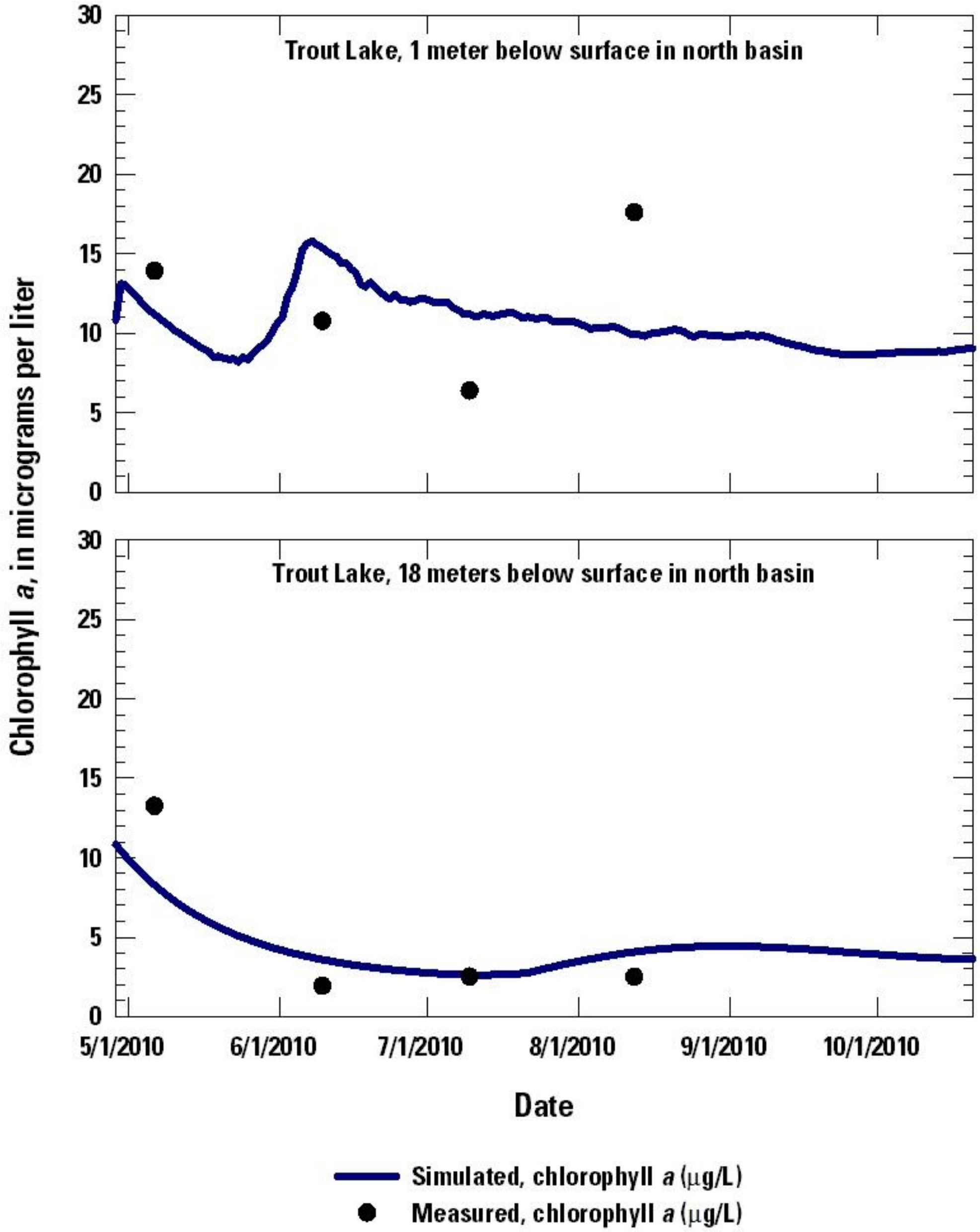

Figure 29. Simulated and measured chlorophyll *a* concentrations (in μg/L for two different depths at north basin hole (USGS station number 475214090100401) in Trout Lake, April 28, 2010 to October 20, 2010..

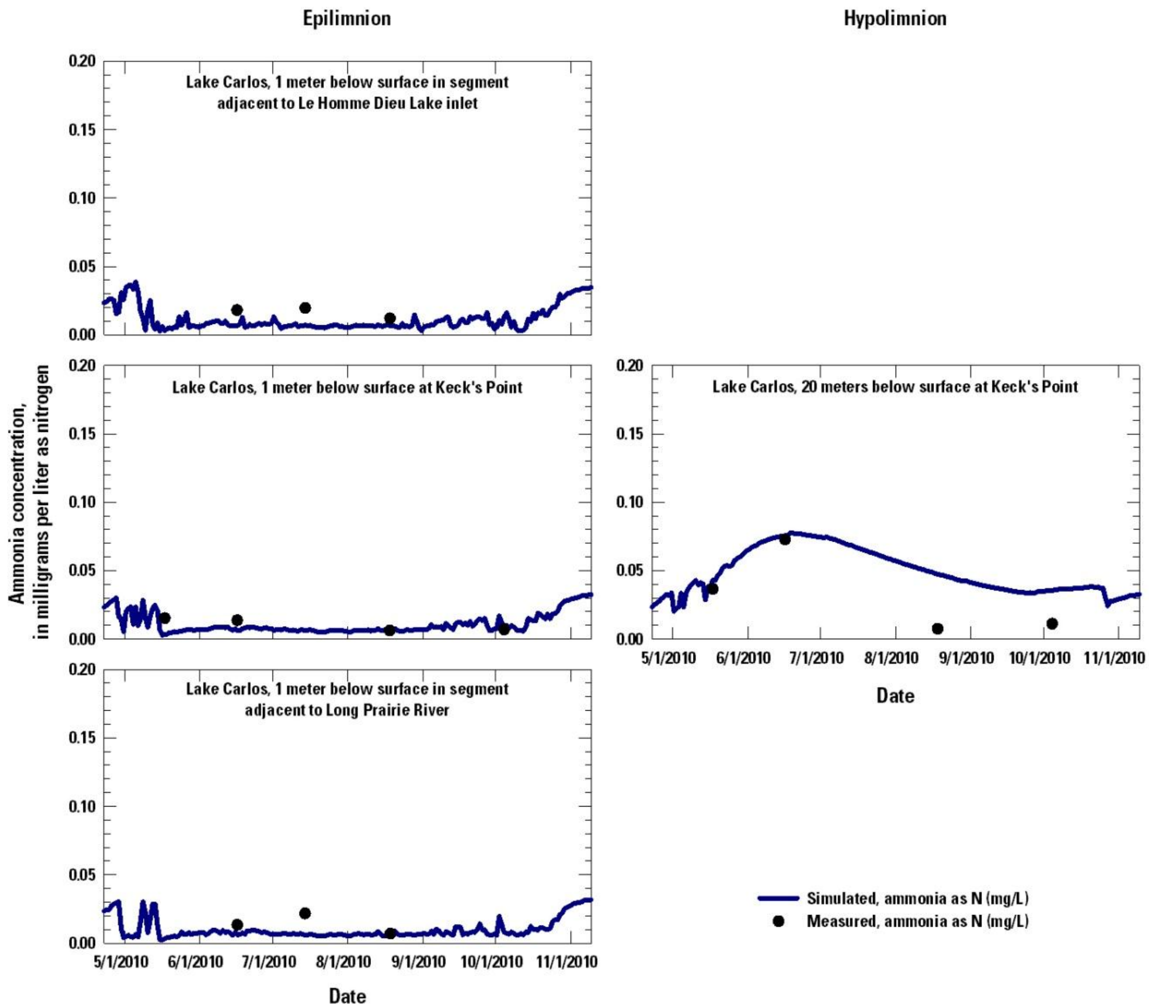

Figure 30. Simulated and measured ammonia (as N) concentrations (in mg/L) for three different segments in Lake Carlos, April 22, 2010 to November 9, 2010.

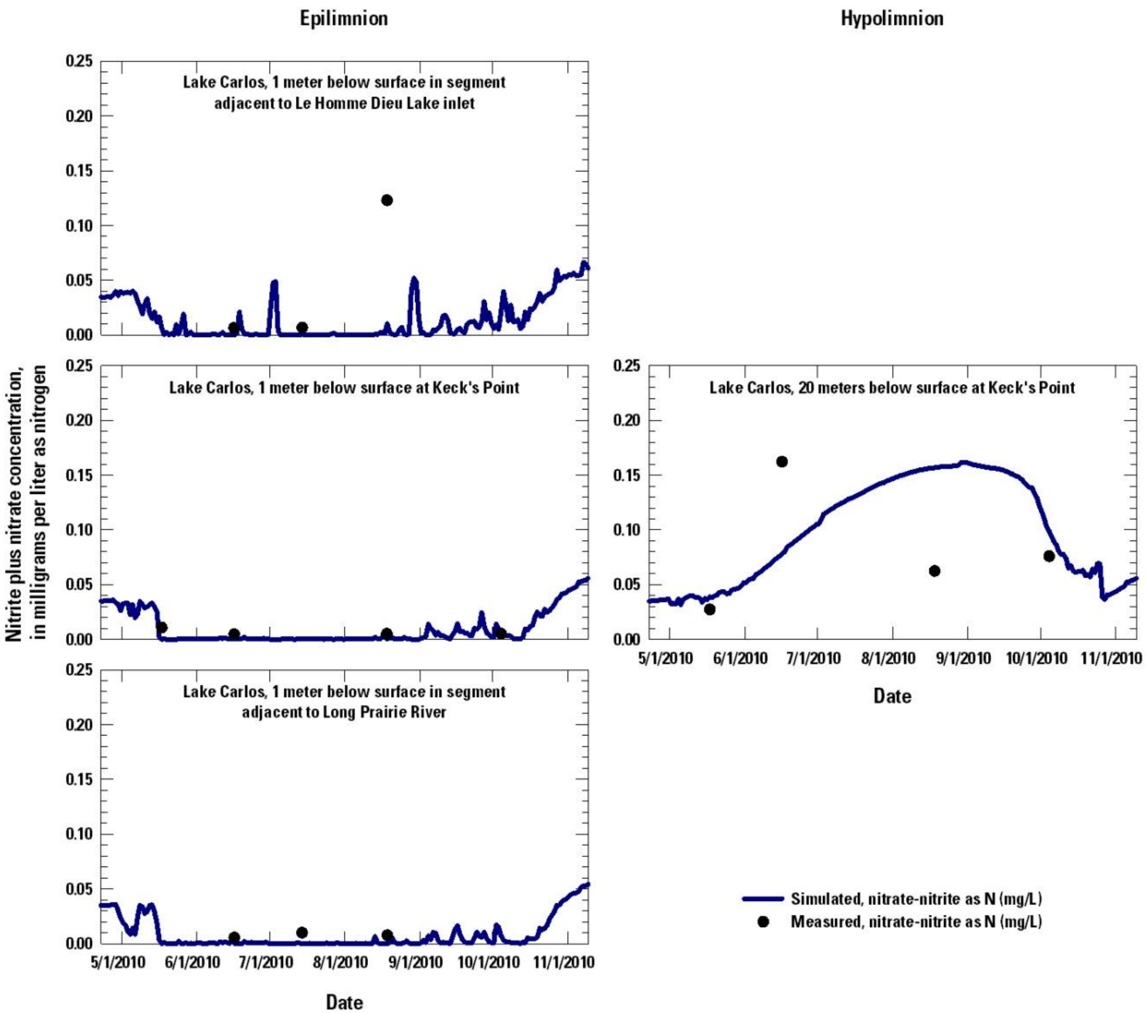

Figure 31. Simulated and measured nitrate-nitrite (as N) concentrations (in mg/L) for three different segments at Kecks Point (USGS station number 455843095212501) in Lake Carlos, April 22, 2010 to November 9, 2010.

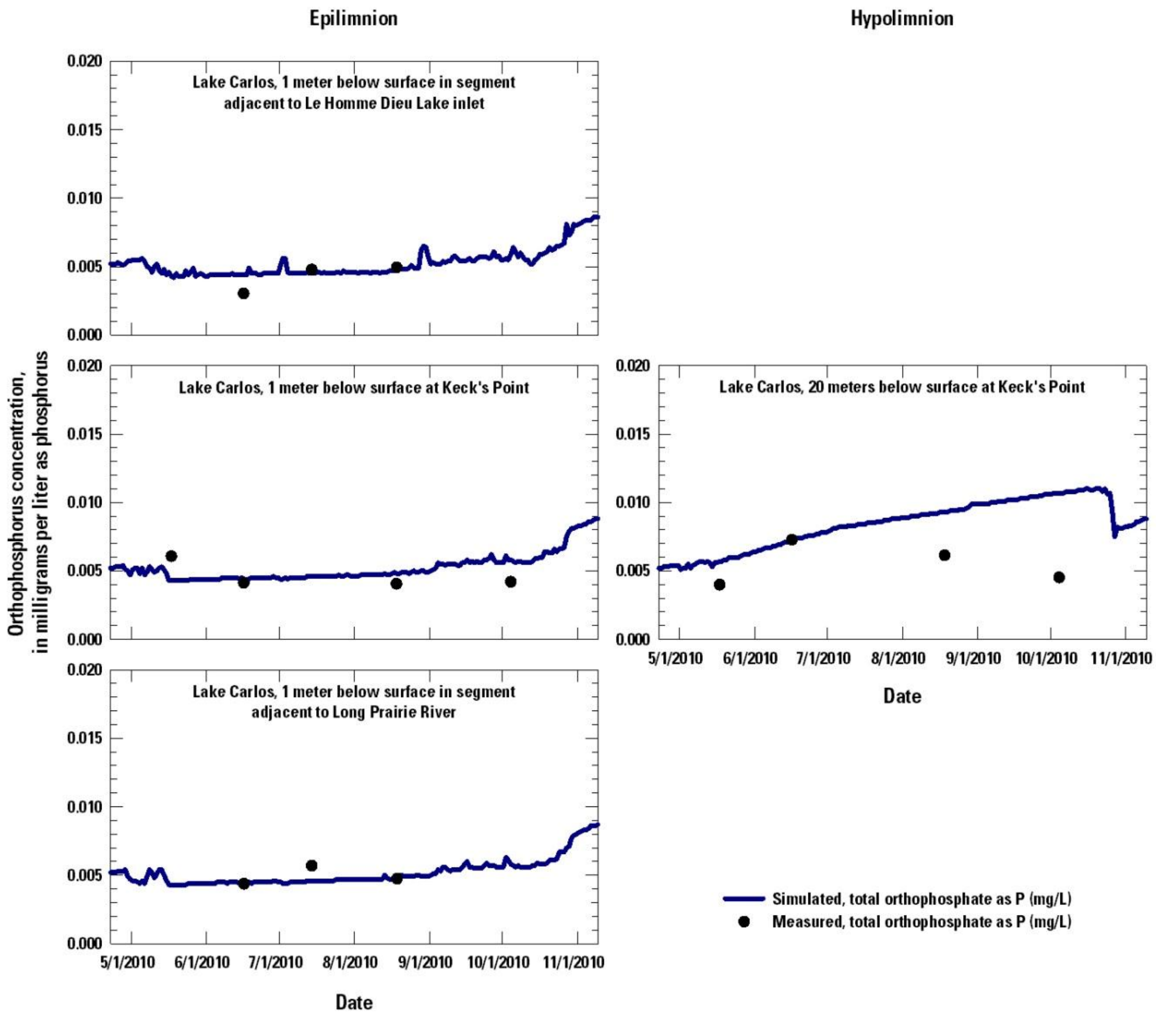

Figure 32. Simulated and measured orthophosphorus (as P) concentrations (in mg/L) for three different segments at Kecks Point (USGS station number 455843095212501) in Lake Carlos, April 22, 2010 to November 9, 2010.

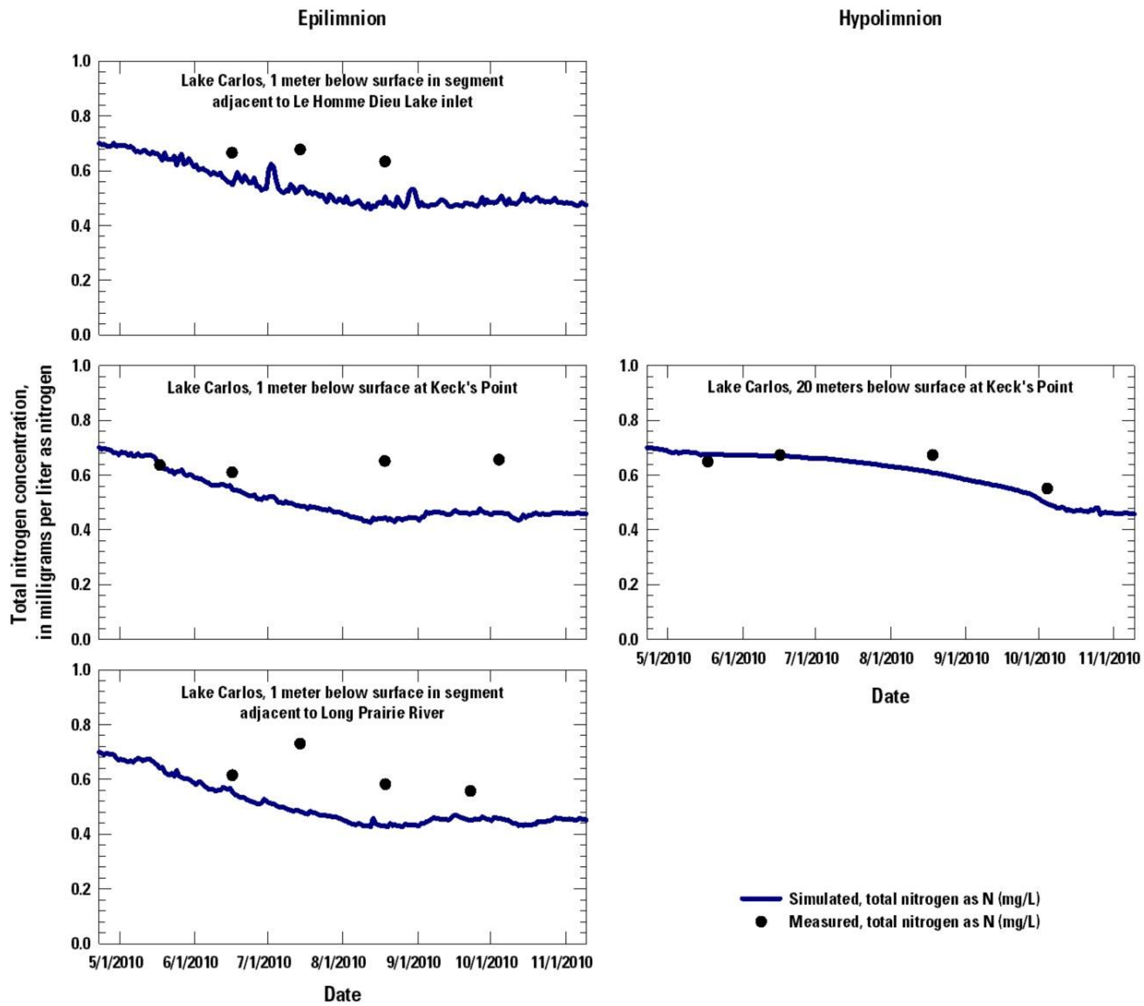

Figure 33. Simulated and measured total nitrogen concentrations (in mg/L) for three different segments at Kecks Point (USGS station number 455843095212501) in Lake Carlos, April 22, 2010 to November 9, 2010.

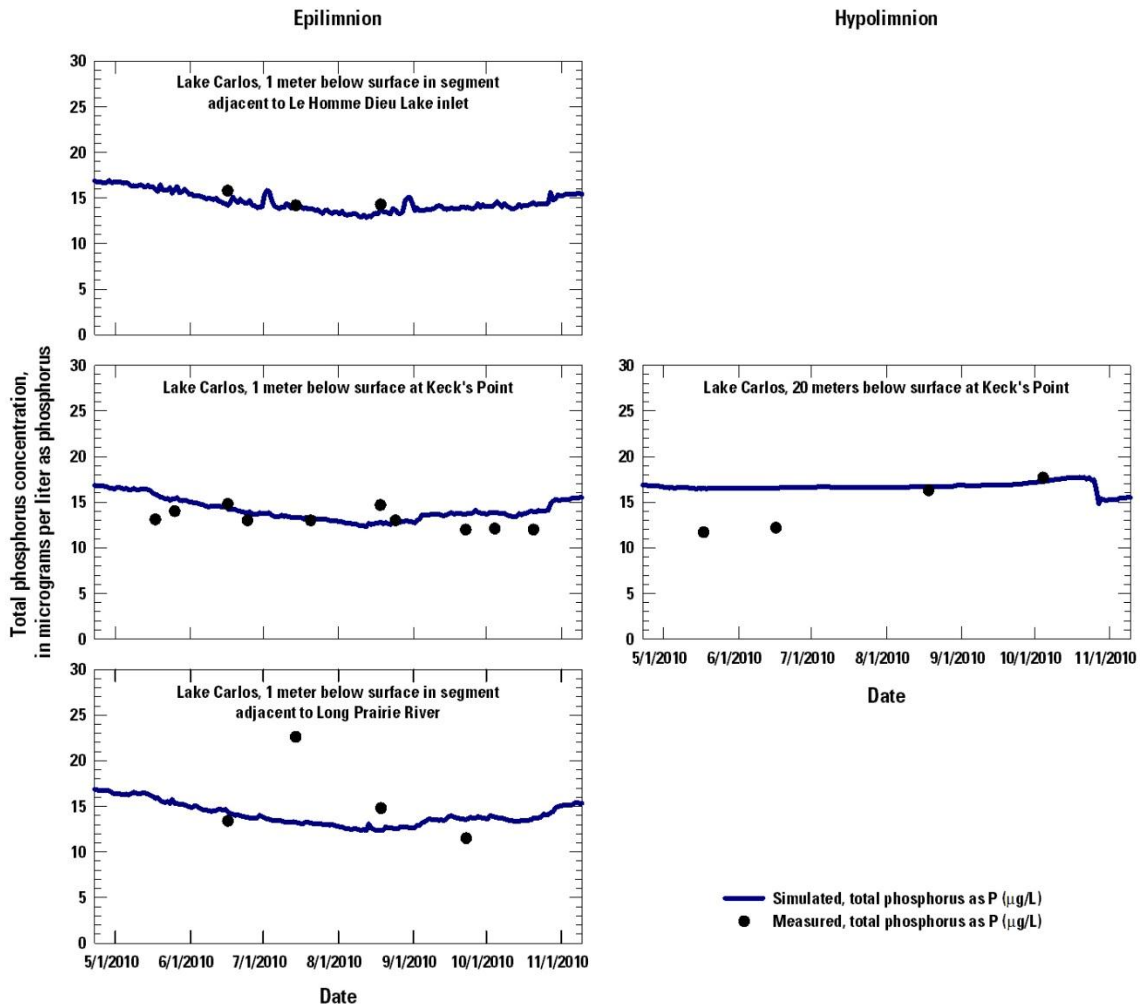

Figure 34. Simulated and measured total phosphorus concentrations (in µg/L) for three different segments at Kecks Point (USGS station number 455843095212501) in Lake Carlos, April 22, 2010 to November 9, 2010.

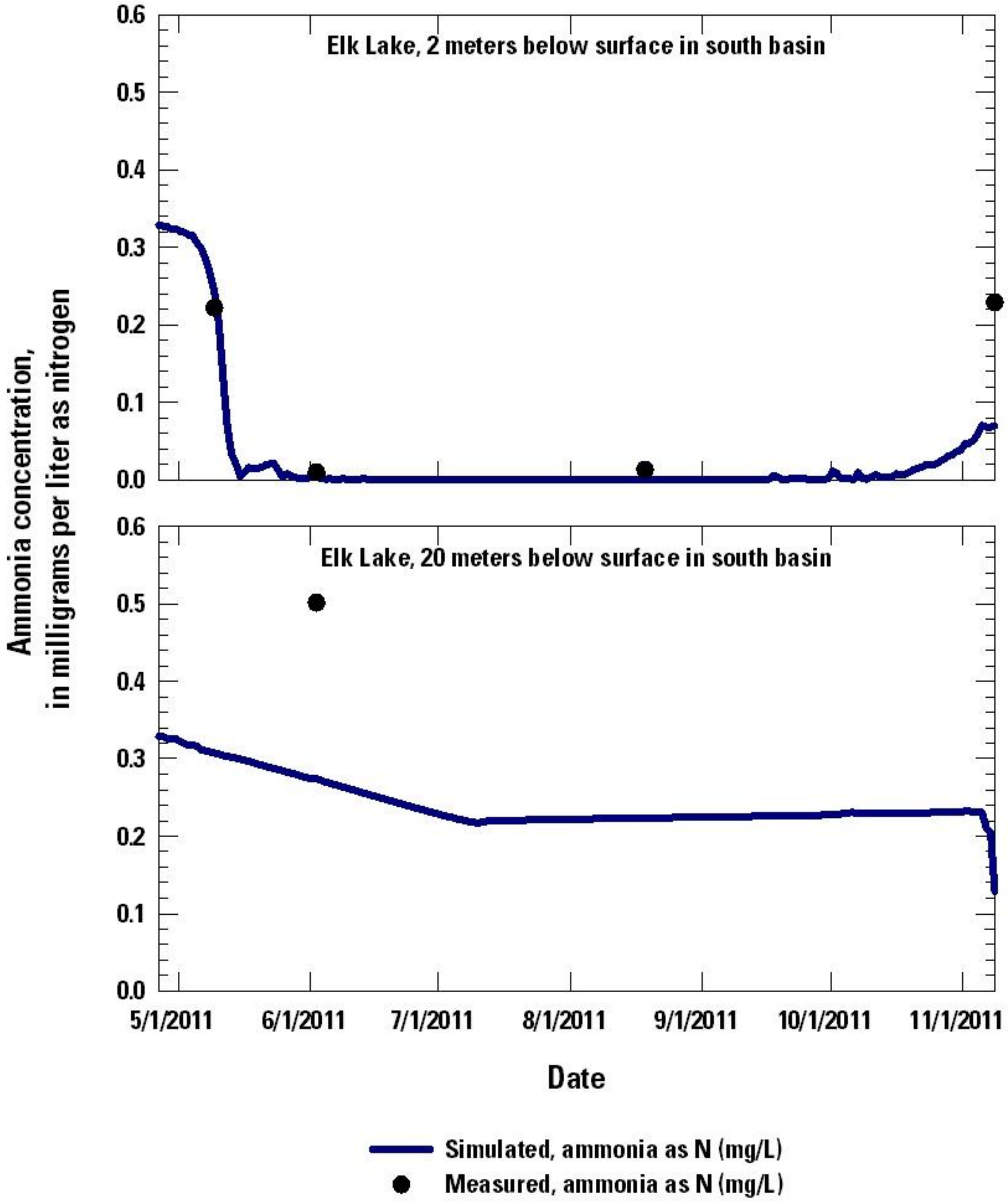

Figure 35. Simulated and measured ammonia (as N) concentrations (in mg/L) for two different depths at south basin hole (USGS station number 471116095125301) in Elk Lake, April 26, 2011 to November 8, 2011.

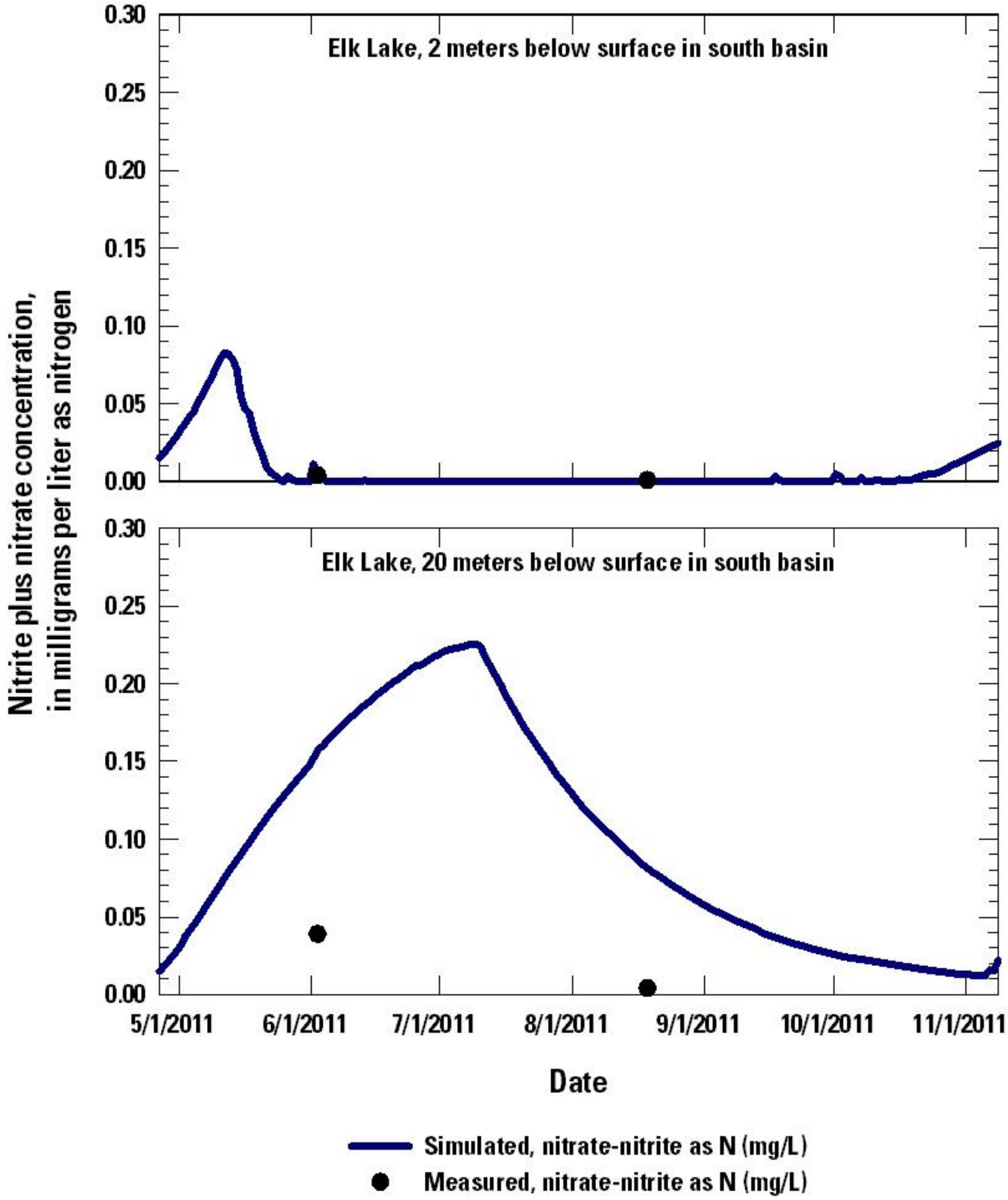

Figure 36. Simulated and measured nitrate-nitrite (as N) concentrations (in mg/L) for two different depths at south basin hole (USGS station number 471116095125301) in Elk Lake, April 26, 2011 to November 8, 2011.

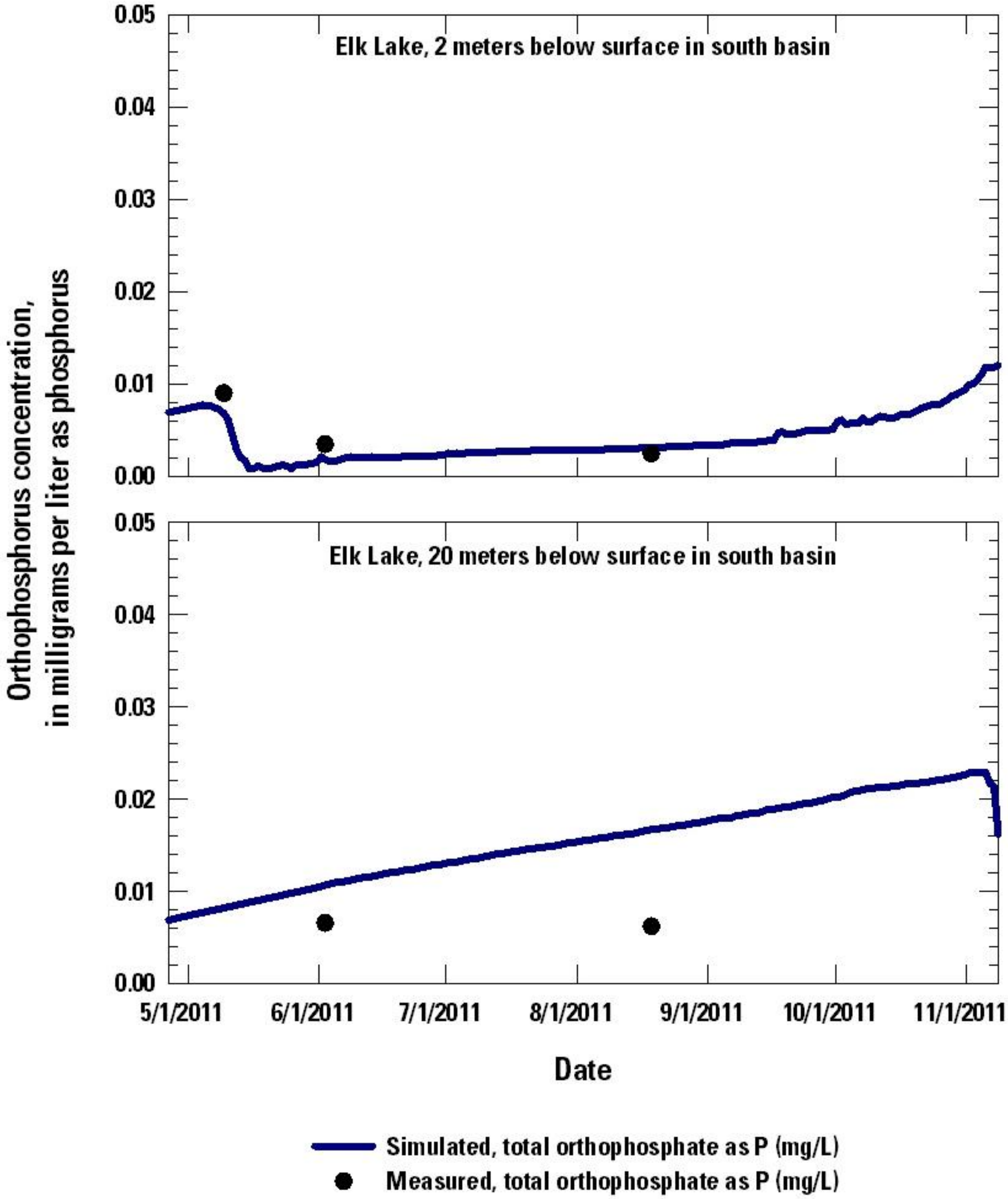

Figure 37. Simulated and measured orthophosphorus (as P) concentrations (in mg/L) for two different depths at south basin hole (USGS station number 471116095125301) in Elk Lake, April 26, 2011 to November 8, 2011.

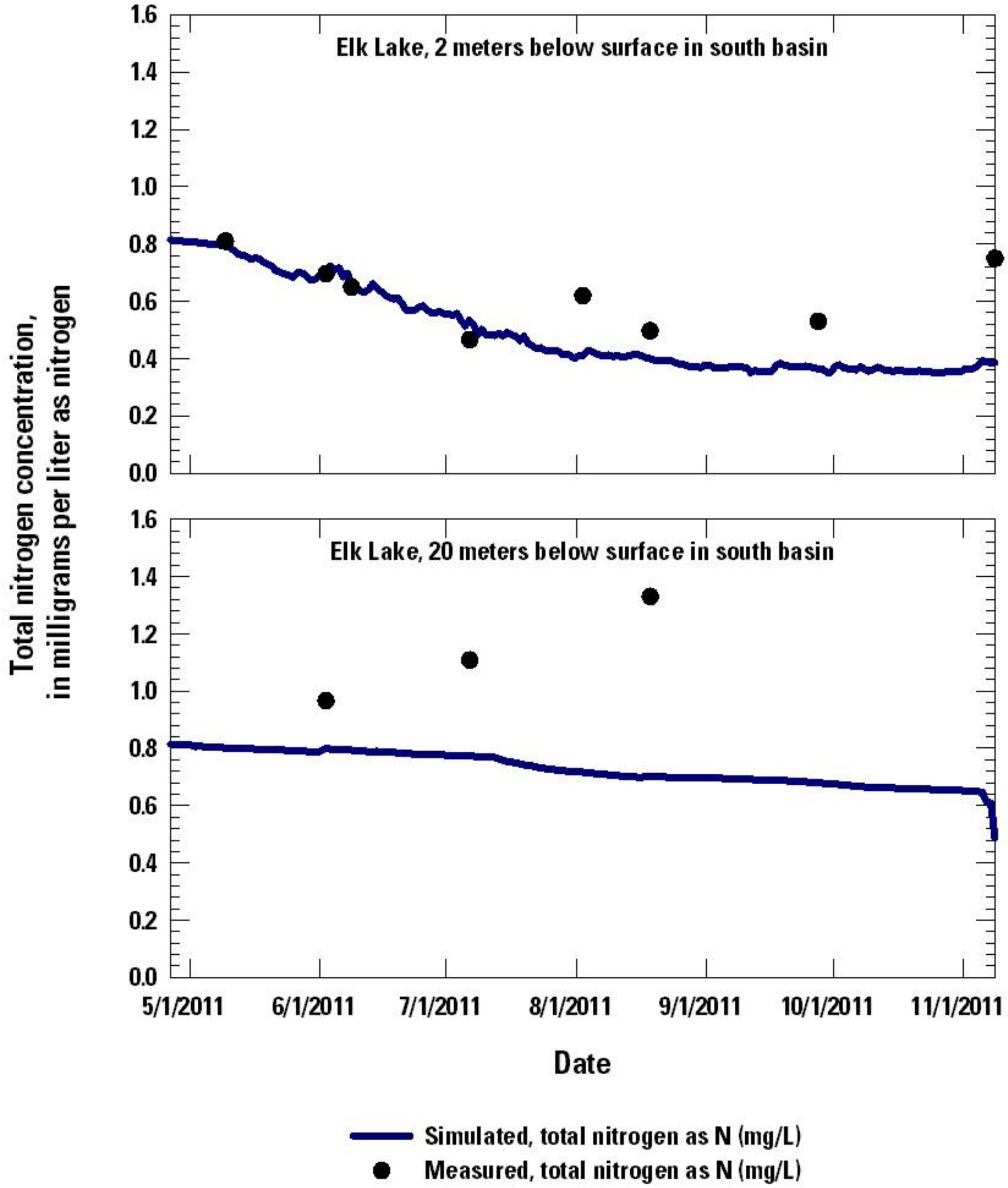

Figure 38. Simulated and measured total nitrogen concentrations (in mg/L) for two different depths at south basin hole (USGS station number 471116095125301) in Elk Lake, April 26, 2011 to November 8, 2011.

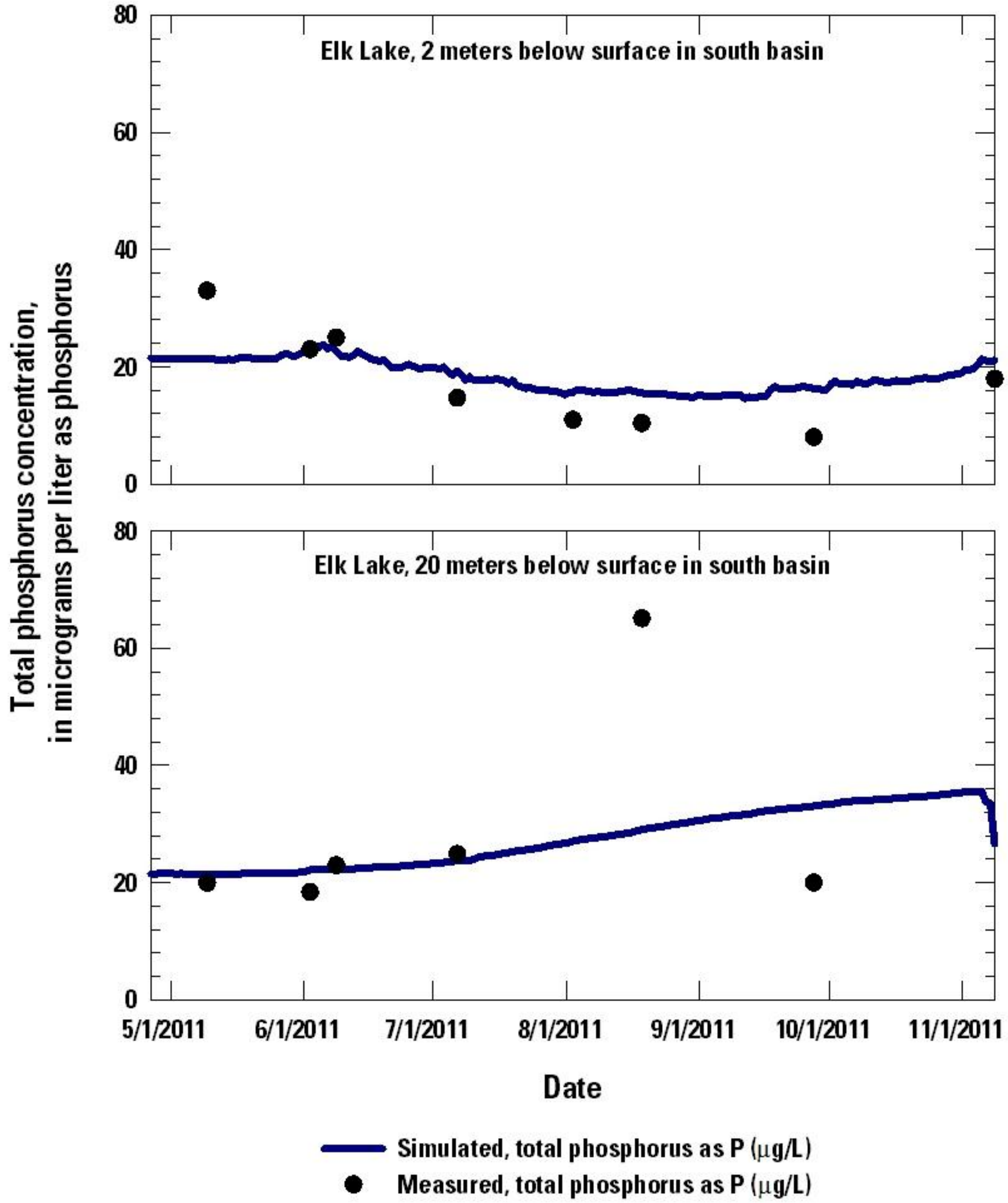

Figure 39. Simulated and measured total phosphorus concentrations (in µg/L) for two different depths at south basin hole (USGS station number 471116095125301) in Elk Lake, April 26, 2011 to November 8, 2011.

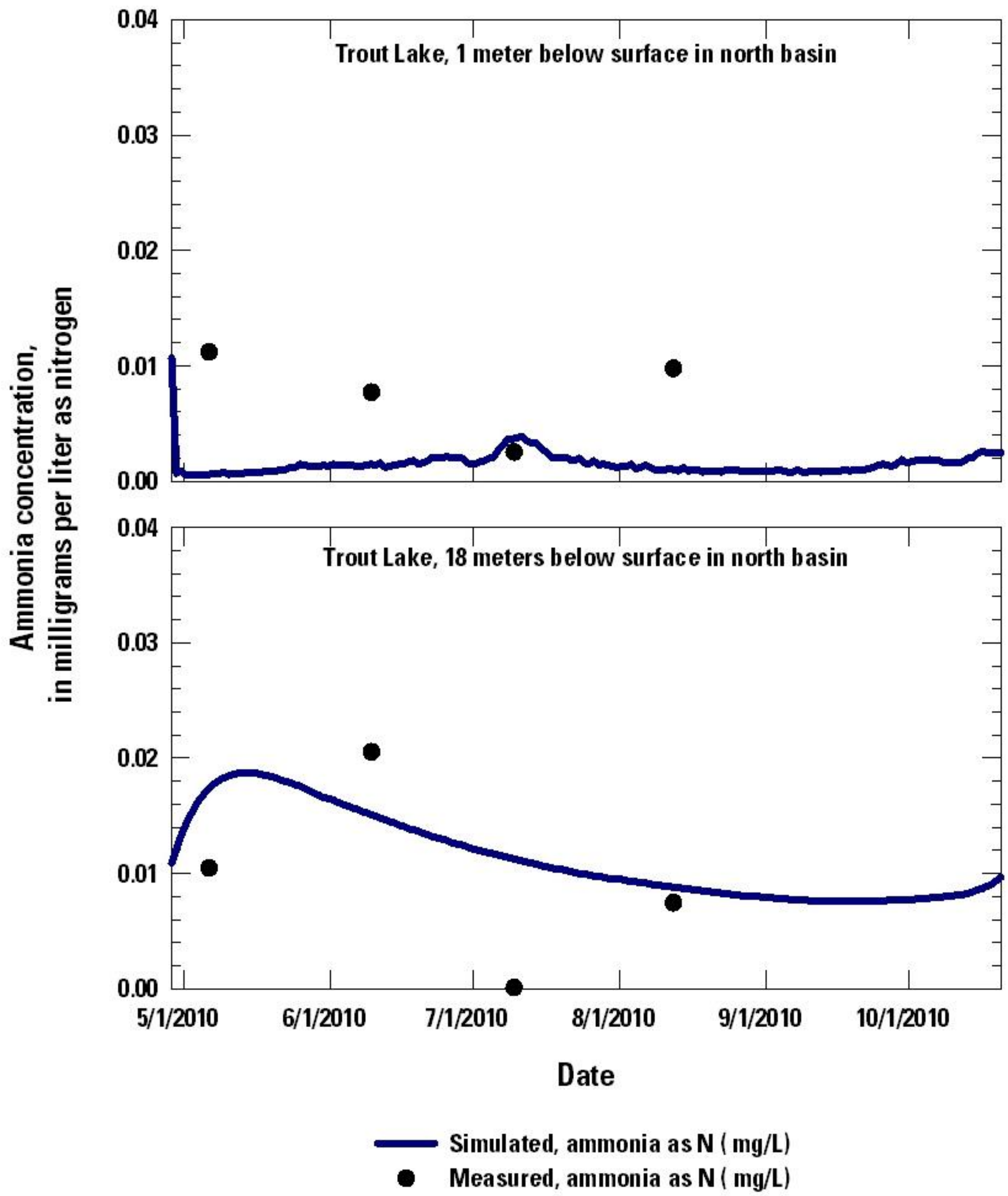

Figure 40. Simulated and measured ammonia (as N) concentrations (in mg/L) for two different depths at north basin hole (USGS station number 475214090100401) in Trout Lake, April 28, 2010 to October 20, 2010.

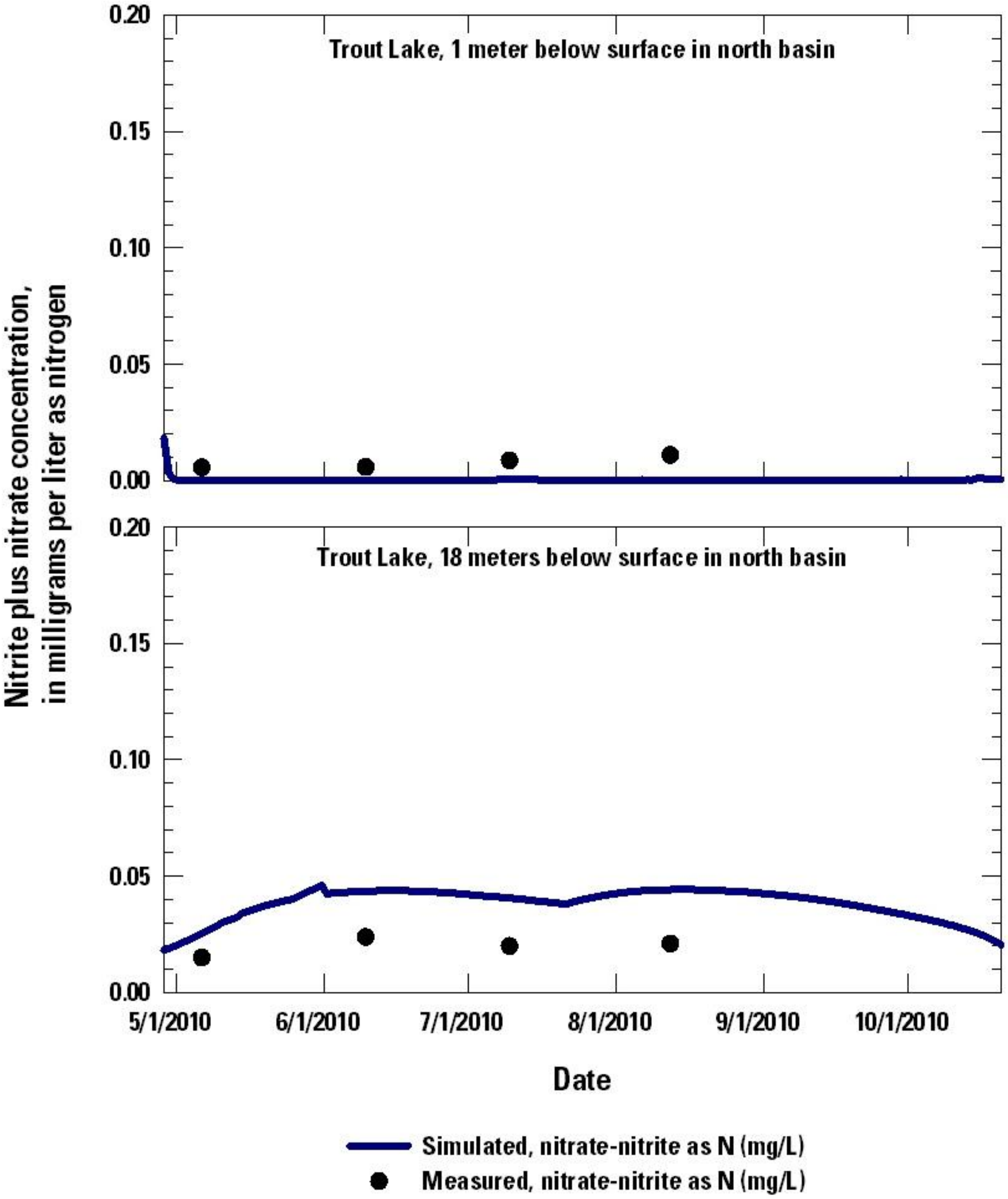

Figure 41. Simulated and measured nitrate-nitrite (as N) concentrations (in mg/L) for two different depths at north basin hole (USGS station number 475214090100401) in Trout Lake, April 28, 2010 to October 20, 2010.

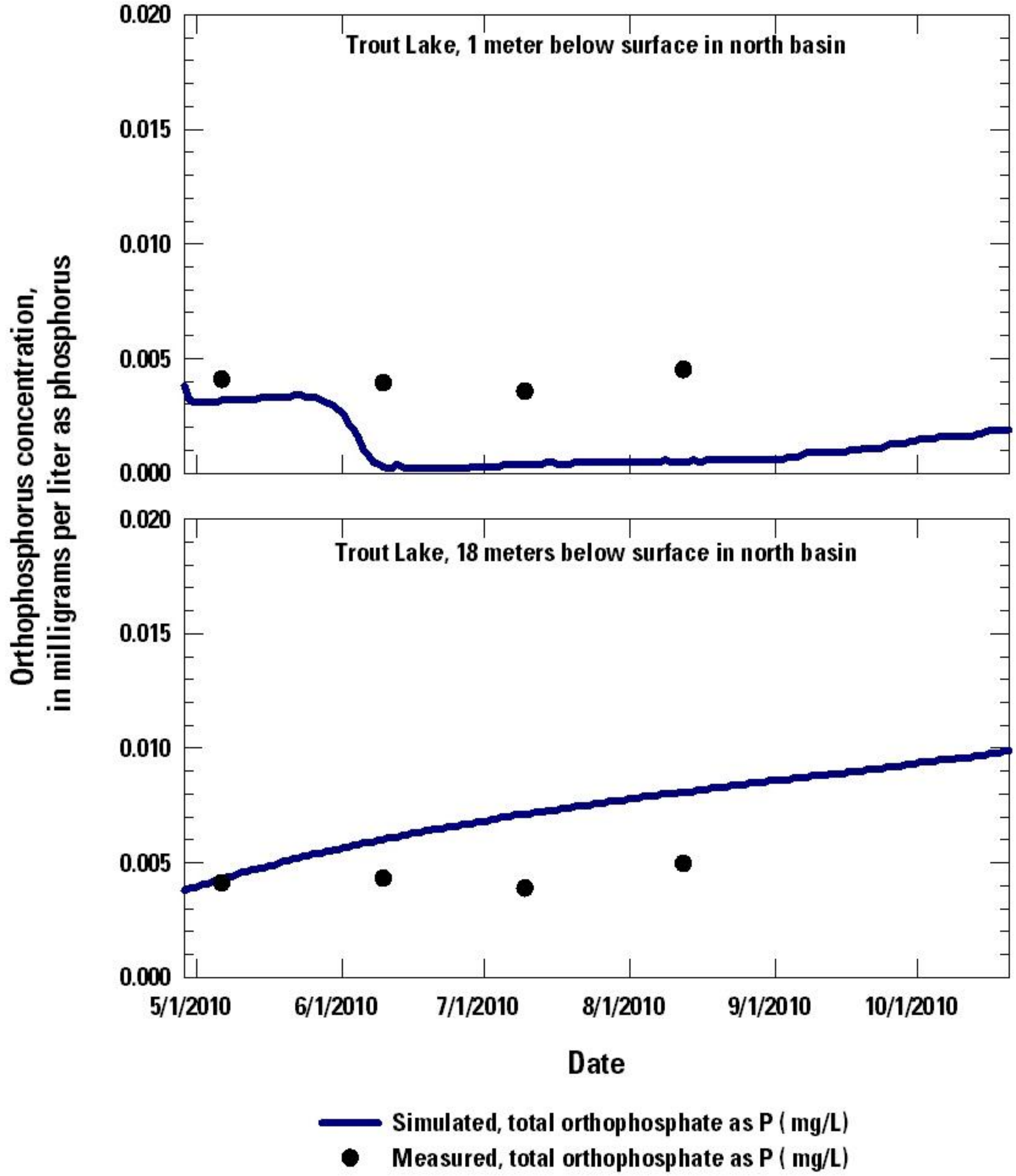

Figure 42. Simulated and measured orthophosphorus (as P) concentrations (in mg/L) for two different depths at north basin hole (USGS station number 475214090100401) in Trout Lake, April 28, 2010 to October 20, 2010.

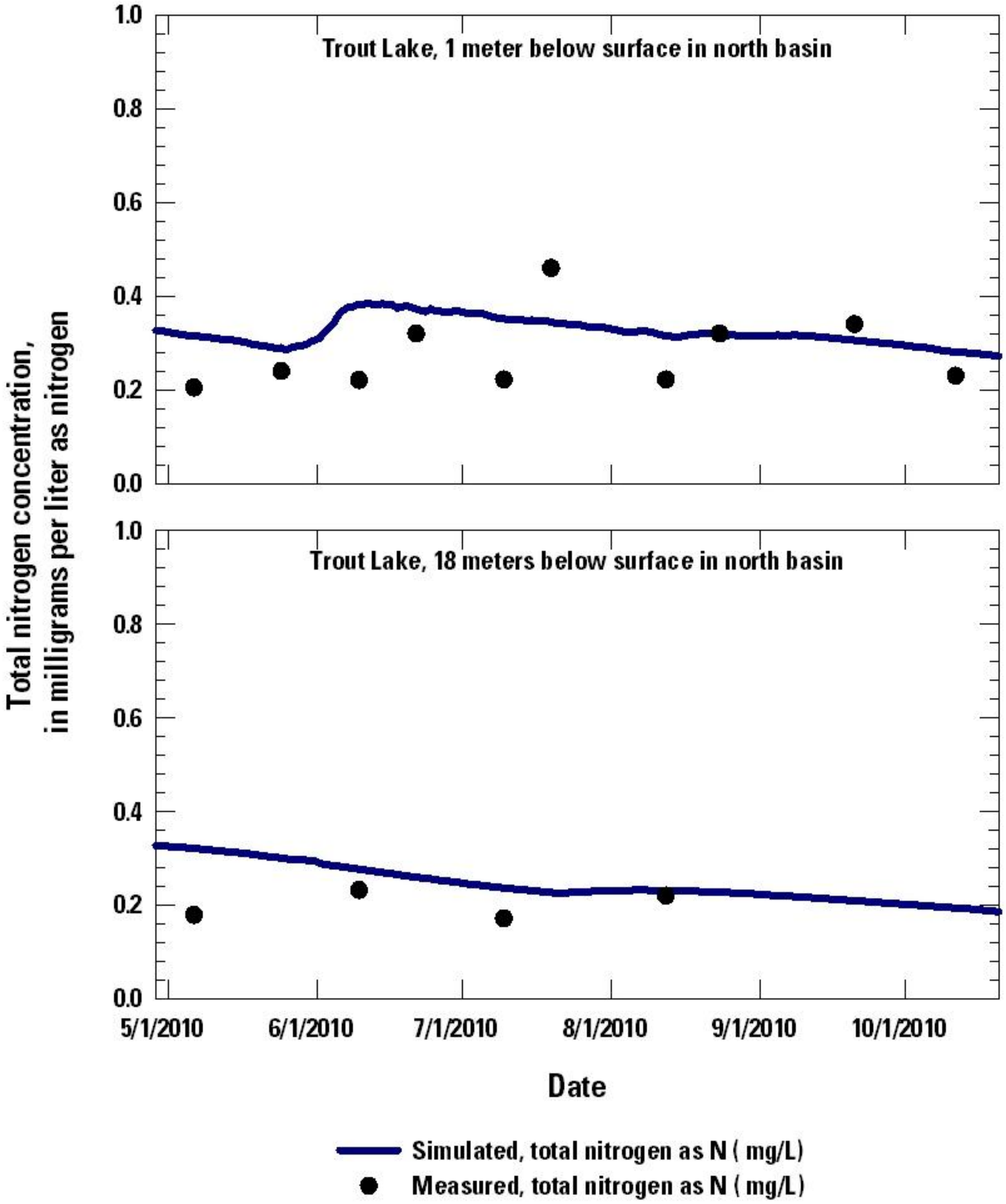

Figure 43. Simulated and measured total nitrogen concentrations (in mg/L) for two different depths at north basin hole (USGS station number 475214090100401) in Trout Lake, April 28, 2010 to October 20, 2010.

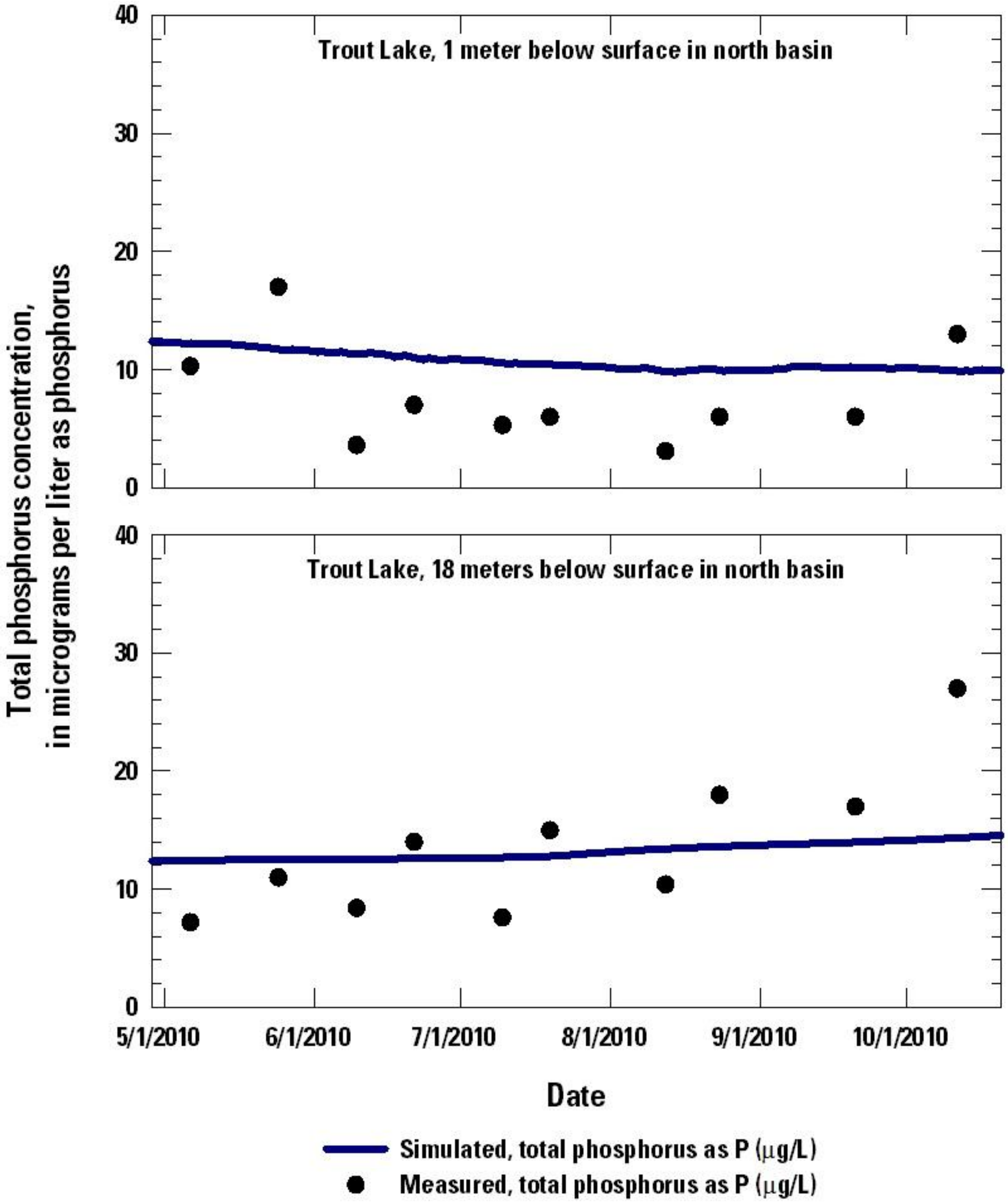

Figure 44. Simulated and measured total phosphorus concentrations (in µg/L) for two different depths at north basin hole (USGS station number 475214090100401) in Trout Lake, April 28, 2010 to October 20, 2010.

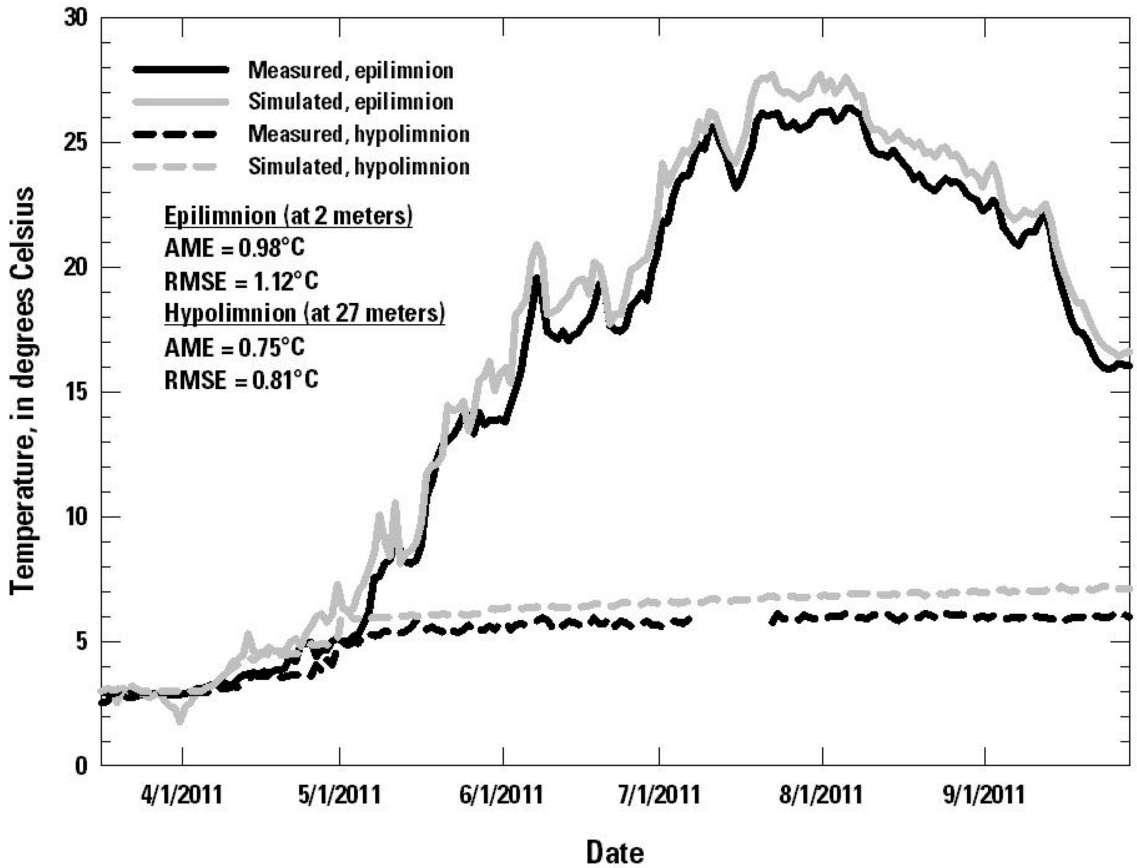

Figure 45. Simulated and measured water temperature for the epilimnion (2-m) and hypolimnion (37-m) at Kecks Point (USGS station number 455843095212501) in Lake Carlos, March 16, 2011 to September 28, 2011.

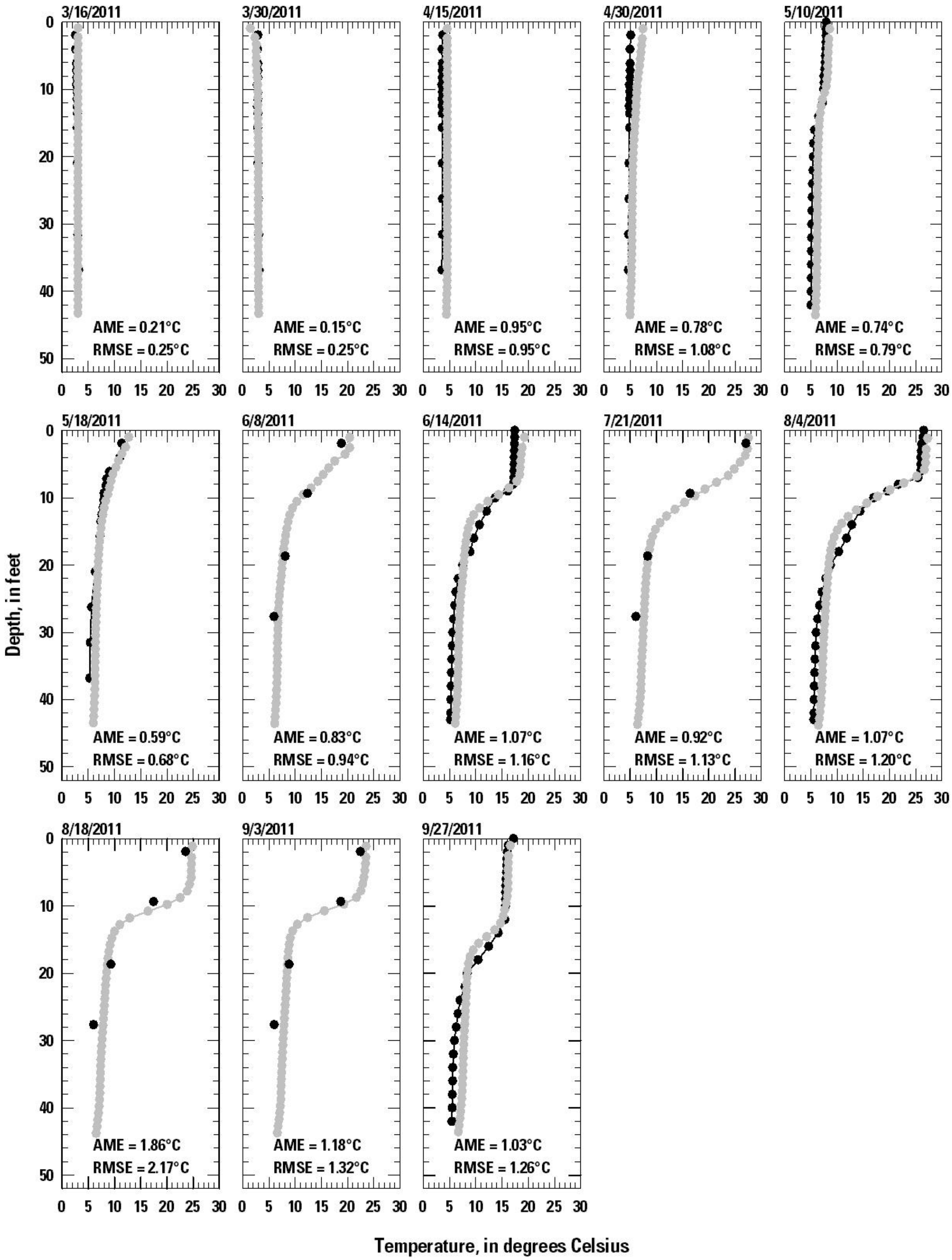

Figure 46. Simulated (gray) and measured (black) water temperature at Kecks Point (USGS station number 455843095212501) in Lake Carlos for 11 dates in 2011, with AME and RMSE quantities.

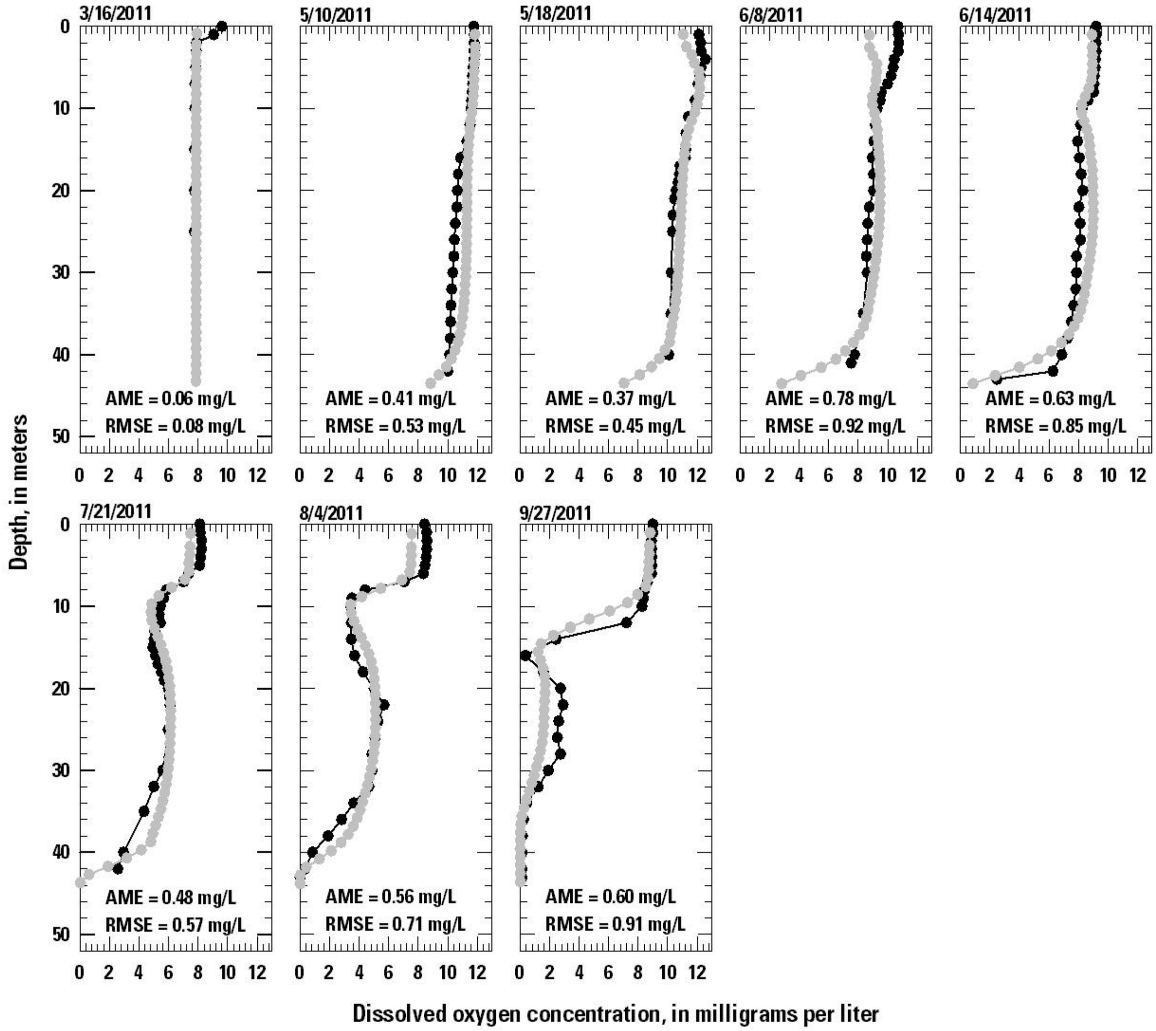

Figure 47. Simulated (gray) and measured (black) dissolved oxygen concentrations at Kecks Point (USGS station number 455843095212501) in Lake Carlos for 8 dates in 2011, with AME and RMSE quantities.

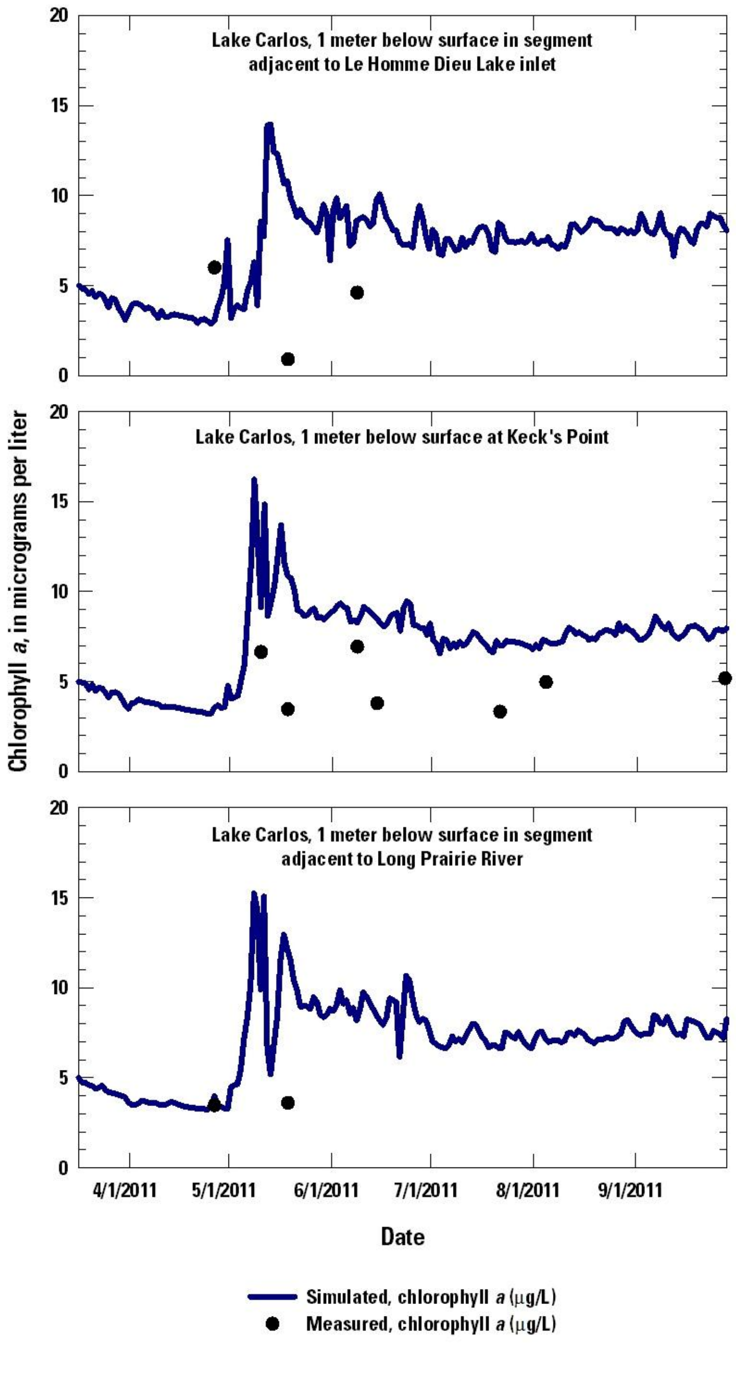

Figure 48. Simulated and measured chlorophyll *a* concentrations (in µg/L) for three different segments in Lake Carlos, March 16, 2011 to September 28, 2011.

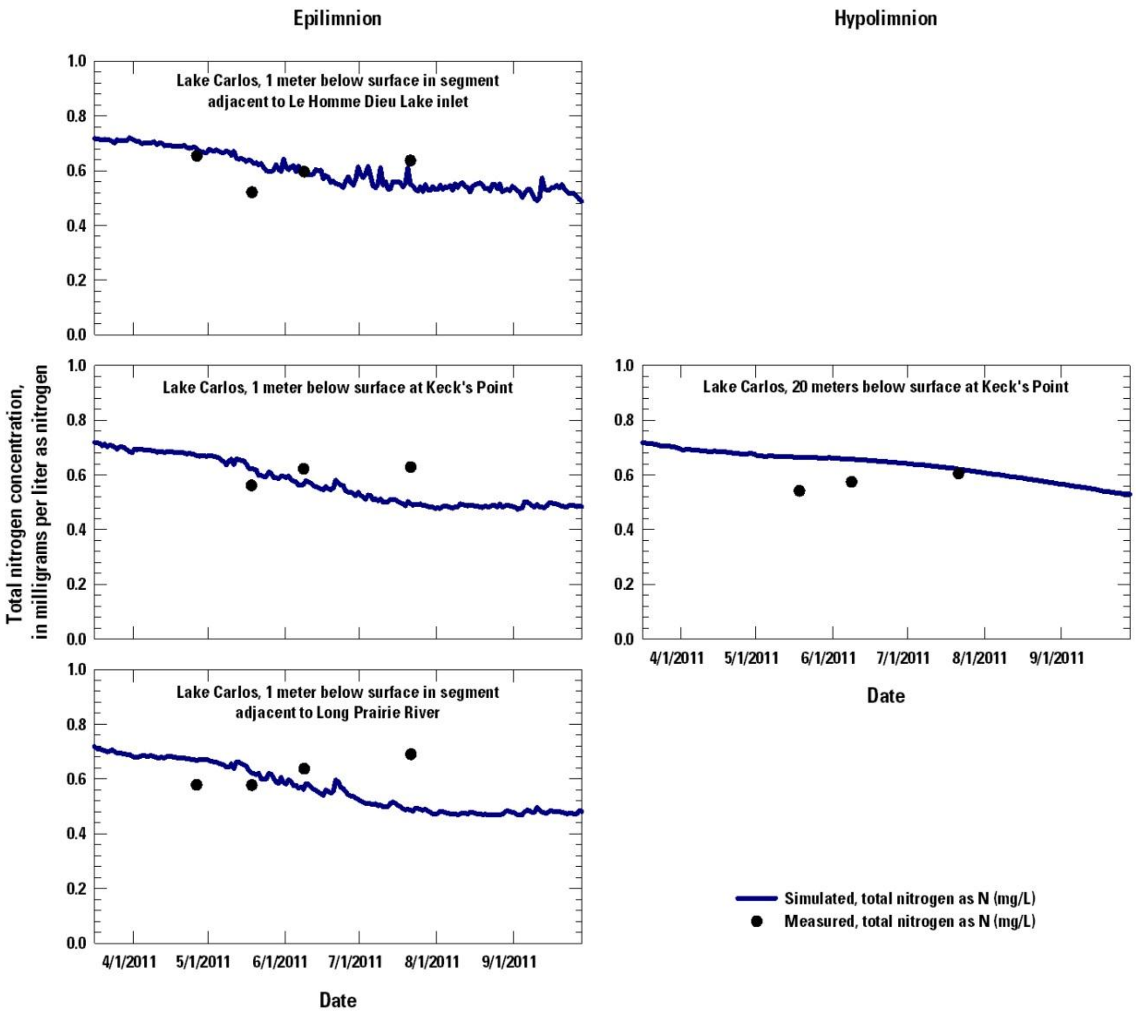

Figure 49. Simulated and measured total nitrogen concentrations (in mg/L) for three different segments in Lake Carlos, March 16, 2011 to September 28, 2011.

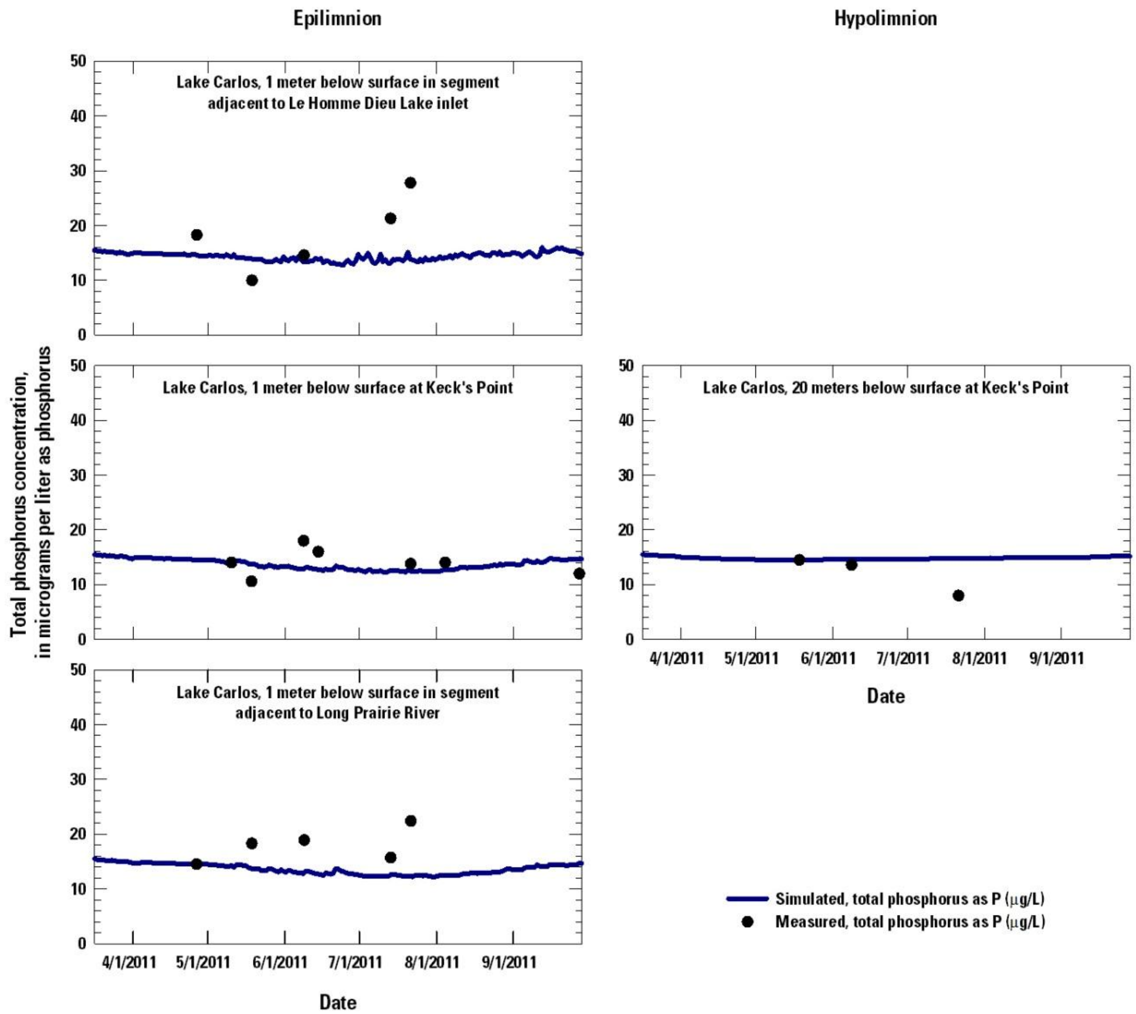

Figure 50. Simulated and measured total phosphorus concentrations (in µg/L) for three different segments in Lake Carlos, March 16, 2011 to September 28, 2011.

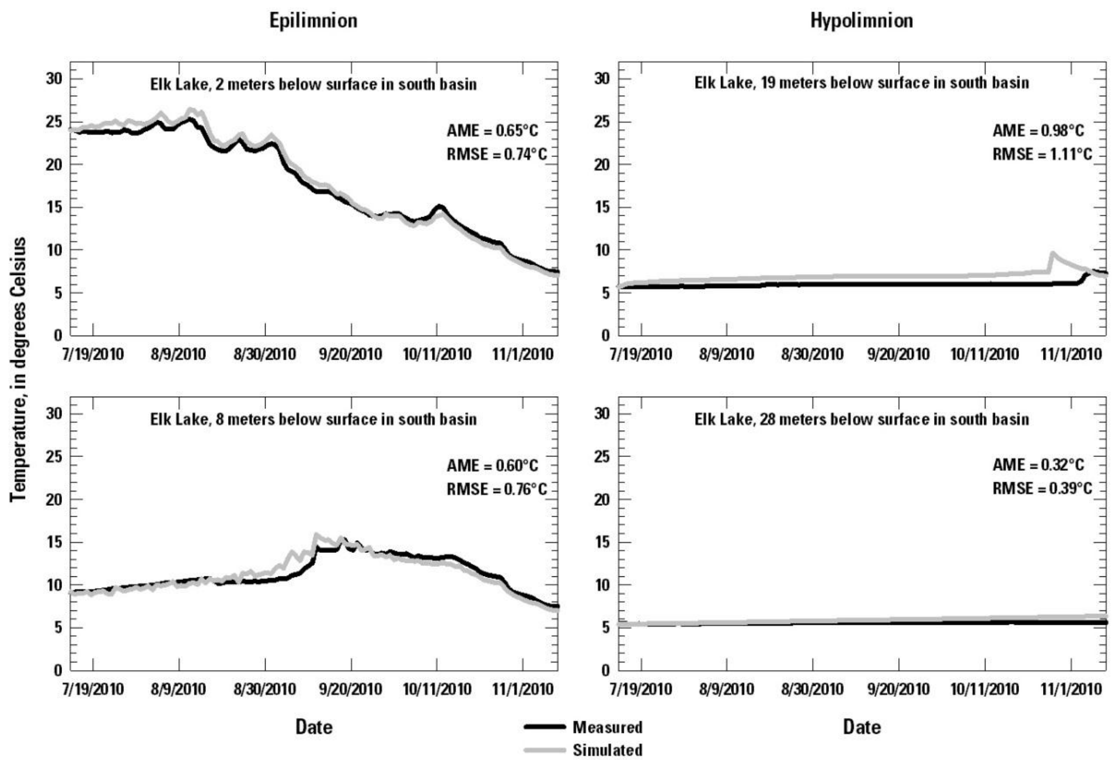

Figure 51. Simulated (gray) and measured (black) water temperature for the epilimnion (2-m and 8-m) and hypolimnion (19-m and 28-m) at south basin hole (USGS station number 471116095125301) in Elk Lake, July 13, 2010 to November 9, 2010.

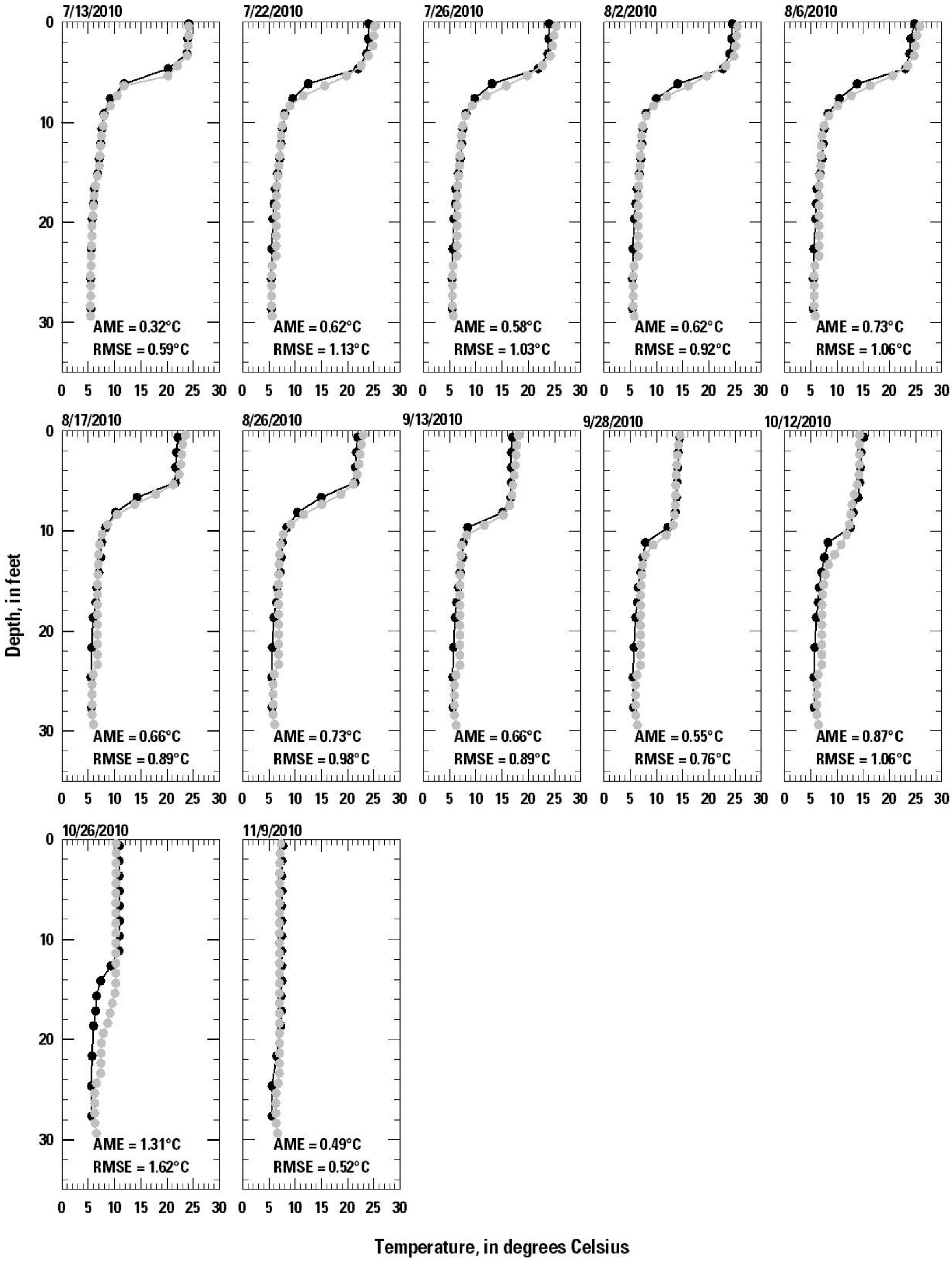

Figure 52. Simulated (gray) and measured (black) water temperature at south basin hole (USGS station number 471116095125301) in Elk Lake for 12 dates in 2010, with AME and RMSE quantities.

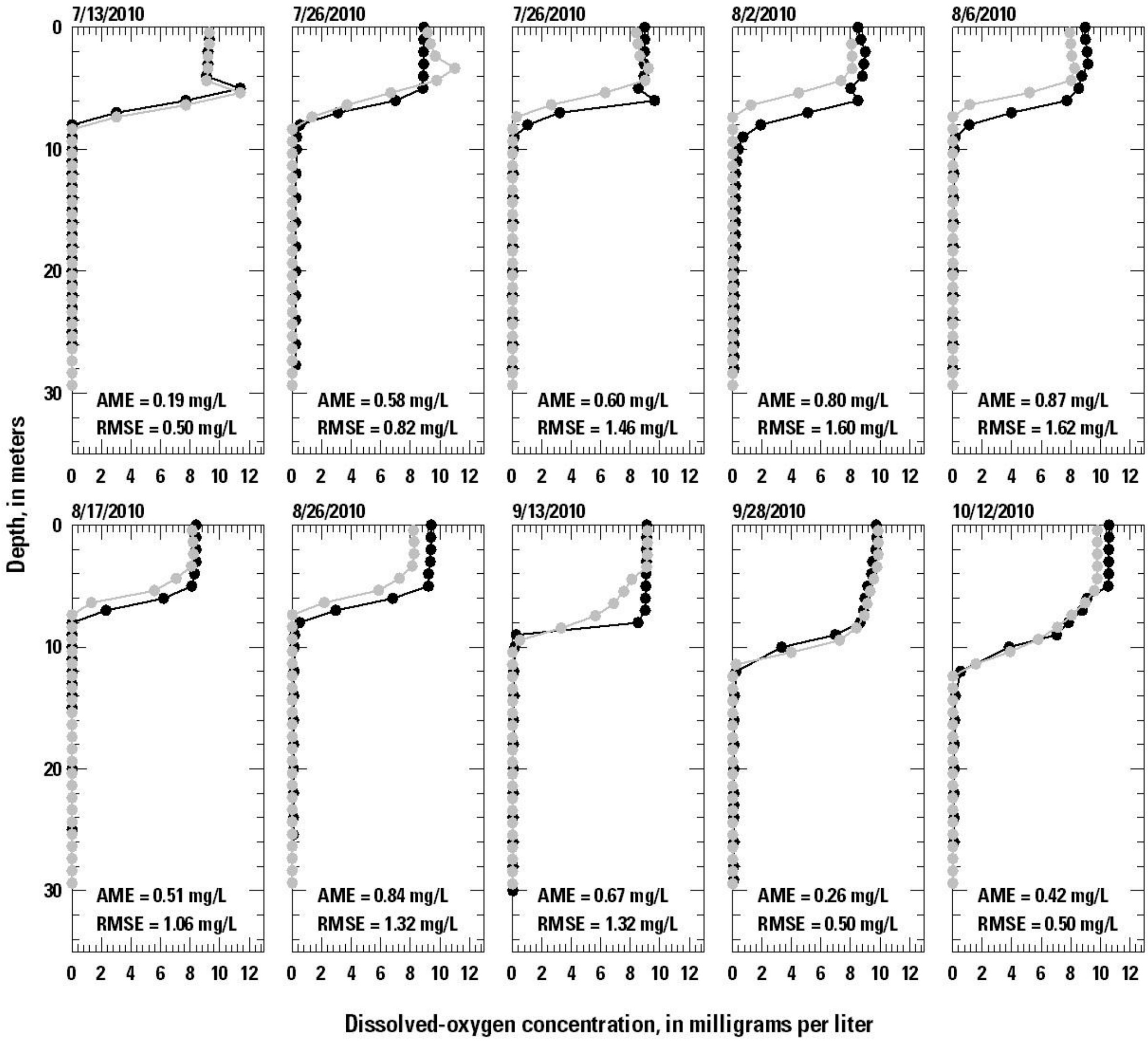

Figure 53. Simulated (gray) and measured (black) dissolved oxygen concentrations at south basin hole (USGS station number 471116095125301) in Elk Lake for 10 dates in 2010, with AME and RMSE quantities.

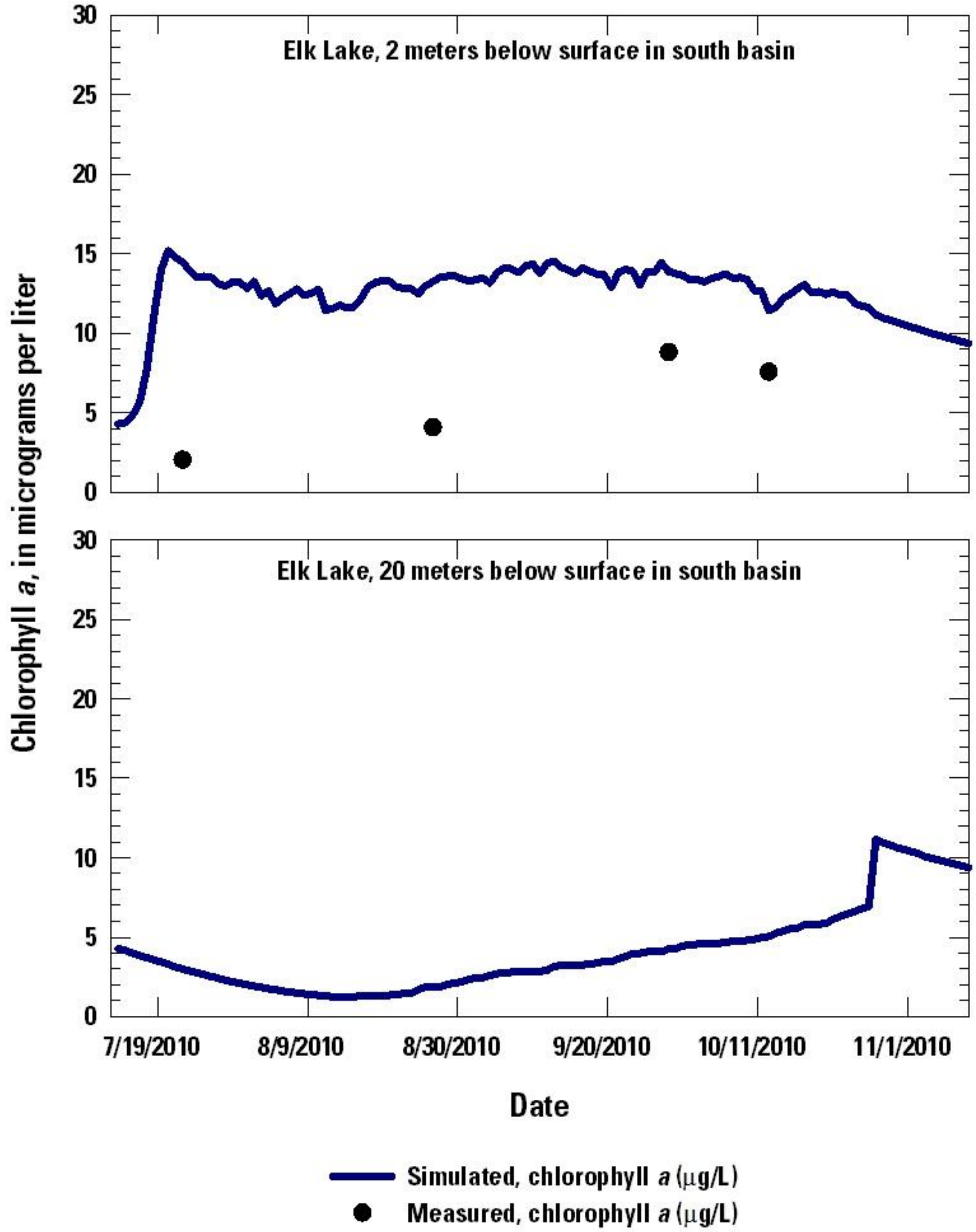

Figure 54. Simulated and measured chlorophyll *a* concentrations (in µg/L) for two different depths at south basin hole (USGS station number 471116095125301) in Elk Lake, July 13, 2010 to November 9, 2010.

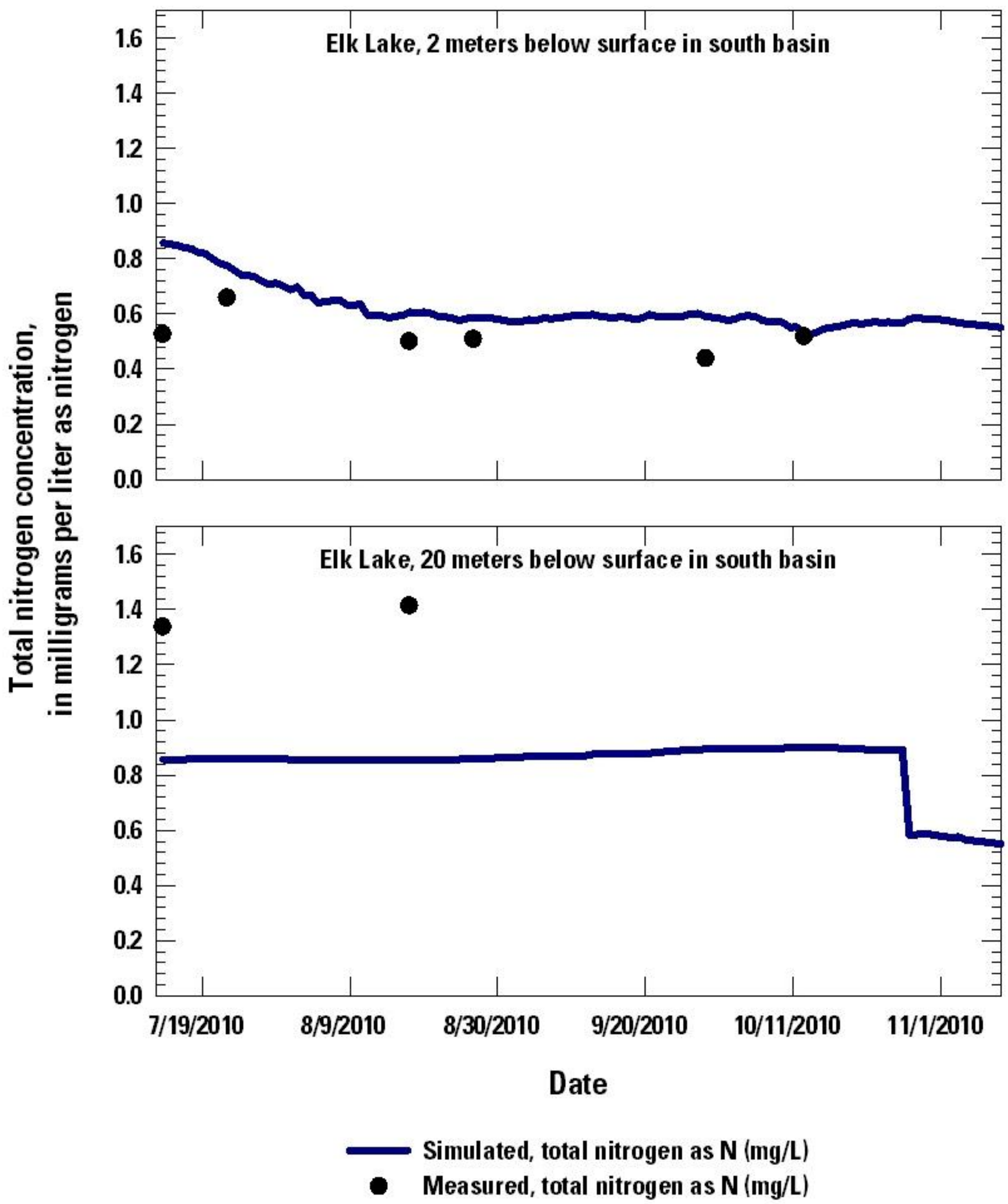

Figure 55. Simulated and measured total nitrogen concentrations (in mg/L) for two different depths at south basin hole (USGS station number 471116095125301) in Elk Lake, July 13, 2010 to November 9, 2010.

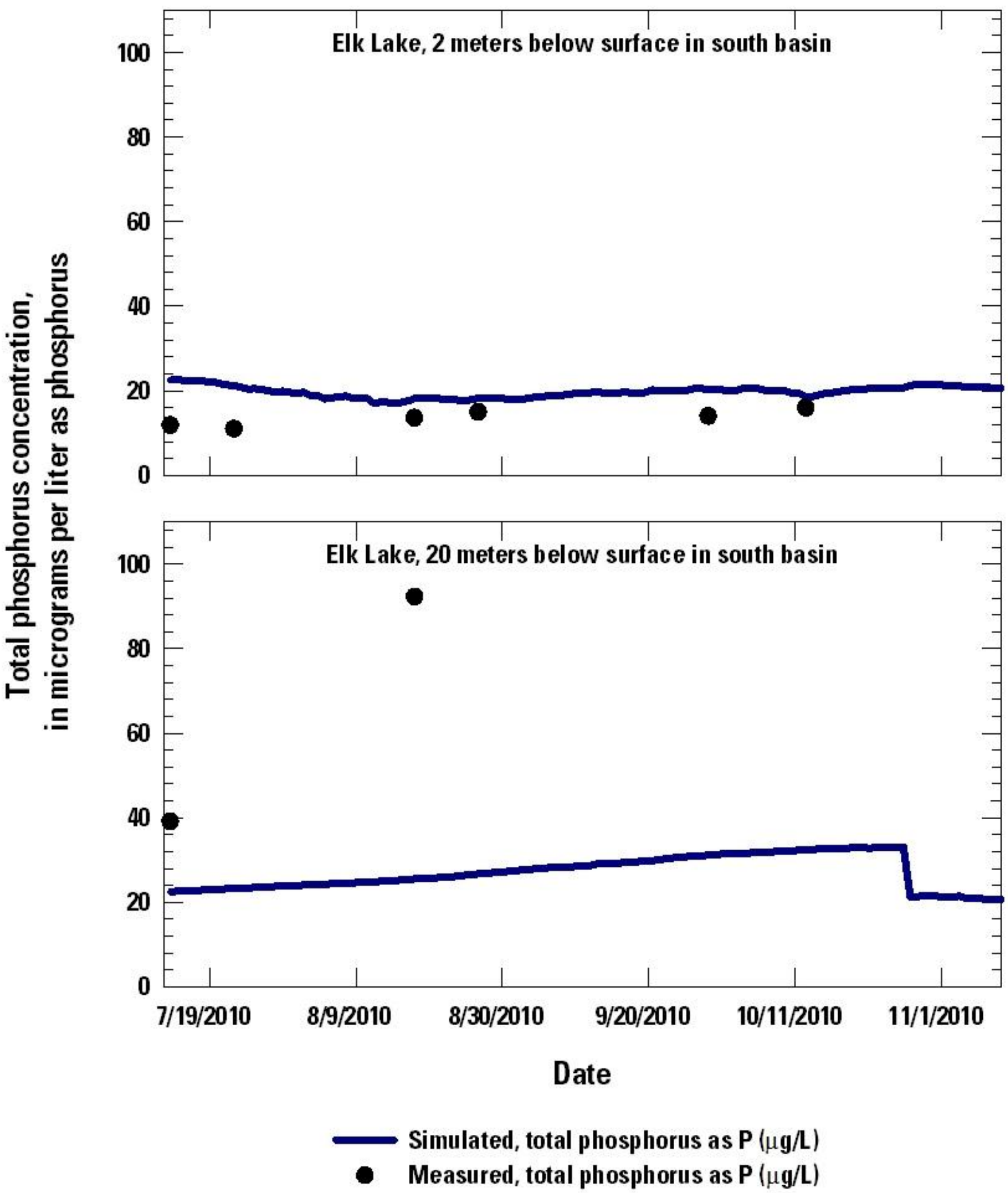

Figure 56. Simulated and measured total phosphorus concentrations (in µg/L) for two different depths at south basin hole (USGS station number 471116095125301) in Elk Lake, July 13, 2010 to November 9, 2010.

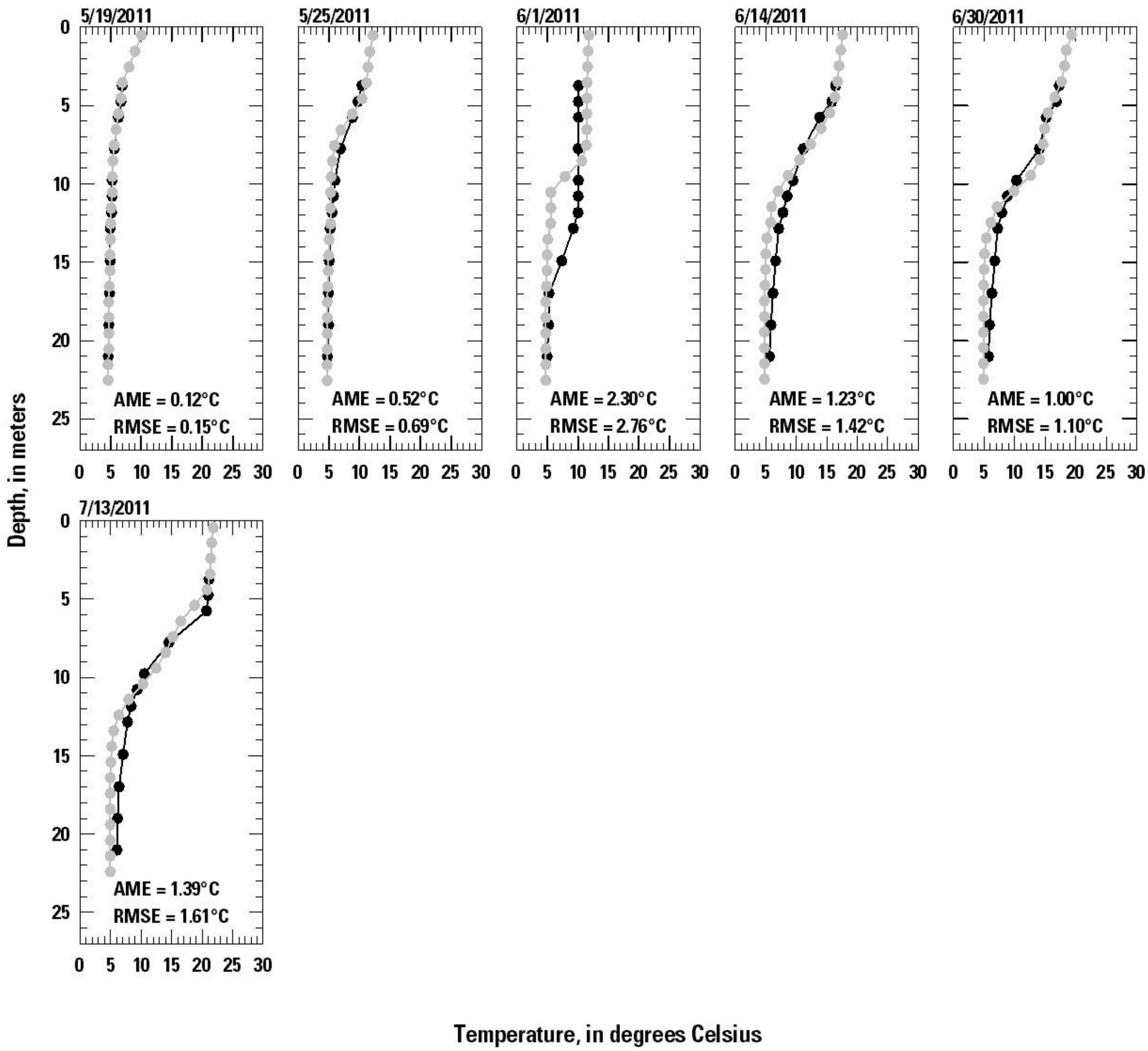

Figure 57. Simulated (gray) and measured (black) water temperature at north basin hole (USGS station number 475214090100401) in Trout Lake for six dates in 2011, with AME and RMSE quantities.

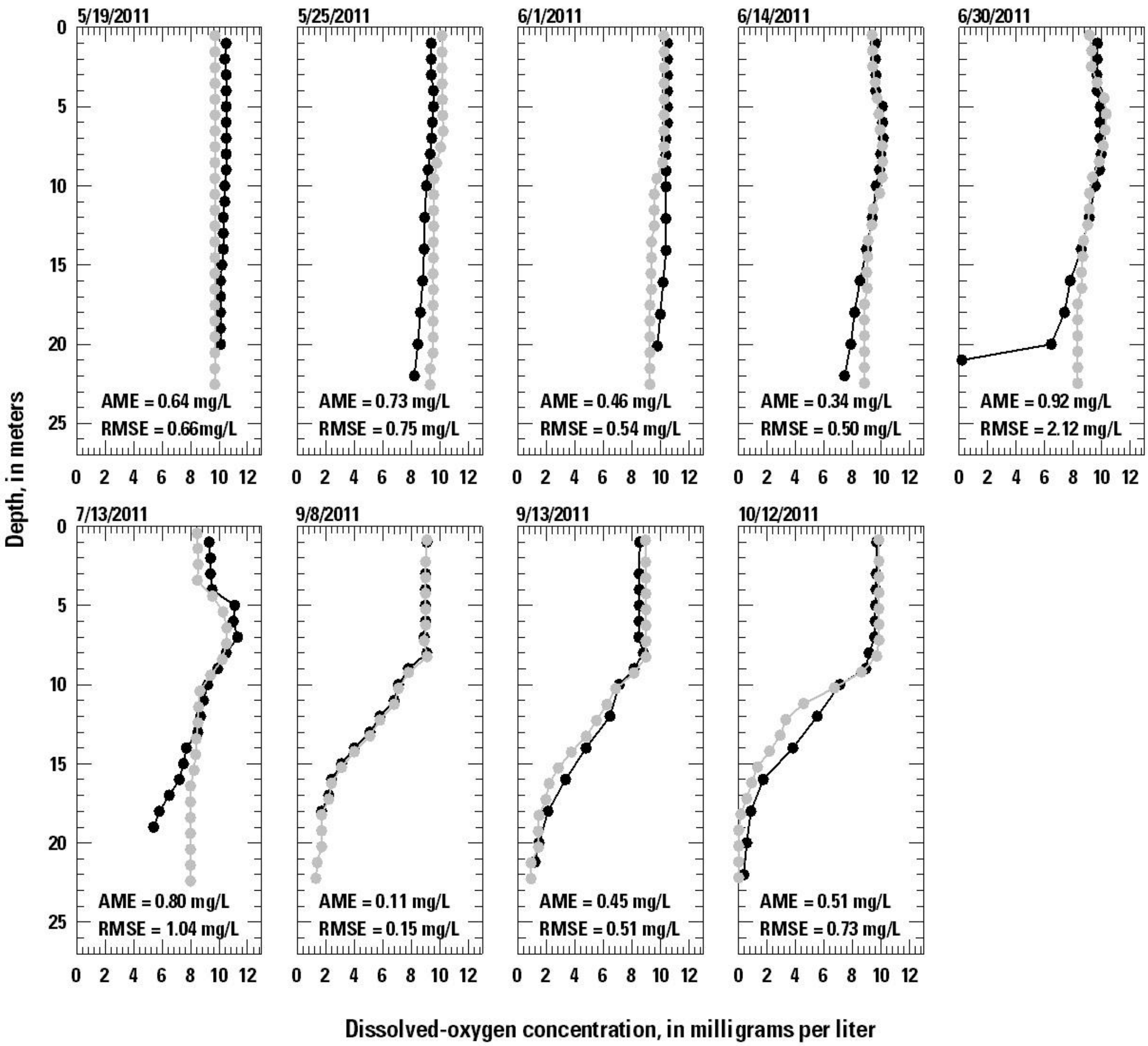

Figure 58. Simulated (gray) and measured (black) dissolved oxygen concentrations at north basin hole (USGS station number 475214090100401) in Trout Lake for nine dates in 2011, with AME and RMSE quantities.

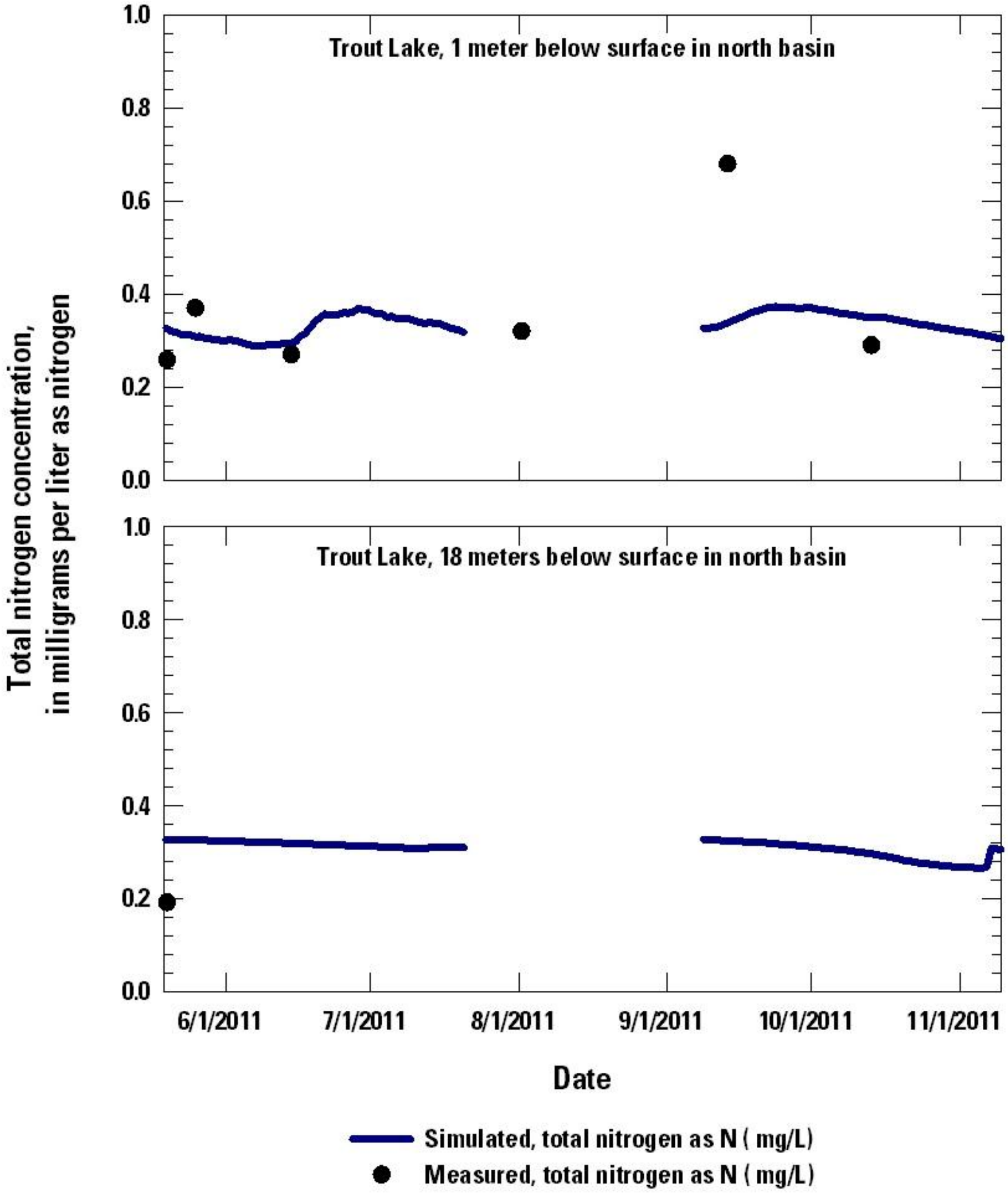

Figure 59. Simulated and measured total nitrogen concentrations (in mg/L) for two different depths at north basin hole (USGS station number 475214090100401) in Trout Lake, May 19, 2011 to July 20, 2011 and September 8, 2011 to November 9, 2011.

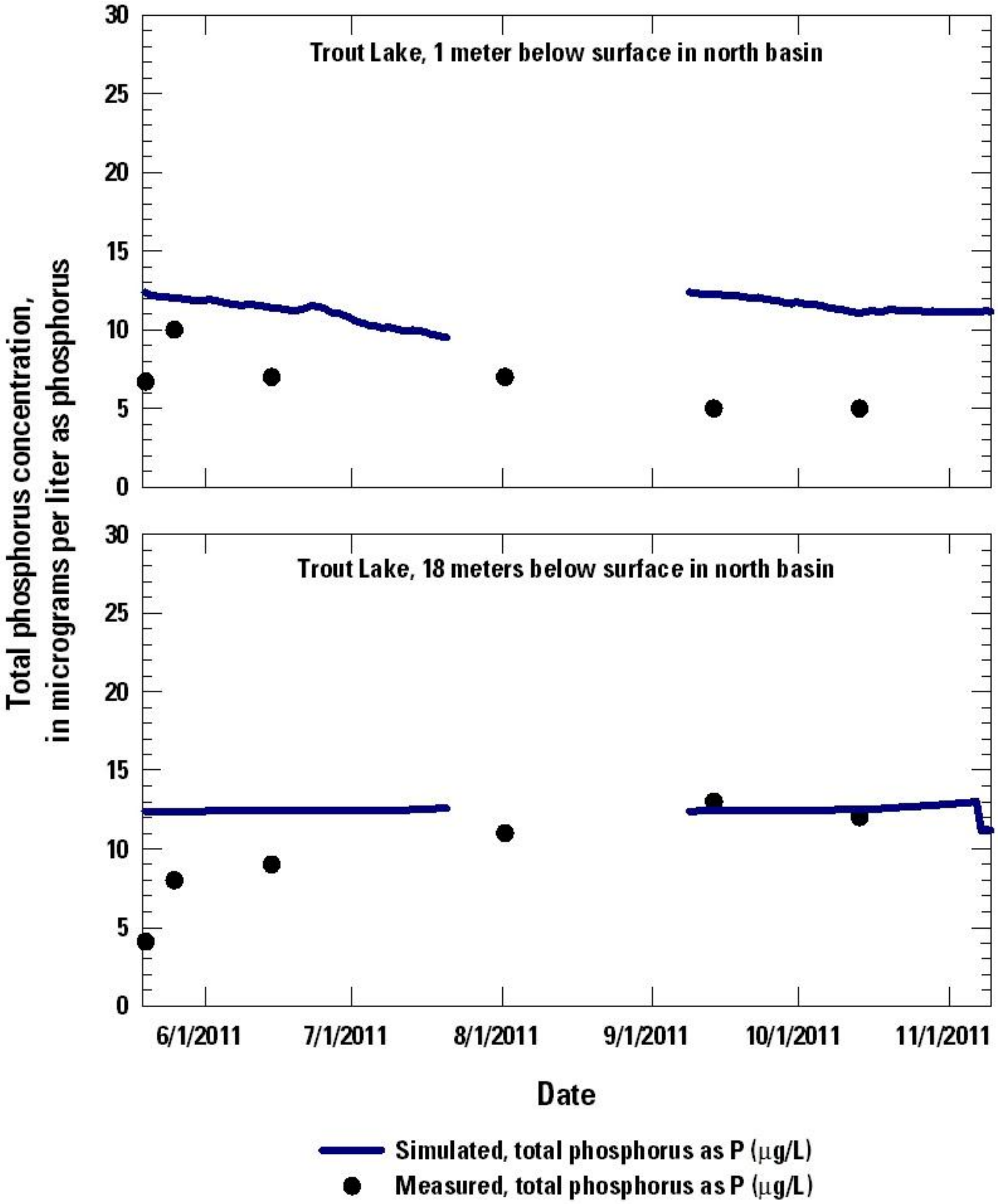

Figure 60. Simulated and measured total phosphorus concentrations (in μg/L) for two different depths at north basin hole (USGS station number 475214090100401) in Trout Lake, May 19, 2011 to July 20, 2011 and September 8, 2011 to November 9, 2011.

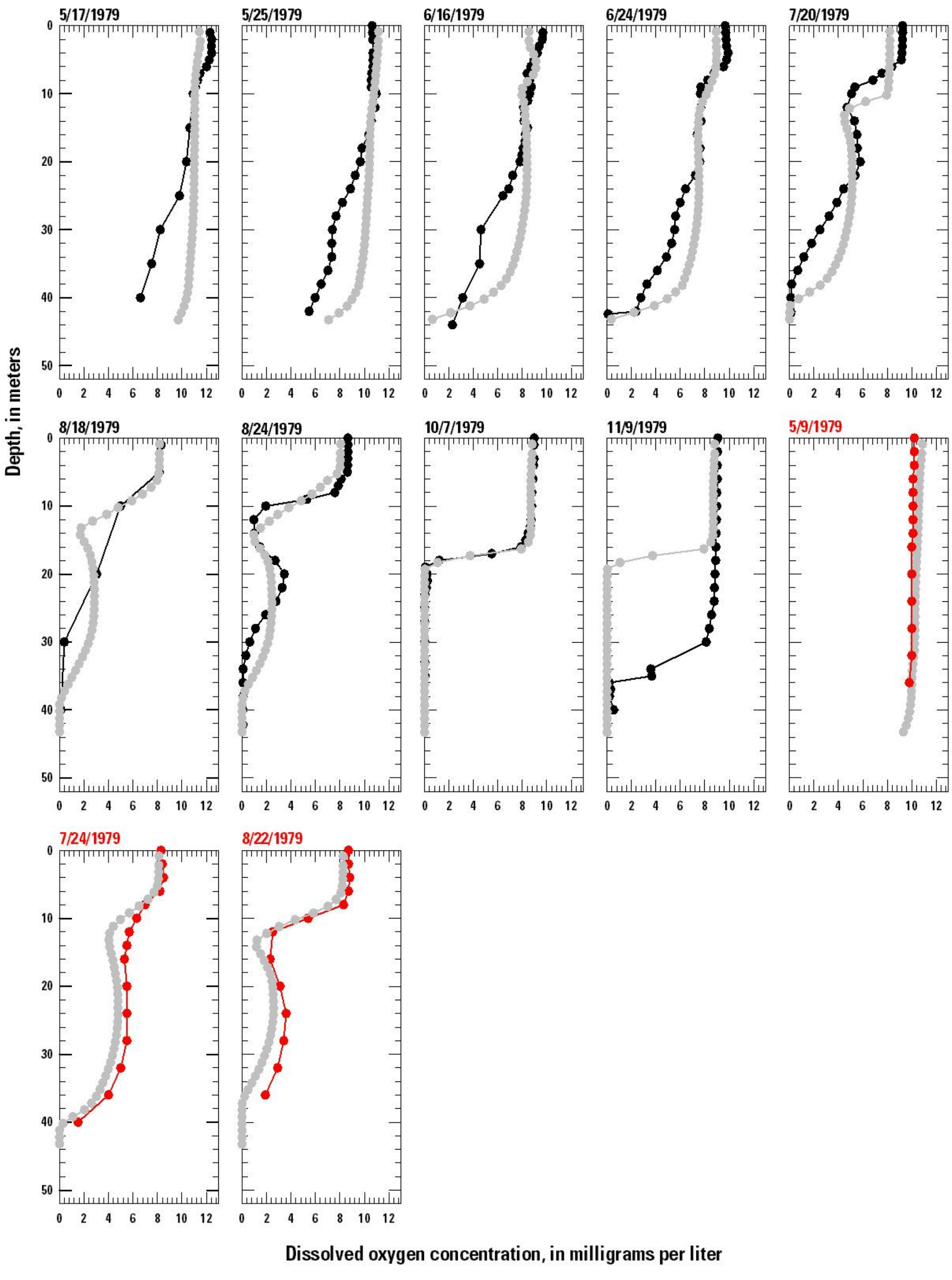

Figure 61. Simulated (gray) and measured (black) dissolved oxygen concentrations for Kecks Point (USGS station number 455843095212501) for 12 dates in 1979. Results from the 1979 simulation are shown in gray with data from 2010 (black) and from 1979 (red) shown for comparison.

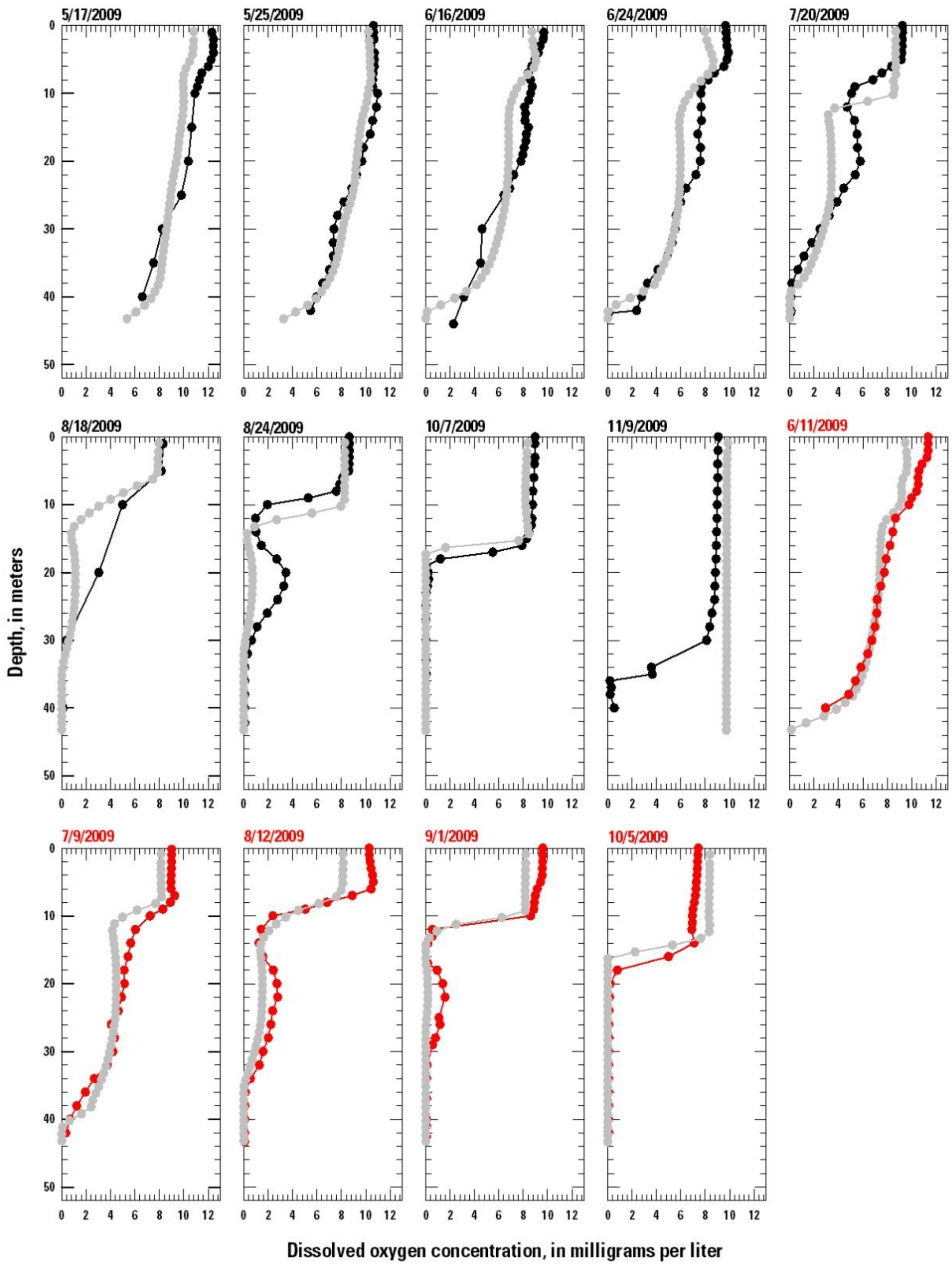

Figure 62. Simulated (gray) and measured (black) dissolved oxygen concentrations for Kecks Point (USGS station number 455843095212501) for 14 dates in 2009, with AME and RMSE quantities. Results from the 2009 simulation are shown in gray with data from 2010 (black) and from 1979 (red) shown for comparison.

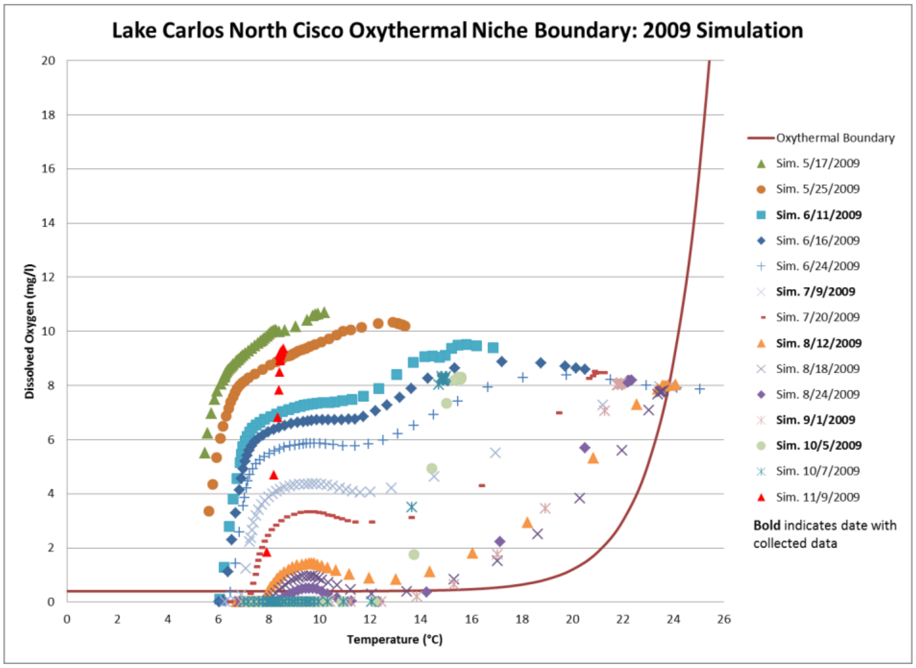

a.

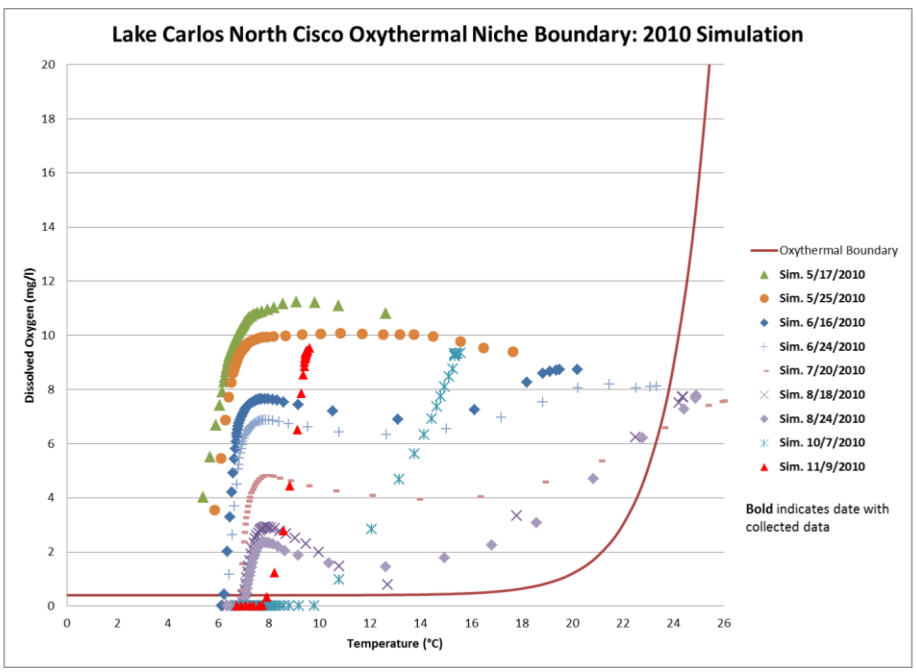

b.

Figure 63. Plots of the simulated dissolved oxygen output from Keck's point, Lake Carlos MN, for 2009 (1a) and 2010 (1b) compared to Jacobson et al. (2008) model of niche boundaries for lake cisco *Coregonus artedi*. In this model $O_{lethal} = c + \alpha e^{\beta T(lethal)}$ where O_{lethal} and $T_{(lethal)}$ are the oxygen concentrations and temperature values that define the lethal niche boundary, c is a vertical (y-axis) shift parameter, and α and β are exponential function parameters.

Table 1. Location of continuous pressure transducers, water-quality sondes, thermistors, and discrete water-quality measurements used for the development of either model input or calibration of water temperature, dissolved oxygen, and water-quality constituents in the three Sentinel Lakes studies.

[All continuous measurements included regular, monthly visits to download and calibrate continuous pressure transducers, water-quality sondes, and thermistors. Continuous constituents: S, water stage level; S→Q, discharge/flow (derived from stage); DO, dissolved oxygen; SC, specific conductance; T, water temperature.
Discrete constituents: MI, major inorganics; L-L N, low-level nutrients; TC/TN, total carbon/total nitrogen; Alk, alkalinity.
Use: C, calibration; I, input; WQ, water-quality (including discrete constituents).
CE-QUAL-W2 segment: Number identifies segment inflow/outflow attached to in model; I, inflow; O, outflow

Site name	Site Number	Latitude / Longitude	Continuous constituents	Discrete constituents	Use	Model segment
Lake Carlos						
Lake Darling Outlet near Alexandria, MN	05244780	45° 55' 53" -95° 22' 50"	S, S→Q, T	DO, pH, SC, T, MI, L-L N, TC/TN, Alk	I	2 (I)
Lake Le Homme Dieu Outlet at Alexandria, MN	05244810	45° 56' 24" -95° 21' 35"	S, S→Q, T	DO, pH, SC, T, MI, L-L N, TC/TN, Alk	I	5 (I)
Long Prairie River below Lake Carlos near Alexandria, MN	05244820	45° 58' 57" -95° 19' 43"	S, S→Q, T	DO, pH, SC, T, MI, L-L N, TC/TN, Alk	S (C), I (S→Q), T (C)	22 (O)
Lake Carlos west of Kecks Point near Alexandria, MN	455843095212501	45° 58' 43" -95° 21' 25"	DO, pH, SC, T	DO, pH, SC, T, MI, L-L N, TC/TN, Alk	WQ (I), T (C), DO (C)	18
Elk Lake						
Unnamed tributary to Elk Lake near Hubbard, MN	05199935	47° 11' 04" -95° 13' 13"	--	DO, pH, SC, T, MI, L-L N, TC/TN, Alk	I	2 (I)
GA-GWA-Dosh Creek near Hubbard, MN	05199940	47° 11' 04" -95° 12' 42"	--	DO, pH, SC, T, MI, L-L N, TC/TN, Alk	I	3 (I)
Unnamed tributary (Spring 4) to Elk Lake near Hubbard, MN	05199943 / 471127095124101	47° 11' 25" -95° 12' 42"	--	DO, pH, SC, T, MI, L-L N, TC/TN, Alk	I	3 (I)

Site name	Site Number	Latitude / Longitude	Continuous constituents	Discrete constituents	Use	Model segment
Siegfried Creek near Hubbard, MN	05199945	47° 11' 30" -95° 13' 34"	--	DO, pH, SC, T, MI, L-L N, TC/TN, Alk	I	4 (I)
Elk Lake Outlet in Itasca State Park, MN	05199950	47° 11' 47" -95° 13' 19"	S, S→Q, T	DO, pH, SC, T, MI, L-L N, TC/TN, Alk	S (C), I (S→Q), T (C)	6 (O)
Elk Lake, South End, near Hubbard, MN	471116095125301	47° 11' 16" -95° 12' 53"	DO, pH, SC, T	DO, pH, SC, T, MI, L-L N, TC/TN, Alk	WQ (I,C), T (I,C), DO (I,C)	3
Unnamed spring to Elk Lake near Hubbard, MN	471123095132901	47° 11' 23" -95° 13' 29"	--	DO, pH, SC, T, MI, L-L N, TC/TN, Alk	I	--
Piezometer by Spring 1 near Hubbard, MN	471124095132901	47° 11' 23.8" -95° 13' 29.4"	--	DO, SC, MI, L-L N	I	--
Elk Lake (Piezometer 1) near Hubbard, MN	471126095124301	47° 11' 26" -95° 12' 43"	--	DO, pH, SC, MI, L-L N	I	--
Trout Lake						
Trout Lake Tributary, northwest side, near Covill, MN	04011140	47° 52' 27" -90° 11' 00"	--	DO, pH, SC, T, MI, L-L N, TC/TN, Alk	I	2 (I)
Marsh Lake Outlet at Forest Rd 308 near Covill, MN	04011145	47° 52' 16" -90° 11' 04"	--	DO, pH, SC, T, MI, L-L N, TC/TN, Alk	I	4 (I)
Trout Lake Outlet near Covill, MN	04011150	47° 51' 58" -90° 10' 34"	S, S→Q, T	DO, pH, SC, T, MI, L-L N, TC/TN, Alk	S (C), I (S→Q), T (C)	4 (O)
Trout Lake, East Side, near Grand Marais, MN	475214090100401	47° 52' 14" -90° 10' 04"	DO, pH, SC, T	DO, pH, SC, T, MI, L-L N, TC/TN, Alk	WQ (I,C), T (I,C), DO (I,C)	2

Table 2. Initial constituent concentrations for all three sentinel lakes, both calibration and validation runs.

Constituent	Value					
	Calibration			Validation		
	Lake Carlos (2010)	Elk Lake (2011)	Trout Lake (2010)	Lake Carlos (2011)	Elk Lake (2010)	Trout Lake (2011)
Initial Water level, m	413.58	448.08	505.69	413.53	447.98	505.86
Total dissolved solids (TDS), g m^3	258.97	172.23	29.68	255.58	172.23	29.68
Orthophosphate, g m^3	0.0052	0.0069	0.0038	0.0041	0.0069	0.0038
Ammonia, g m^3	0.0234	0.329	0.0109	0.0241	0.329	0.0109
Nitrate-Nitrite, g m^3	0.0348	0.015	0.0183	0.0686	0.015	0.0183
Dissolved silica, g m^3	6.9983	10.7815	6.4142	7.697	10.7815	6.4142
Particulate silica, g m^3	1	1	1	1	1	1
Total iron, g m^3	0.0002	0.0073	0.0109	0.0002	0.0073	0.0109
Labile dissolved organic matter (DOM), g m^3	1.8736	2.0877	1.5349	1.7206	2.0877	1.5349
Refractory DOM, g m^3	4.3716	2.0877	0.6578	4.0148	2.0877	0.6578
Labile particulate organic matter (POM), g m^3	0.3099	0.5941	0.3739	0.4027	0.5941	0.3739
Refractory POM, g m^3	0.7231	0.5941	0.1602	0.9397	0.5941	0.1602
Diatoms, g m^3	0.3	0.3	1	0.3	1	1
Green algae, g m^3	0.1	0.1	0.2	0.1	0.1	0.2
Blue-green algae, g m^3	0.1	0.2	0.1	0.1	0.1	0.1
Dissolved oxygen, g m^3	6	2.0-4.9*	7.3-9.4*	7.86	0.0-9.3*	9.7
Inorganic carbon, g m^3	194.4	185.1	20.5	195.6	185.1	20.5
Alkalinity, day^{-1}	163.8	152.3	15.8	165.3	152.3	15.8
Initial Temperature, °C	4	4.1	7.5	3	5.4-24.1*	4.6-10.0*
Sediment Temperature, °C	4	8	7.7	4	8	7.7

Table 3. Parameters used for the water-quality algorithms for Lake Carlos, Elk Lake and Trout Lake.

Parameter	Description	Value		
		Lake Carlos	Elk Lake	Trout Lake
EXH2O	Light extinction for pure water, m^{-1}	0.45	0.45	0.25
EXSS	Light extinction due to inorganic suspended solids, m^{-1}	0.05	0.05	0.01
EXOM	Light extinction due to organic suspended solids, m^{-1}	0.05	0.05	0.01
BETA	Fraction of incident solar radiation absorbed at water surface	0.38	0.45	0.45
EXA1	Light extinction due to algae (diatoms), $m^{-1}/(gm^{-3})$	0.25	0.2	0.2
EXA2	Light extinction due to algae (green), $m^{-1}/(gm^{-3})$	0.2	0.15	0.15
EXA3	Light extinction due to algae (blue-green), $m^{-1}/(gm^{-3})$	0.2	0.15	0.15
AG	Maximum algal growth rate (diatoms), day^{-1}	2.3	2.3	2.3
AG	Maximum algal growth rate (green), day^{-1}	2.1	2.1	2.1
AG	Maximum algal growth rate (blue-green), day^{-1}	2.0	2.0	2.0
AR	Maximum algal respiration rate (diatoms), day^{-1}	0.04	0.04	0.02
AR	Maximum algal respiration rate (green), day^{-1}	0.04	0.04	0.02
AR	Maximum algal respiration rate (blue-green), day^{-1}	0.04	0.04	0.02
AE	Maximum algal excretion rate (diatoms), day^{-1}	0.1	0.1	0.02
AE	Maximum algal excretion rate (green), day^{-1}	0.1	0.1	0.02
AE	Maximum algal excretion rate (blue-green), day^{-1}	0.1	0.1	0.02
AM	Maximum algal mortality rate (diatoms), day^{-1}	0.1	0.12	0.04
AM	Maximum algal mortality rate (green), day^{-1}	0.1	0.03	0.07
AM	Maximum algal mortality rate (blue-green), day^{-1}	0.15	0.07	0.12
AS	Algal settling rate (diatoms), m day^{-1}	0.18	0.15	0.05
AS	Algal settling rate (green), m day^{-1}	0.18	0.15	0.07
AS	Algal settling rate (blue-green), m day^{-1}	0.18	0.15	0.15
AHSP	Algal half-saturation for phosphorus limited growth (diatoms), g m^{-3}	0.002	0.004	0.001
AHSP	Algal half-saturation for phosphorus limited growth (green), g m^{-3}	0.003	0.0018	0.003
AHSP	Algal half-saturation for phosphorus limited growth (blue-green), g m^{-3}	0.002	0.002	0.003
AHSN	Algal half-saturation for nitrogen limited growth (diatoms), g m^{-3}	0.03	0.03	0.023
AHSN	Algal half-saturation for nitrogen limited growth (green), g m^{-3}	0.03	0.012	0.012
AHSN	Algal half-saturation for nitrogen limited growth (blue-green), g m^{-3}	0.02	0.006	0
AHSSI	Algal half-saturation for silica limited growth (diatoms), g m^{-3}	0	0	0
AHSSI	Algal half-saturation for silica limited growth (green), g m^{-3}	0	0	0

Parameter	Description	Value		
		Lake Carlos	Elk Lake	Trout Lake
AHSSI	Algal half-saturation for silica limited growth (blue-green), g m^{-3}	0	0	0
ASAT	Light saturation intensity at maximum photosynthetic rate (diatoms), W m^{-2}	90	90	90
ASAT	Light saturation intensity at maximum photosynthetic rate (green), W m^{-2}	60	60	60
ASAT	Light saturation intensity at maximum photosynthetic rate (blue-green), W m^{-2}	40	40	40
AT1	Lower temperature for algal growth (diatoms), °C	5	5	5
AT1	Lower temperature for algal growth (green), °C	10	10	10
AT1	Lower temperature for algal growth (blue-green), °C	13	13	13
AT2	Lower temperature for maximum algal growth (diatoms), °C	10	10	10
AT2	Lower temperature for maximum algal growth (green), °C	17	17	17
AT2	Lower temperature for maximum algal growth (blue-green), °C	20	20	20
AT3	Upper temperature for maximum algal growth (diatoms), °C	13	13	13
AT3	Upper temperature for maximum algal growth (green), °C	30	30	30
AT3	Upper temperature for maximum algal growth (blue-green), °C	32	32	32
AT4	Upper temperature for algal growth (diatoms), °C	25	25	25
AT4	Upper temperature for algal growth (green), °C	32	32	32
AT4	Upper temperature for algal growth (blue-green), °C	35	35	35
AK1	Fraction of algal growth rate at AT1 (diatoms)	0.1	0.1	0.1
AK1	Fraction of algal growth rate at AT1 (green)	0.1	0.1	0.1
AK1	Fraction of algal growth rate at AT1 (blue-green)	0.1	0.1	0.1
AK2	Fraction of maximum algal growth rate at AT2 (diatoms)	0.99	0.99	0.99
AK2	Fraction of maximum algal growth rate at AT2 (green)	0.99	0.99	0.99
AK2	Fraction of maximum algal growth rate at AT2 (blue-green)	0.99	0.99	0.99
AK3	Fraction of maximum algal growth rate at AT3 (diatoms)	0.99	0.99	0.99
AK3	Fraction of maximum algal growth rate at AT3 (green)	0.99	0.99	0.99
AK3	Fraction of maximum algal growth rate at AT3 (blue-green)	0.99	0.99	0.99
AK4	Fraction of algal growth rate at AT4 (diatoms)	0.1	0.1	0.1
AK4	Fraction of algal growth rate at AT4 (green)	0.1	0.1	0.1
AK4	Fraction of algal growth rate at AT4 (blue-green)	0.1	0.1	0.1
ALGP	Stoichiometric equivalent between algal biomass and phosphorus (diatoms)	0.0015	0.0018	0.002
ALGP	Stoichiometric equivalent between algal biomass and phosphorus (green)	0.0015	0.0022	0.002
ALGP	Stoichiometric equivalent between algal biomass and phosphorus (blue-green)	0.0015	0.0022	0.002
ALGN	Stoichiometric equivalent between algal biomass and nitrogen (diatoms)	0.0825	0.07	0.08

Parameter	Description	Value		
		Lake Carlos	Elk Lake	Trout Lake
ALGN	Stoichiometric equivalent between algal biomass and nitrogen (green)	0.0825	0.07	0.072
ALGN	Stoichiometric equivalent between algal biomass and nitrogen (blue-green)	0.0825	0.07	0.072
ALGC	Stoichiometric equivalent between algal biomass and carbon (diatoms)	0.45	0.45	0.45
ALGC	Stoichiometric equivalent between algal biomass and carbon (green)	0.45	0.45	0.45
ALGC	Stoichiometric equivalent between algal biomass and carbon (blue-green)	0.45	0.45	0.45
ALGSI	Stoichiometric equivalent between algal biomass and silica (diatoms)	0.18	0.18	0.18
ALGSI	Stoichiometric equivalent between algal biomass and silica (green)	0.18	0.18	0.18
ALGSI	Stoichiometric equivalent between algal biomass and silica (blue-green)	0.18	0.18	0.18
ACHLA	Ratio between algal biomass and chlorophyll a in terms of mg algae/µg chl a (diatoms)	0.1	0.28	0.12
ACHLA	Ratio between algal biomass and chlorophyll a in terms of mg algae/µg chl a (green)	0.1	0.28	0.12
ACHLA	Ratio between algal biomass and chlorophyll a in terms of mg algae/µg chl a (blue-green)	0.1	0.28	0.12
ALPOM	Fraction of algal biomass that is converted to particulate organic matter when algae die (diatoms)	0.5	0.5	0.5
ALPOM	Fraction of algal biomass that is converted to particulate organic matter when algae die (green)	0.5	0.5	0.5
ALPOM	Fraction of algal biomass that is converted to particulate organic matter when algae die (blue-green)	0.5	0.5	0.5
ANEQN	Equation number for algal ammonium preference (diatoms)	2	2	2
ANEQN	Equation number for algal ammonium preference (green)	2	2	2
ANEQN	Equation number for algal ammonium preference (blue-green)	2	2	2
ANPR	Algal half saturation constant for ammonium preference (diatoms)	0.003	0.003	0.003
ANPR	Algal half saturation constant for ammonium preference (green)	0.003	0.003	0.003
ANPR	Algal half saturation constant for ammonium preference (blue-green)	0.003	0.003	0.003
O2AR	Oxygen stoichiometry for algal respiration	1.1	1.1	1.1
O2AR	Oxygen stoichiometry for algal respiration	1.1	1.1	1.1
O2AR	Oxygen stoichiometry for algal respiration	1.1	1.1	1.1
O2AG	Oxygen stoichiometry for algal primary production	1.6	1.6	1.6
O2AG	Oxygen stoichiometry for algal primary production	1.6	1.6	1.6

Parameter	Description	Value		
		Lake Carlos	Elk Lake	Trout Lake
O2AG	Oxygen stoichiometry for algal primary production	1.6	1.6	1.6
LDOMDK	Labile dissolved organic matter (DOM) decay rate, day $^{-1}$	0.1	0.12	0.04
RDOMDK	Refractory DOM decay rate, day $^{-1}$	0.006	0.01	0.003
LRDDK	Labile to refractory DOM decay rate, day $^{-1}$	0.005	0.003	0.001
LPOMDK	Labile particulate organic matter (POM) decay rate, day $^{-1}$	0.05	0.1	0.05
RPOMDK	Refractory POM decay rate, day $^{-1}$	0.003	0.002	0.003
LRPDK	Labile to refractory POM decay rate, day $^{-1}$	0.005	0.02	0.007
POMS	POM settling rate, m day $^{-1}$	0.18	0.15	0.09
ORGP	Stoichiometric equivalent between organic matter and phosphorus	0.0015	0.0025	0.0022
ORGN	Stoichiometric equivalent between organic matter and nitrogen	0.0825	0.08	0.072
ORGC	Stoichiometric equivalent between organic matter and carbon	0.45	0.45	0.45
ORGSI	Stoichiometric equivalent between organic matter and silica	0.18	0.18	0.18
OMT1	Lower temperature for organic matter decay, °C	4	4	4
OMT2	Upper temperature for organic matter decay, °C	30	30	30
OMK1	Fraction of organic matter decay at OMT1	0.1	0.1	0.1
OMK2	Fraction of organic matter decay at OMT2	0.99	0.99	0.99
PO4R	Sediment release rate of phosphorus, fraction of sediment oxygen demand (SOD)	0.001	0.001	0.001
PARTP	Phosphorus partitioning coefficient for suspended solids	0	0	0
NH4R	Sediment release rate of ammonium, fraction of SOD	0.001	0.001	0.001
NH4DK	Ammonium decay rate, day-1	0.12	0.09	0.4
NH4T1	Lower temperature for ammonia decay, °C	4	4	4
NH4T2	Lower temperature for maximum ammonia decay, °C	25	25	25
NH4K1	Fraction of nitrification rate at NH4T1	0.1	0.1	0.1
NH4K2	Fraction of nitrification rate at NH4T2	0.99	0.99	0.99
NO3DK	Nitrate decay rate, day $^{-1}$	0.2	0.1	0.4
NO3S	Denitrification rate from sediments, m day $^{-1}$	0.5	0.5	0.5
FNO3SED	Fraction of NO_3-N diffused into the sediments that become part of organic N in the sediments	0	0	0
NO3T1	Lower temperature for nitrate decay, °C	5	5	5
NO3T2	Lower temperature for maximum nitrate decay, °C	25	25	25
NO3K1	Fraction of denitrification rate at NO3T1	0.1	0.1	0.1
NO3K2	Fraction of denitrification rate at NO3T2	0.99	0.99	0.99
DSIR	Dissolved silica sediment release rate, fraction of SOD	0.1	0.1	0.1
PSIS	Particulate biogenic settling rate, m sec $^{-1}$	0.1	0.1	0.1
PSIDK	Particulate biogenic silica decay rate, day $^{-1}$	0.1	0.1	0.1
PARTSI	Dissolved silica partitioning coefficient	0.2	0.2	0.2
SOD	Zero-order SOD	1 or 3	2	0.33

Parameter	Description	Value		
		Lake Carlos	Elk Lake	Trout Lake
O2LIM	Dissolved oxygen half-saturation constant or concentration at which aerobic processes are at 50% of their maximum, g m^{-3}	0.1	0.1	0.1
FER	Iron sediment release rate, fraction of SOD	0.1	0.1	0.5
FES	Iron settling velocity, m day-1	2	2	2
CO2R	Sediment carbon dioxide release rate, fraction of sediment oxygen demand	1	1	1
O2NH4	Oxygen stoichiometry for nitrification	4.57	4.57	4.57
O2OM	Oxygen stoichiometry for organic matter decay	1.4	1.4	1.4
TYPE	Type of waterbody	LAKE	LAKE	LAKE
EQN#	Equation number used for determining reaeration	5	5	5

Table 4. Summary of AME and RMSE quantities for all three Sentinel lakes for the calibration runs.

Constituent	Site name	Site Number	Depth (meters)	Number of compared data points	AME	RMSE
Lake Carlos						
Temperature, °C	Lake Le Homme Dieu Outlet at Alexandria, MN	05244810	1.00	202	1.69	2.16
	Long Prairie River below Lake Carlos near Alexandria, MN	05244820	1.00	201	1.71	1.91
	Lake Carlos west of Kecks Point near Alexandria, MN	455843095212501	1.00	174	0.61	0.75
	Lake Carlos west of Kecks Point near Alexandria, MN	455843095212501	1.65	174	0.48	0.67
	Lake Carlos west of Kecks Point near Alexandria, MN	455843095212501	20.00	173	0.57	0.70
	Lake Carlos west of Kecks Point near Alexandria, MN	455843095212501	40.65	173	0.99	1.01
	Lake Carlos west of Kecks Point near Alexandria, MN[1]	455843095212501	--	263	0.97	1.18
Dissolved oxygen, mg L^{-1}	Lake Carlos west of Kecks Point near Alexandria, MN[1]	455843095212501	--	242	0.93	1.64
Chlorophyll *A*, $\mu g\ L^{-1}$	Lake Le Homme Dieu Outlet at Alexandria, MN	05244810	1.00	1	0.1	0.1
	Long Prairie River below Lake Carlos near Alexandria, MN	05244820	1.00	1	0.5	0.5
	Lake Carlos west of Kecks Point near Alexandria, MN	455843095212501	1.00	10	2.7	2.9
	Lake Carlos west of Kecks Point near Alexandria, MN	455843095212501	20.00	3	3.4	4.9
Orthophosphate, mg L^{-1}	Lake Le Homme Dieu Outlet at Alexandria, MN	05244810	1.00	4	<0.01	<0.01
	Long Prairie River below Lake Carlos near Alexandria, MN	05244820	1.00	4	<0.01	<0.01
	Lake Carlos west of Kecks Point near Alexandria, MN	455843095212501	1.00	5	<0.01	<0.01
	Lake Carlos west of Kecks Point near Alexandria, MN	455843095212501	20.00	4	<0.01	<0.01
Ammonia, mg L^{-1}	Lake Le Homme Dieu Outlet at Alexandria, MN	05244810	1.00	4	0.01	0.01
	Long Prairie River below Lake Carlos near Alexandria, MN	05244820	1.00	4	<0.01	<0.01
	Lake Carlos west of Kecks Point near Alexandria, MN	455843095212501	1.00	5	<0.01	0.01
	Lake Carlos west of Kecks Point near Alexandria, MN	455843095212501	20.00	4	0.02	0.02
Nitrate-Nitrite, mg L^{-1}	Lake Le Homme Dieu Outlet at Alexandria, MN	05244810	1.00	4	0.04	0.06
	Long Prairie River below Lake Carlos near Alexandria, MN	05244820	1.00	4	<0.01	<0.01
	Lake Carlos west of Kecks Point near Alexandria, MN	455843095212501	1.00	5	0.01	0.02
	Lake Carlos west of Kecks Point near Alexandria, MN	455843095212501	20.00	4	0.05	0.06
Total nitrogen, mg L^{-1}	Lake Le Homme Dieu Outlet at Alexandria, MN	05244810	1.00	4	0.12	0.12
	Long Prairie River below Lake Carlos near Alexandria, MN	05244820	1.00	5	0.12	0.14

Constituent	Site name	Site Number	Depth (meters)	Number of compared data points	AME	RMSE
	Lake Carlos west of Kecks Point near Alexandria, MN	455843095212501	1.00	5	0.12	0.14
	Lake Carlos west of Kecks Point near Alexandria, MN	455843095212501	20.00	4	0.04	0.05
Total phosphorus, $\mu g\ L^{-1}$	Lake Le Homme Dieu Outlet at Alexandria, MN	05244810	1.00	4	1	1
	Long Prairie River below Lake Carlos near Alexandria, MN	05244820	1.00	5	3	4
	Lake Carlos west of Kecks Point near Alexandria, MN	455843095212501	1.00	11	1	2
	Lake Carlos west of Kecks Point near Alexandria, MN	455843095212501	20.00	4	2	3
Elk Lake						
Temperature, °C	Elk Lake Outlet in Itasca State Park, MN	05199950	1.00	197	1.54	1.76
	Elk Lake, South End, near Hubbard, MN	471116095125301	2.00	197	0.65	0.80
	Elk Lake, South End, near Hubbard, MN	471116095125301	7.00	170	0.78	1.08
	Elk Lake, South End, near Hubbard, MN	471116095125301	20.00	197	0.69	0.69
	Elk Lake, South End, near Hubbard, MN	471116095125301	28.00	176	0.54	0.74
	Elk Lake, South End, near Hubbard, MN[2]	471116095125301	--	527	0.49	0.80
Dissolved oxygen, $mg\ L^{-1}$	Elk Lake, South End, near Hubbard, MN	471116095125301	2.00	182	0.83	1.01
	Elk Lake, South End, near Hubbard, MN	471116095125301	7.00	170	0.89	1.33
	Elk Lake, South End, near Hubbard, MN	471116095125301	20.00	120	0.28	0.37
	Elk Lake, South End, near Hubbard, MN[2]	471116095125301	--	540	0.53	1.08
Chlorophyll *A*, $\mu g\ L^{-1}$	Elk Lake, South End, near Hubbard, MN	471116095125301	2.00	7	2.7	3.4
Orthophosphate, $mg\ L^{-1}$	Elk Lake Outlet in Itasca State Park, MN	05199950	1.00	3	<0.01	<0.01
	Elk Lake, South End, near Hubbard, MN	471116095125301	2.00	4	<0.01	<0.01
	Elk Lake, South End, near Hubbard, MN	471116095125301	20.00	2	0.10	0.10
Ammonia, $mg\ L^{-1}$	Elk Lake Outlet in Itasca State Park, MN	05199950	1.00	3	0.12	0.17
	Elk Lake, South End, near Hubbard, MN	471116095125301	2.00	3	0.07	0.09
	Elk Lake, South End, near Hubbard, MN	471116095125301	20.00	2	0.42	0.46
Nitrate-Nitrite, $mg\ L^{-1}$	Elk Lake Outlet in Itasca State Park, MN	05199950	1.00	3	0.02	0.03
	Elk Lake, South End, near Hubbard, MN	471116095125301	2.00	2	<0.01	<0.01
	Elk Lake, South End, near Hubbard, MN	471116095125301	20.00	2	0.10	0.10
Total nitrogen, $mg\ L^{-1}$	Elk Lake Outlet in Itasca State Park, MN	05199950	1.00	3	0.17	0.18
	Elk Lake, South End, near Hubbard, MN	471116095125301	2.00	8	0.12	0.17
	Elk Lake, South End, near Hubbard, MN	471116095125301	20.00	3	0.45	0.48

Constituent	Site name	Site Number	Depth (meters)	Number of compared data points	AME	RMSE
Total phosphorus, $\mu g\ L^{-1}$	Elk Lake Outlet in Itasca State Park, MN	05199950	1.00	3	6	7
	Elk Lake, South End, near Hubbard, MN	471116095125301	2.00	8	5	6
	Elk Lake, South End, near Hubbard, MN	471116095125301	20.00	2	10	16
Trout Lake						
Temperature, °C	Trout Lake Outlet near Covill, MN	04011150	1.00	176	0.63	0.78
	Trout Lake, East Side, near Grand Marais, MN	475214090100401	1.00	134	0.54	0.61
	Trout Lake, East Side, near Grand Marais, MN	475214090100401	18.00	134	0.23	0.23
	Trout Lake, East Side, near Grand Marais, MN[3]	475214090100401	--	154	0.66	1.01
Dissolved oxygen, $mg\ L^{-1}$	Trout Lake, East Side, near Grand Marais, MN[3]	475214090100401	--	313	0.83	1.51
Chlorophyll *A*, $\mu g\ L^{-1}$	Trout Lake Outlet near Covill, MN	04011150	1.00	4	3.5	4.1
	Trout Lake, East Side, near Grand Marais, MN	475214090100401	1.00	4	5.0	5.3
	Trout Lake, East Side, near Grand Marais, MN	475214090100401	18.00	4	2.1	2.8
Orthophosphate, $mg\ L^{-1}$	Trout Lake Outlet near Covill, MN	04011150	1.00	5	<0.01	<0.01
	Trout Lake, East Side, near Grand Marais, MN	475214090100401	1.00	5	<0.01	<0.01
	Trout Lake, East Side, near Grand Marais, MN	475214090100401	18.00	5	<0.01	<0.01
Ammonia, $mg\ L^{-1}$	Trout Lake Outlet near Covill, MN	04011150	1.00	5	0.02	0.03
	Trout Lake, East Side, near Grand Marais, MN	475214090100401	1.00	5	<0.01	<0.01
	Trout Lake, East Side, near Grand Marais, MN	475214090100401	18.00	5	0.01	0.02
Nitrate-Nitrite, $mg\ L^{-1}$	Trout Lake Outlet near Covill, MN	04011150	1.00	5	0.04	0.04
	Trout Lake, East Side, near Grand Marais, MN	475214090100401	1.00	5	<0.01	<0.01
	Trout Lake, East Side, near Grand Marais, MN	475214090100401	18.00	5	0.02	0.02
Total nitrogen, $mg\ L^{-1}$	Trout Lake Outlet near Covill, MN	04011150	1.00	5	0.09	0.09
	Trout Lake, East Side, near Grand Marais, MN	475214090100401	1.00	11	0.05	0.08
	Trout Lake, East Side, near Grand Marais, MN	475214090100401	18.00	5	0.07	0.08
Total phosphorus, $\mu g\ L^{-1}$	Trout Lake Outlet near Covill, MN	04011150	1.00	5	3	4
	Trout Lake, East Side, near Grand Marais, MN	475214090100401	1.00	11	5	6
	Trout Lake, East Side, near Grand Marais, MN	475214090100401	18.00	11	4	5

Table 5. Summary of AME and RMSE quantities for all three Sentinel lakes for the validation runs.

Constituent	Site name	Site Number	Depth (meters)	Number of compared data points	AME	RMSE
Lake Carlos						
Temperature, °C	Lake Le Homme Dieu Outlet at Alexandria, MN	05244810	1.00	197	1.25	1.42
	Long Prairie River below Lake Carlos near Alexandria, MN	05244820	1.00	197	1.57	1.95
	Lake Carlos west of Kecks Point near Alexandria, MN	455843095212501	1.90	197	0.98	1.12
	Lake Carlos west of Kecks Point near Alexandria, MN	455843095212501	27.00	182	0.75	0.81
	Lake Carlos west of Kecks Point near Alexandria, MN[1]	455843095212501	--	192	0.87	1.06
Dissolved oxygen, mg L^{-1}	Lake Carlos west of Kecks Point near Alexandria, MN[1]	455843095212501	--	181	0.53	0.71
Chlorophyll *A*, $\mu g\ L^{-1}$	Lake Le Homme Dieu Outlet at Alexandria, MN	05244810	1.00	3	3.1	3.8
	Long Prairie River below Lake Carlos near Alexandria, MN	05244820	1.00	2	4.6	6.1
	Lake Carlos west of Kecks Point near Alexandria, MN	455843095212501	1.00	3	4.1	4.8
Orthophosphate, mg L^{-1}	Lake Le Homme Dieu Outlet at Alexandria, MN	05244810	1.00	5	<0.01	<0.01
	Long Prairie River below Lake Carlos near Alexandria, MN	05244820	1.00	5	<0.01	<0.01
	Lake Carlos west of Kecks Point near Alexandria, MN	455843095212501	1.00	4	<0.01	<0.01
	Lake Carlos west of Kecks Point near Alexandria, MN	455843095212501	20.00	4	<0.01	<0.01
Ammonia, mg L^{-1}	Lake Le Homme Dieu Outlet at Alexandria, MN	05244810	1.00	5	0.03	0.05
	Long Prairie River below Lake Carlos near Alexandria, MN	05244820	1.00	5	0.02	0.02
	Lake Carlos west of Kecks Point near Alexandria, MN	455843095212501	1.00	4	<0.01	<0.01
	Lake Carlos west of Kecks Point near Alexandria, MN	455843095212501	20.00	4	<0.01	0.01
Nitrate-Nitrite, mg L^{-1}	Lake Le Homme Dieu Outlet at Alexandria, MN	05244810	1.00	5	0.03	0.04
	Long Prairie River below Lake Carlos near Alexandria, MN	05244820	1.00	5	0.02	0.03
	Lake Carlos west of Kecks Point near Alexandria, MN	455843095212501	1.00	4	0.02	0.04
	Lake Carlos west of Kecks Point near Alexandria, MN	455843095212501	20.00	4	0.01	0.02
Total nitrogen, mg L^{-1}	Lake Le Homme Dieu Outlet at Alexandria, MN	05244810	1.00	5	0.05	0.07
	Long Prairie River below Lake Carlos near Alexandria, MN	05244820	1.00	5	0.10	0.12
	Lake Carlos west of Kecks Point near Alexandria, MN	455843095212501	1.00	4	0.10	0.10
	Lake Carlos west of Kecks Point near Alexandria, MN	455843095212501	20.00	4	0.06	0.08
Total phosphorus, $\mu g\ L^{-1}$	Lake Le Homme Dieu Outlet at Alexandria, MN	05244810	1.00	6	6	7
	Long Prairie River below Lake Carlos near Alexandria, MN	05244820	1.00	6	4	5

Constituent	Site name	Site Number	Depth (meters)	Number of compared data points	AME	RMSE
	Lake Carlos west of Kecks Point near Alexandria, MN	455843095212501	1.00	4	3	3
	Lake Carlos west of Kecks Point near Alexandria, MN	455843095212501	20.00	4	2	3
Elk Lake						
Temperature, °C	Elk Lake Outlet in Itasca State Park, MN	05199950	1.00	120	1.06	1.32
	Elk Lake, South End, near Hubbard, MN	471116095125301	2.00	120	0.65	0.74
	Elk Lake, South End, near Hubbard, MN	471116095125301	8.00	120	0.60	0.76
	Elk Lake, South End, near Hubbard, MN	471116095125301	19.00	120	0.98	1.11
	Elk Lake, South End, near Hubbard, MN	471116095125301	28.00	120	0.32	0.39
	Elk Lake, South End, near Hubbard, MN[2]	471116095125301	--	192	0.68	0.99
Dissolved oxygen, mg L^{-1}	Elk Lake, South End, near Hubbard, MN[2]	471116095125301	--	204	0.57	1.16
Chlorophyll *A*, μg L^{-1}	Elk Lake, South End, near Hubbard, MN	471116095125301	2.00	4	7.6	8.4
Orthophosphate, mg L^{-1}	Elk Lake Outlet in Itasca State Park, MN	05199950	1.00	2	<0.01	<0.01
	Elk Lake, South End, near Hubbard, MN	471116095125301	2.00	2	<0.01	<0.01
	Elk Lake, South End, near Hubbard, MN	471116095125301	20.00	2	<0.01	<0.01
Ammonia, mg L^{-1}	Elk Lake Outlet in Itasca State Park, MN	05199950	1.00	2	0.16	0.22
	Elk Lake, South End, near Hubbard, MN	471116095125301	2.00	2	0.16	0.23
	Elk Lake, South End, near Hubbard, MN	471116095125301	20.00	2	0.37	0.38
Nitrate-Nitrite, mg L^{-1}	Elk Lake Outlet in Itasca State Park, MN	05199950	1.00	2	0.01	0.01
	Elk Lake, South End, near Hubbard, MN	471116095125301	2.00	2	0.01	0.02
	Elk Lake, South End, near Hubbard, MN	471116095125301	20.00	2	<0.01	<0.01
Total nitrogen, mg L^{-1}	Elk Lake Outlet in Itasca State Park, MN	05199950	1.00	2	0.16	0.22
	Elk Lake, South End, near Hubbard, MN	471116095125301	2.00	6	0.13	0.16
	Elk Lake, South End, near Hubbard, MN	471116095125301	20.00	2	0.52	0.52
Total phosphorus, μg L^{-1}	Elk Lake Outlet in Itasca State Park, MN	05199950	1.00	2	54	76
	Elk Lake, South End, near Hubbard, MN	471116095125301	2.00	6	6	7
	Elk Lake, South End, near Hubbard, MN	471116095125301	20.00	2	42	49
Trout Lake						
Temperature, °C	Trout Lake Outlet near Covill, MN	04011150	1.00	126	0.91	1.16
	Trout Lake, East Side, near Grand Marais, MN	475214090100401	18.00	163	0.89	0.97
	Trout Lake, East Side, near Grand Marais, MN[3]	475214090100401	--	72	1.00	1.46

Constituent	Site name	Site Number	Depth (meters)	Number of compared data points	AME	RMSE
Dissolved oxygen, mg L^{-1}	Trout Lake, East Side, near Grand Marais, MN[3]	475214090100401	--	149	0.56	0.94
Chlorophyll *A*, μg L^{-1}	Trout Lake, East Side, near Grand Marais, MN	475214090100401	1.00	4	9.8	10.0
Orthophosphate, mg L^{-1}	Trout Lake Outlet near Covill, MN	04011150	1.00	1	<0.01	<0.01
	Trout Lake, East Side, near Grand Marais, MN	475214090100401	1.00	1	<0.01	<0.01
	Trout Lake, East Side, near Grand Marais, MN	475214090100401	18.00	1	<0.01	<0.01
Ammonia, mg L^{-1}	Trout Lake Outlet near Covill, MN	04011150	1.00	1	<0.01	<0.01
	Trout Lake, East Side, near Grand Marais, MN	475214090100401	1.00	1	<0.01	<0.01
	Trout Lake, East Side, near Grand Marais, MN	475214090100401	18.00	1	<0.01	<0.01
Nitrate-Nitrite, mg L^{-1}	Trout Lake Outlet near Covill, MN	04011150	1.00	1	<0.01	<0.01
	Trout Lake, East Side, near Grand Marais, MN	475214090100401	1.00	1	0.03	0.03
	Trout Lake, East Side, near Grand Marais, MN	475214090100401	18.00	1	0.03	0.03
Total nitrogen, mg L^{-1}	Trout Lake Outlet near Covill, MN	04011150	1.00	1	0.09	0.09
	Trout Lake, East Side, near Grand Marais, MN	475214090100401	1.00	5	0.11	0.16
	Trout Lake, East Side, near Grand Marais, MN	475214090100401	18.00	1	0.14	0.14
Total phosphorus, μg L^{-1}	Trout Lake Outlet near Covill, MN	04011150	1.00	1	7	7
	Trout Lake, East Side, near Grand Marais, MN	475214090100401	1.00	5	5	5
	Trout Lake, East Side, near Grand Marais, MN	475214090100401	18.00	5	6	7

Table 6. Summary of sensitivity analysis for all three Sentinel lakes, in percent change from calibration run.

		Output, in percent change from calibrated value					
Constituent	Input, in percent change from calibrated value	Water tempature, in °C	Dissolved oxygen, in mg L^{-1}	Ammonia, in mg L^{-1} as N	Nitrite + nitrate, in mg L^{-1} as N	Ortho-phosphate, in mg L^{-1} as P	Chlorophyll *A*, in μg L^{-1}
Lake Carlos							
wind sheltering coefficient	-20	-14.1	-17.5	16.5	7.5	-1.9	13.2
	+20	11.9	15.4	-8.8	-12.9	0.6	1.5
inflow phosphorus	-20	0.0	0.0	0.0	0.0	-1.8	0.0
	+20	0.0	0.0	0.0	0.0	1.4	0.0
inflow nitrogen	-20	0.0	0.0	-0.2	-0.7	0.2	-1.1
	+20	0.0	0.0	0.2	0.7	-0.3	1.1
inflow organic matter	-20	0.0	0.6	-1.9	-0.7	-0.8	-2.9
	+20	0.0	-0.6	2.0	0.6	0.8	2.9
sediment oxygen demand	-20	0.0	5.4	-2.7	8.4	-3.7	0.2
	+20	0.0	-4.4	3.1	-8.0	4.2	-0.5
extinction coefficient	-20	0.8	1.9	-0.4	-6.8	-2.2	12.8
	+20	-0.4	-0.9	0.3	4.7	1.2	-7.1
Elk Lake							
wind sheltering coefficient	-20	-5.1	-4.9	3.1	4.5	-4.6	6.6
	+20	9.5	8.0	-5.6	-17.2	5.8	-6.5
inflow phosphorus	-20	0.0	-0.1	0.1	0.1	-1.6	-0.4
	+20	0.0	0.0	0.0	-0.1	1.6	0.2
inflow nitrogen	-20	0.1	0.3	-0.4	-0.3	0.2	-0.9
	+20	-0.1	-0.3	0.5	0.2	-0.4	0.9
inflow organic matter	-20	0.1	0.8	-0.7	-0.4	-0.9	-1.9
	+20	-0.1	-0.7	0.8	-0.1	0.6	1.9

Constituent	Input, in percent change from calibrated value	Output, in percent change from calibrated value					
		Water tempature, in °C	Dissolved oxygen, in mg L^{-1}	Ammonia, in mg L^{-1} as N	Nitrite + nitrate, in mg L^{-1} as N	Ortho-phosphate, in mg L^{-1} as P	Chlorophyll *A*, in $\mu g\ L^{-1}$
sediment oxygen demand	-20	0.0	4.8	-3.0	10.0	-6.4	-0.1
	+20	0.0	-4.1	2.6	-8.1	6.8	0.2
extinction coefficient	-20	1.8	8.3	-2.7	-5.5	-3.6	16.9
	+20	-1.1	-5.4	1.5	2.5	2.1	-11.8
Trout Lake							
wind sheltering coefficient	-20	-0.6	-2.4	1.9	3.6	2.3	-0.6
	+20	0.3	3.7	-1.8	-0.2	-4.3	1.9
inflow phosphorus	-20	0.0	0.0	-0.2	-0.4	-0.3	-0.7
	+20	0.0	0.0	0.3	0.4	0.3	0.7
inflow nitrogen	-20	0.0	0.0	0.0	-0.1	0.0	0.0
	+20	0.0	0.0	0.1	0.1	0.0	0.0
inflow organic matter	-20	0.1	0.1	-0.5	-0.8	-0.4	-0.9
	+20	-0.1	-0.1	0.7	0.7	0.3	0.9
sediment oxygen demand	-20	0.0	2.8	-2.1	2.3	-0.6	0.0
	+20	0.0	-2.5	2.5	-2.6	0.9	0.0
extinction coefficient	-20	3.0	1.3	-6.6	-28.0	-7.3	9.0
	+20	-1.9	-2.2	7.2	13.9	4.8	-5.3